

IMPROVED AGE ESTIMATION FOR SOLAR-TYPE DWARFS USING ACTIVITY-ROTATION DIAGNOSTICS

ERIC E. MAMAJEK^{1,2,3} AND LYNNE A. HILLENBRAND⁴

Received 2008 April 26; accepted 2008 July 10

ABSTRACT

While the strong anticorrelation between chromospheric activity and age has led to the common use of the Ca II H and K emission index ($R'_{\text{HK}} = L_{\text{HK}}/L_{\text{bol}}$) as an empirical age estimator for solar-type dwarfs, existing activity-age relations produce implausible ages at both high and low activity levels. We have compiled R'_{HK} data from the literature for young stellar clusters, richly populating for the first time the young end of the activity-age relation. Combining the cluster activity data with modern cluster age estimates and analyzing the color dependence of the chromospheric activity age index, we derive an improved activity-age calibration for F7–K2 dwarfs ($0.5 \text{ mag} < B - V < 0.9 \text{ mag}$). We also present a more fundamentally motivated activity-age calibration that relies on conversion of R'_{HK} values through the Rossby number to rotation periods and then makes use of improved gyrochronology relations. We demonstrate that our new activity-age calibration has typical age precision of ~ 0.2 dex for normal solar-type dwarfs aged between the Hyades and the Sun (~ 0.6 – 4.5 Gyr). Inferring ages through activity-rotation-age relations accounts for some color-dependent effects and systematically improves the age estimates (albeit only slightly). We demonstrate that coronal activity as measured through the fractional X-ray luminosity ($R_X = L_X/L_{\text{bol}}$) has nearly the same age- and rotation-inferring capability as chromospheric activity measured through R'_{HK} . As a first application of our calibrations, we provide new activity-derived age estimates for a volume-limited sample of the 108 solar-type field dwarfs within 16 pc.

Subject headings: stars: activity — stars: chromospheres — stars: coronae — stars: fundamental parameters — stars: rotation — X-rays: stars

1. INTRODUCTION

Age is, arguably, the most difficult basic stellar quantity to estimate for low-mass field dwarfs (see, e.g., Mamajek et al. 2008). Yet, the temporal evolution of phenomena such as stellar activity, surface abundances, rotation, and circumstellar matter is of current interest and within observational means for nearby stars. Our particular motivation for improving field star age estimates stems from our interest in circumstellar disk evolution as executed via the *Spitzer Space Telescope* Formation and Evolution of Planetary Systems⁵ (FEPS) Legacy Science program, which is surveying the dust surrounding solar-type stars between ~ 3 Myr and ~ 3 Gyr (Meyer et al. 2004, 2006; Kim et al. 2005; Stauffer et al. 2005; Hines et al. 2006, 2007; Silverstone et al. 2006; Moro-Martín et al. 2007; Bouwman et al. 2008; Meyer et al. 2008; Hillenbrand et al. 2008; J. M. Carpenter et al. 2008, in preparation).

The most theoretically grounded stellar age estimator is the Hertzsprung-Russell diagram, which predicts ages based on our understanding of nuclear physics, stellar interior structure, and stellar atmospheres. It can be employed in stellar clusters for which main-sequence (MS) turnoff and/or turn-on ages are typically available and to field stars of known distance that are in the pre-MS or post-MS phases of stellar evolution. Field stars, however, are generally MS objects and, by definition, lack coeval accompanying stellar populations that might enable accurate age dating via standard H-R diagram techniques. Thus, proxy indicators of age are necessary.

1.1. Chromospheric Activity as an Age Indicator

Historically, a popular age estimator for field stars of roughly solar mass has been the R'_{HK} index, which measures chromospheric emission in the cores of the broad photospheric Ca II H and K absorption lines, normalized to the underlying photospheric spectrum. Chromospheric activity is generated through the stellar magnetic dynamo, the strength of which appears to scale with rotation velocity (Kraft 1967; Noyes et al. 1984; Montesinos et al. 2001). Both chromospheric emission and rotation are observationally constrained to decay with age (Wilson 1963; Skumanich 1972; Soderblom 1983; Soderblom et al. 1991). The angular momentum loss is theoretically understood as due to mass loss in a magnetized wind (Schatzman 1962; Weber & Davis 1967; Mestel 1968).

The chromospheric activity index R'_{HK} is calculated from a band ratio measurement of the Ca H and K emission line strength (the “S-index” or, when converted to the Mount Wilson system, S_{MW} ; Vaughan et al. 1978; Vaughan & Preston 1980; Duncan et al. 1991) from which the underlying stellar photospheric contribution is then subtracted. We refer the reader to papers by Noyes et al. (1984), Baliunas et al. (1995, 1996), Henry et al. (1996), Wright et al. (2004), and references therein for in-depth discussion of how to measure S_{MW} and R'_{HK} , as well as the history of studies using this index. Our simple goal for this study is to provide an R'_{HK} versus age relation applicable to sets of R'_{HK} and $(B - V)_0$ data (the latter derived from a spectral type or from a color) for solar-type and near-solar-metallicity dwarfs.

The activity-age data pair of highest quality is that for the Sun, and our adopted values are listed in Table 1. The solar age is presumed coincident with that of the oldest portions of meteorites (the Ca-Al-rich inclusions; 4.570 Gyr; Baker et al. 2005). However, the Sun and presumably most other stars exhibit activity cycles (with period 11 yr in the case of the Sun), as well as longer term variations (e.g., the so-called Maunder minimum in the case

¹ Harvard-Smithsonian Center for Astrophysics, Cambridge, MA 02138; emamajek@cfa.harvard.edu.

² Clay Postdoctoral Fellow.

³ Current address: Department of Physics and Astronomy, University of Rochester, Rochester, NY 14627-0171.

⁴ Department of Astronomy and Astrophysics, California Institute of Technology, Pasadena, CA 91125; lah@astro.caltech.edu.

⁵ See <http://feps.as.arizona.edu>.

TABLE 1
ADOPTED SOLAR DATA

Parameter	Value	References
$(B - V)_0$	0.65 mag	1
Age.....	4.570 Gyr	2
\bar{S}_\odot	0.176	3
$\log R'_{\text{HK}}$	-4.906 dex	4
$\log R'_{\text{HK}}$ 68% Range.....	-4.942 to -4.865 dex	5
$\log R'_{\text{HK}}$ 95% Range.....	-4.955 to -4.832 dex	5
$\log L_X$	27.35 ergs s ⁻¹	6
$\log R_X$ [=log (L_X/L_{bol})].....	-6.24 dex	6

NOTES.—An uncertainty in the solar $(B - V)_0$ of ± 0.01 mag produces a systematic uncertainty of the $\log R'_{\text{HK}}$ values by ∓ 0.004 dex. Note that the absolute calibration of the $\log R'_{\text{HK}}$ values (as a physical metric of chromospheric line losses) is probably only accurate to $\sim 10\%$ (Hartmann et al. 1984; Noyes et al. 1984).

REFERENCES.—(1) Cox 2000; (2) minimum age from Baker et al. 2005; (3) time-weighted average of Baliunas et al. 1996 and Hall et al. 2007 for 1966–2006; (4) calculated using $(B - V)_0$ and mean \bar{S}_\odot via Noyes et al. 1984; (5) calculating using solar 1 Å K index data from Livingston et al. 2007 using relations from Radick et al. 1998 and Noyes et al. 1984 and adopting the solar $(B - V)_0$ color listed; (6) soft X-ray (0.1–2.4 keV) luminosity and fraction luminosity estimated from Judge et al. (2003) with 50% uncertainty.

of the Sun). Over the period 1966–1993, covering mostly solar cycles 20, 21, and 22, Baliunas et al. (1995) estimated the solar Mount Wilson S -index to be $\bar{S}_\odot = 0.179$. Over the period 1994–2006, mostly solar cycle 23, Hall et al. (2007) measured $\bar{S}_\odot = 0.170$. Using a mean solar S -value that is approximately weighted by the span of measurements ($\bar{S}_\odot = 0.176$; for ~ 1966 –2006) and a mean solar color of $B - V = 0.65$ (Cox 2000), and using the equations from Noyes et al. (1984), we estimate the mean solar activity to be $\log R'_{\text{HK}} = -4.91$. We also give in Table 1 the 68% and 95% range of the observed solar $\log R'_{\text{HK}}$ due to variability.

1.2. Shortcomings of Previous Activity-Age Calibrations

Using the Sun as one anchor point, we can look to open clusters with ages derived from other methods (e.g., the H-R diagram) in order to populate an activity-age calibration. There are four such R'_{HK} versus age relations in the literature that have been used in age-dating field stars: two from Soderblom et al. (1991) and one each from Donahue (1993) and Lachaume et al. (1999). The activity-age relations from Soderblom et al. (1991) include a linear fit to age versus activity for members of clusters and binaries. The second relation, often overlooked, assumes a constant star formation history and takes into account kinematic disk heating. D. Soderblom (2008, private communication) has kindly provided an analytic version of this alternative activity-age relation.

That there are deficiencies with these existing calibrations can be easily demonstrated. For the Lachaume et al. (1999) calibration, the solar R'_{HK} value adopted here (-4.91) would imply a solar age of 7.2 Gyr, which is clearly in error. The other two calibrations used the Sun as one of their anchor points, but with slightly different R'_{HK} values (for the calibrations of Soderblom et al. [1991] and Donahue [1993] one derives ages of 4.1 and 4.0 Gyr, respectively). Soderblom et al. (1991) do not advocate extrapolating either of their activity-age relations to the young/active regime ($\log R'_{\text{HK}} > -4.4$); however, Donahue (1993) explicitly fits his activity-age relation to age ~ 10 Myr and $\log R'_{\text{HK}} \simeq -4.2$ (anchoring his fit to data for NGC 2264). Given the observed activity levels in the ~ 5 –15 Myr Sco-Cen OB association ($\log R'_{\text{HK}} \simeq -4.05$; § 2), neither the fit from Donahue (1993) or extrapolating the two fits from Soderblom et al. (1991) estimates an age similar to the isochronal value. Indeed, the commonly used fit of Donahue

(1993) would estimate an age of 1 minute for a star with $\log R'_{\text{HK}} \simeq -4.05$. Given the paucity of young stars in the previous calibrations, we should not be too surprised at the lack of agreement with other age-dating methods at the high-activity end of the relation.

1.3. Potential for Improved Activity-Age Calibrations

Clearly, an improved activity-age calibration is needed. Further, we would like to understand and quantify the limitations of any such relationship and hence its practical application. We focus this paper primarily on refining the age-activity relation for solar-type dwarfs. By “solar type” we mean $\sim F7$ –K2 or $0.5 \text{ mag} < (B - V)_0 < 0.9 \text{ mag}$, which is approximately the color range over which the Noyes et al. (1984) relation for the photospheric contribution to the S -index is applicable, as well as the color range blanketed by recent activity surveys. The F3 V–F6 V temperature region [$0.42 \text{ mag} < (B - V)_0 < 0.5 \text{ mag}$] appears to mark the transition where the rotation-activity correlation breaks down, chromospheric activity diminishes, stellar convective envelopes thin, and magnetic braking becomes inefficient (Kraft 1967; Wolff et al. 1985; Garcia-Lopez et al. 1993). By “dwarfs” we mean MS and pre-MS stars, and we explicitly exclude evolved stars more than 1 mag above the MS.

There are three developments that make our investigation timely:

1. Recently measured R'_{HK} values for stars that belong to age-dated young stellar aggregates (e.g., Sco-Cen, β Pic). These additions to the literature both broaden and strengthen modern activity-age derivations relative to the data landscape of 1–2 decades ago.
2. The ages of well-studied nearby open clusters (e.g., α Per, Pleiades) have been updated during the past decade. The most noticeable difference relative to traditionally accepted age values is the systematic shift toward older ages driven by results using the Li depletion boundary age estimation method (e.g., Stauffer et al. 1998; Barrado y Navascués et al. 2004).
3. Interest in circumstellar disk and planetary system evolution has increased dramatically over the past 5 years. The availability of relevant infrared data, e.g., from *Spitzer* observations, begs for a robust stellar age estimator in order to probe the collisional and radiative evolution of debris disks and the connection of such phenomena to exosolar planetary system dynamics. Similarly, exoplanet discoveries over the past decade have motivated interest in the ages of the parent field stars for comparison to the Sun and solar system. In this paper we derive, using samples drawn from cluster and moving group populations (§ 2), a new R'_{HK} activity versus age relation (§ 3). In § 4 we tie both chromospheric activity index (R'_{HK}) and coronal activity index [$R_X = \log (L_X/L_{\text{bol}})$] data to stellar rotation rates via the Rossby number (i.e., secure an activity-rotation relation) and attempt to derive independently an activity-age relation based on the “gyrochronology” rotation evolution formalism of Barnes (2007) although with newly derived coefficients. In the Appendix we quantify the correlation between fractional X-ray luminosity and Ca H and K activity for solar-type stars and demonstrate that R_X , like R'_{HK} , can be used to derive quantitative age estimates.

2. DATA

2.1. Ca II H and K Data

We have collected R'_{HK} indices derived from S -values in the tradition of the Mount Wilson HK project. Typical errors for single observations due to measurement uncertainty and calibration to the standard system combine to typically ~ 0.1 dex (e.g., Henry

et al. 1996; Paulson et al. 2002; White et al. 2007). Given the ubiquity of the R'_{HK} index in the literature and the uniformity in its calculation and calibration by previous authors, we make no attempt either to improve on the R'_{HK} index or to correct for other effects (i.e., metallicity,⁶ gravity, etc.).

R'_{HK} values were taken from many sources, including the large multi-epoch surveys of Duncan et al. (1991), Baliunas et al. (1996), Wright et al. (2004), and Hall et al. (2007); the large single-epoch surveys of Henry et al. (1996) and Gray et al. (2003, 2006); and the smaller, focused surveys of Soderblom et al. (1993, 1998), Paulson et al. (2002), Tinney et al. (2002), Jenkins et al. (2006, 2008), and White et al. (2007). The S -values from Duncan et al. (1991) were converted to R'_{HK} following Noyes et al. (1984) using $B - V$ colors from Perryman et al. (1997). Discussion of the calibration of the HK observations onto the Mount Wilson system are addressed in the individual studies. Single-epoch surveys typically give consistent $\log R'_{\text{HK}}$ values that agree at the ~ 0.1 dex rms level (e.g., Jenkins et al. 2008), likely due to observational errors in evaluating the S -index plus intrinsic stellar variability.

As solar-type stars undergo major changes in their interior structure at the end of their MS lifetime, and Wright et al. (2004) have demonstrated that evolved stars show systematically lower activity levels, we restrict our sample to stars that are consistent with being MS stars (here defined as being within ΔM_V of 1 mag of the MS defined by Wright 2005). We specifically retain pre-MS stars, however, as we are interested in probing the activity-age relation toward the youngest ages.

Although stellar rotation varies slowly with time, rotation-driven stellar activity varies on much shorter timescales, e.g., years, weeks, and days. This variability is also taken, in and of itself, as an age indicator with more rapid, stochastic, and high-amplitude variability indicative of younger stars, while regularly periodic, long-cycle, and low-amplitude variability characterizes older stars (e.g., Radick et al. 1995, 1998; Hempelmann et al. 1996; Baliunas et al. 1998). Lockwood et al. (2007) and Hall et al. (2007) also provide recent synopses.

The physical mechanisms producing such variability include changes in the filling factor of emitting regions, growth and decay of individual emitting regions, and short- and long-term activity cycles. For example, in the Sun, as well as in other stars, there is considerable variation in the observable S through an 11 yr cycle, by 10% (White & Livingston 1981). In M67 a substantial fraction of the stars exhibit even larger variations (Giampapa et al. 2006). Evidence from the California Planet Search (Wright et al. 2004; D. Fischer & H. Isaacson 2008, private communication) shows that the bulk of the sample exhibits variations of a few to $\sim 10\%$ in S at activity levels $-4.9 < \log R'_{\text{HK}} < -4.4$ with less variation at lower activity levels, $< 2\%$ in S at $\log R'_{\text{HK}} < -5.1$. Within samples of presumably coeval cluster stars, there is similar evidence of scatter in $\log R'_{\text{HK}}$ values for a given color (as we illustrate for our sample in § 3.1), which can be interpreted as a mix of high and low activity levels about the mean level characteristic of the cluster age. Estimated variations on timescales up to a few percent of the solar age correspond to ~ 0.15 in $\log R'_{\text{HK}}$.

In Table 1 we list the 68% and 95% ranges for the solar $\log R'_{\text{HK}}$ value from 1977 to 2008 as estimated from the data of Livingston et al. (2007). During recent solar maxima $\log R'_{\text{HK}} \simeq -4.83$, and

during recent solar minima $\log R'_{\text{HK}} \simeq -4.96$. Through extrapolation of the chromospheric activity–cycle length relation, Baliunas & Soon (1995) extrapolate the solar activity during the Maunder minimum period (~ 1645 – 1715) to be roughly $\log R'_{\text{HK}} \simeq -5.10$.

All of this implies errors in ages that we could quantify if we understood the probability that an individual measurement reflects the mean activity level for that star. For our sample, the $\log R'_{\text{HK}}$ data are a mix of long-term multi-epoch averages along with some single/few-epoch observations. Most of the X-ray data (discussed next) are single-epoch observations of length a few hundred seconds. The evidence on variability suggests caution in age derivation for stars lacking activity index monitoring of sufficient duration such that mean activity levels can be determined. Hence, we expect some uncertainty in ages derived from activity levels to be due to variability.

2.2. Rotation and X-Ray Data

To augment our understanding of the activity-age relation, we also compiled data that allowed us to explore the more fundamental rotation-age relation. We created a database of solar-type stars having $\log R'_{\text{HK}}$ with complimentary estimates of color, rotation period, and, when available, fractional X-ray luminosity [$\log (L_X/L_{\text{bol}}) = \log R_X$]. We started with the compiled catalog of Pizzolato et al. (2003) and added stars from the FEPS program that had new rotation periods measured by G. Henry (2006, private communication). We removed stars from the Pizzolato et al. (2003) sample that had periods inferred from chromospheric activity levels as in Saar & Osten (1997); i.e., we retain only those rotation periods measured from the observed modulation of star-spots or chromospheric activity.

X-ray luminosities for sample stars were calculated using the 0.1–2.4 keV X-ray count rates and HR1 hardness ratios from the *ROSAT* All-Sky Survey (Voges et al. 1999, 2000).⁷ X-ray count rate f_X (counts s^{-1}) can be converted to X-ray flux (ergs $\text{cm}^{-2} \text{s}^{-1}$) in the low column density regime via a conversion factor (C_X) formula from Fleming et al. (1995):

$$C_X = (8.31 + 5.30 \text{ HR1}) \times 10^{-12} \text{ ergs cm}^{-2} \text{ count}^{-1}. \quad (1)$$

Combining the X-ray flux f_X and conversion factor C_X with distance D , one can estimate the stellar X-ray luminosity L_X (ergs s^{-1}):

$$L_X = 4\pi D^2 C_X f_X. \quad (2)$$

The final conversion to X-ray and bolometric luminosities used parallaxes, V -band photometry, and $B - V$ colors from *Hipparcos* (Perryman et al. 1997) and bolometric corrections from Kenyon & Hartmann (1995).

Our rotation-activity sample consists of 167 MS and pre-MS stars of near-solar color ($0.5 \text{ mag} < B - V < 0.9 \text{ mag}$) with measured periods and $\log R'_{\text{HK}}$. Of these, 166 have X-ray luminosities and $\log R_X$ values that can be estimated. The three lacking X-ray data are unsurprisingly inactive ($\log R'_{\text{HK}} < -5.0$). While the primary focus on this paper is on using chromospheric activity to gauge stellar ages, we recognize that X-ray luminosities are calculable for many more stars than those with published $\log R'_{\text{HK}}$ measurements. Hence, in the Appendix we quantify the correlation between chromospheric and X-ray activity for solar-type dwarfs.

⁶ The near-solar metallicity (rms $\simeq 0.1$ dex in Fe/H; Twarog et al. 1997) of many of the nearest young open clusters and stellar aggregates that anchor the activity-age relation is well established. This finding extends to T Tauri stars in the nearest star-forming regions (Padgett 1996). However, recent analysis of the California-Carnegie Planet Search Project sample by J. Wright (2008, private communication; J. Wright 2008, in preparation) suggests that there are metallicity effects that can bias R'_{HK} , most severely for stars older than the Sun.

⁷ One can convert count rates and fluxes between *ROSAT* and other X-ray bands using the PIMMS tool (<http://cxc.harvard.edu/toolkit/pimms.jsp>). For a brief discussion regarding converting *ROSAT* and *Chandra* fluxes, see Preibisch & Feigelson (2005).

TABLE 2
 $\log R'_{\text{HK}}$ FOR COLOR-SEPARATED SOLAR-TYPE DWARF BINARIES

A Name	B Name	A $B - V$	B $B - V$	A $\log R'_{\text{HK}}$	B $\log R'_{\text{HK}}$	References
HD 531B.....	HD 531A	0.67	0.75	-4.28	-4.39	1, 2
HD 5190.....	HD 5208	0.52	0.68	-4.96	-5.13	1, 3
HD 6872A.....	HD 6872B	0.47	0.54	-4.86	-4.96	1, 2
HD 7439.....	HD 7438	0.45	0.81	-4.75	-4.67	1, 2, 4
HD 13357A.....	HD 13357B	0.67	0.72	-4.74	-4.61	1, 2*
HD 14082A.....	HD 14082B	0.52	0.62	-4.41	-4.37	1, 2
HD 26923.....	HD 26913	0.57	0.68	-4.50	-4.39	1, 5
HD 28255A.....	HD 28255B	0.62	0.69	-4.89	-4.65	1, 6
HD 53705.....	HD 53706	0.62	0.78	-4.93	-5.01	1, 3
HD 59099.....	HD 59100	0.49	0.63	-4.72	-4.98	1, 3*
HD 73668A.....	HD 73668B	0.61	0.81	-4.88	-4.66	1, 2
HD 103432.....	HD 103431	0.71	0.76	-4.82	-4.73	1, 2, 7*
HD 116442.....	HD 116443	0.78	0.87	-4.94	-4.94	1, 2
HD 118576.....	GJ 9455B	0.64	0.85	-4.92	-4.73	1, 7
HD 128620.....	HD 128621	0.63	0.84	-5.00	-4.92	3, 8
HD 134331.....	HD 134330	0.62	0.72	-4.82	-4.82	1, 3
HD 135101A.....	HD 135101B	0.68	0.74	-5.11	-5.01	1, 2, 4
HD 137763.....	HD 137778	0.79	0.87	-4.97	-4.37	1, 2
HD 142661.....	HD 142661B	0.55	0.81	-4.94	-4.58	1, 4*
HD 144087.....	HD 144088	0.75	0.85	-4.66	-4.60	1, 2
HD 219175A.....	HD 219175B	0.54	0.65	-4.99	-4.89	1, 2, 7*

NOTE.—An asterisk implies that the published S_{MW} value from the cited survey was converted to $\log R'_{\text{HK}}$ by the author following Noyes et al. (1984).

REFERENCES.—(1) Perryman et al. 1997; (2) Wright et al. 2004; (3) Henry et al. 1996; (4) Gray et al. 2003; (5) Baliunas et al. 1996; (6) Tinney et al. 2002; (7) Duncan et al. 1991; (8) Bessell 1981.

2.3. Field Binaries

Solar-type dwarf binaries are a useful sample for two reasons in the present investigation: examining whether there is a color dependence of $\log R'_{\text{HK}}$ versus age, and gauging the precision of the age estimates derived from activity. The coevality of stellar binary components at the <1 Myr level is well motivated observationally (e.g., Hartigan et al. 1994; Hartigan & Kenyon 2003). We list three useful samples for the purposes of exploring the age-activity relation.

First, for exploring the color dependence of $\log R'_{\text{HK}}$ for a given age, we identify 21 “color-separated” binary systems in the liter-

ature with R'_{HK} measurements that have (1) photospheric $B - V$ colors differing between the two components by >0.05 mag and (2) $B - V$ color for each component between 0.45 and ≈ 0.9 (where the photospheric correction to R'_{HK} is well characterized; Noyes et al. 1984). These systems are listed in Table 2. As our primary focus is on systems of near-solar metallicity, we exclude two very metal-poor systems from the analysis (HD 23439AB and HD 134439/40, both with $[\text{Fe}/\text{H}] \simeq -1.0$; Thévenin & Idriart 1999), although inclusion of the pair would have negligible impact on our findings.

Second, in Table 3 we list solar-type binaries that met the color range criterion $[0.45 \text{ mag} < (B - V)_0 < 0.9 \text{ mag}]$, but whose

TABLE 3
 $\log R'_{\text{HK}}$ FOR NEAR-IDENTICAL SOLAR-TYPE DWARF BINARIES

A Name	B Name	A $B - V$	B $B - V$	A $\log R'_{\text{HK}}$	B $\log R'_{\text{HK}}$	References
HD 9518A.....	HD 9518B	0.53	0.54	-5.12	-5.00	1, 2
HD 10361.....	HD 10360	0.85	0.88	-4.88	-4.75	3, 4
HD 20807.....	HD 20766	0.60	0.64	-4.79	-4.65	1, 4
HD 84612.....	HD 84627	0.52	0.53	-4.83	-4.81	1, 4
HD 92222A.....	HD 92222B	0.59	0.59	-4.44	-4.51	2, 5
HD 98745.....	HD 98744	0.54	0.54	-5.04	-5.21	1, 2
HD 103743.....	HD 103742	0.64	0.67	-4.81	-4.83	1, 4
HD 111484A.....	HD 111484B	0.56	0.56	-4.71	-4.81	1, 2
HD 145958A.....	HD 145958B	0.76	0.80	-4.94	-4.94	1, 2
HD 154195A.....	HD 154195B	0.61	0.61	-4.87	-4.88	1, 4*
HD 155886.....	HD 155885	0.85	0.86	-4.57	-4.56	6, 7, 8*
HD 167216.....	HD 167215	0.53	0.58	-5.05	-5.12	1, 2
HD 179957.....	HD 179958	0.64	0.64	-5.05	-5.08	2, 3
HD 186408.....	HD 186427	0.64	0.66	-5.10	-5.08	1, 2

NOTE.—An asterisk implies that the published S_{MW} value from the cited survey was recalculated to $\log R'_{\text{HK}}$ by the author using the color listed and following Noyes et al. (1984).

REFERENCES.—(1) Perryman et al. 1997; (2) Wright et al. 2004; (3) Mermilliod 1991 (VizieR Online Data Catalog, II/168); (4) Henry et al. 1996; (5) $(B - V)_0$ inferred from spectral type; (6) Gliese & Jahreiss 1991; (7) Baliunas et al. 1996; (8) Baliunas et al. 1995.

TABLE 4
FIELD BINARIES WITH ROTATION PERIODS

A Name	B Name	A $B - V$	B $B - V$	A Period (days)	B Period (days)	References
HD 131156A.....	HD 131156B	0.73	1.16	6.31	11.94	1, 2
HD 128620	HD 128621	0.63	0.84	25.6	36.9	3, 4, 5, 6
HD 155886	HD 155885	0.85	0.86	20.69	21.11	2, 7
HD 201091	HD 201092	1.07	1.31	35.37	37.84	1, 2
HD 219834A.....	HD 219834B	0.79	0.90	42	43	8, 9

NOTE.—The period for HD 128620 (α Cen A) is a mean (25.6 days) from values given by E. Guinan (2008, private communication; 22 ± 3 days) and Hallam et al. (1991; 28.8 ± 2.5 days) and is consistent within the constraints from $v \sin i$ and p -mode rotational splitting (Fletcher et al. 2006; Bazot et al. 2007).

REFERENCES.—(1) Perryman et al. 1997; (2) Donahue et al. 1996; (3) Bessell 1981; (4) E. Guinan 2008, private communication; (5) Jay et al. 1997; (6) Hallam et al. 1991; (7) Hoffleit & Jaschek 1991; (8) Mermilliod 1991; (9) Baliunas et al. 1996.

components had near-identical colors [$|\Delta(B - V)_0| < 0.05$], i.e., “twin” binaries. We include these systems in our analysis of gauging the accuracy to which activity-derived ages can be estimated. Lastly, following Barnes (2007), we also identify five field binaries from the literature having measured rotation periods and list their properties in Table 4. A few have $(B - V)_0$ colors beyond the range where $\log R'_{\text{HK}}$ is well defined [i.e., $(B - V)_0 > 0.9$ mag]; however, we include them in our sample for the purposes of assessing the accuracy of the rotation versus age versus color relation discussed in § 4.2.

2.4. Cluster Ages, Membership, and Activity

We turn now to a detailed discussion of our cluster samples. Kinematic membership of individual stars to their assigned groups was scrutinized with modern astrometric data (i.e., *Hipparcos*, Tycho-2, and UCAC2 catalogs) either by the authors or through examination of recently published kinematic studies, or both. Assessment of whether the stars’ proper motions were consistent with membership follows the methodology in Mamajek (2005). Table 5 lists the members of the stellar groups along with their relevant color and activity, and Table 6 summarizes the cluster ages, the number of published $\log R'_{\text{HK}}$ values for cluster members, and a summary of activity statistics. In total there are 274 published $\log R'_{\text{HK}}$ measurements for 206 stars in our cluster database. In the following subsections we briefly review the stellar groups and references for their membership and ages.

2.4.1. Young Associations

Members of Upper Sco were taken from Preibisch & Zinnecker (1999) and Walter et al. (1994); we adopt the mean group age (5 Myr) from Preibisch et al. (2002). Memberships and mean ages for the β Pic and Tuc-Hor moving groups (12 and 30 Myr ages, respectively) were taken from Zuckerman & Song (2004), and HD 105 was added as a Tuc-Hor member following Mamajek et al. (2004). In Tuc-Hor, only stars demonstrated by Mamajek et al. (2004) to be near and comoving with the β Tuc nucleus were retained for our activity-age calibration. Members of Lower Cen-Cru (LCC) and Upper Cen-Lup (UCL) were taken from de Zeeuw et al. (1999) and Mamajek et al. (2002), and mean group ages were adopted from Mamajek et al. (2002). Preibisch & Mamajek (2008) suggest that LCC shows evidence for substructure and a probable age gradient (the more populous northern part appears to be ~ 17 Myr, while the less populous southern part appears to be ~ 12 Myr); however, 16 Myr is a reasonable mean age for the group, and given the lack of evolution in $\log R'_{\text{HK}}$ between $\sim 10^6$ and 10^8 yr, the choice of adopted age has negligible impact on our analysis. Furthermore, to improve the statistics, we combined the

UCL and LCC groups, which are approximately coeval and whose individual R'_{HK} measurements were similar.

We have decided to not include members of a few nearby stellar groups in our calibration of the activity versus age relation: AB Dor, Her-Lyr, and Castor. Although there are solar-type members of the nearby AB Dor moving group, we do not include its members for the following reasons: (1) its age is controversial (Close et al. 2005; Luhman et al. 2005; Ortega et al. 2007), (2) it is not clear that a clean separation between membership within a supposedly “coeval” AB Dor group (Zuckerman & Song 2004) and the “non-coeval” Pleiades B4 moving group (Asiain et al. 1999; Famaey et al. 2008) has been demonstrated, and (3) the range of acceptable velocities for membership in the AB Dor group seems rather large for a coeval group (Zuckerman & Song 2004) compared to OB associations and clusters (e.g., Briceño et al. 2007). The coevality and evidence for a common origin for members of the Her-Lyr and Castor groups have also not been sufficiently demonstrated for inclusion in a sample of calibration stars.

2.4.2. α Per, Pleiades, and UMa

The α Per members have been confirmed kinematically by Makarov (2006) for all of the cluster candidates except C1 Melotte 20 696 and AP 93. We find that the UCAC2 proper motions for both of these stars are statistically consistent with membership and include them in our α Per sample. For the age of α Per, we adopt the most recent Li depletion boundary value from Barrado y Navascués et al. (2004), 85 Myr.

For the Pleiades, all of the R'_{HK} measurements of candidate members from Duncan et al. (1991), Soderblom et al. (1993), and White et al. (2007) were considered. We independently tested the kinematic membership of each of these stars to the Pleiades using Tycho-2 or UCAC2 proper motions and the group proper motion from Robichon et al. (1999). All of the objects have motions within 2σ of the Pleiades mean motion (although star 571 is a marginal case, but supporting evidence suggests that this is probably a bona fide member). Deacon & Hambly (2004) independently assign high membership probability to the Pleiades for stars 102, 129, 173, 296, 314, 514, 923, 1776, 1015, 1207, and 3097. For the age of the Pleiades, we adopt the recent Li depletion boundary estimate from Barrado y Navascués et al. (2004), 130 Myr.

An extensive study of the age, membership, and activity of the Ursa Major cluster was undertaken by King et al. (2003), and we include their “Y” or “Y?” candidate members in our census for that cluster. Recently, King & Schuler (2005) reevaluated the age of UMa and claimed that the system appears to be approximately

TABLE 5
MEMBERS OF STELLAR AGGREGATES WITH $\log R'_{\text{HK}}$ MEASUREMENTS

Name	Alias	Alias	$B - V$ (mag)	References	$E(B - V)$ (mag)	References	$(B - V)_0$ (mag)	References	$\log R'_{\text{HK}}$ (dex)	N_{obs}	References	Group
TYC 6779-1372-1.....	ScoPMS 5	HD 142361	0.71	1	0.10	2, 11	0.62	2, 11	-4.01	2	22	US
TYC 6793-501-1.....	ScoPMS 60	HD 146516	0.79	2	0.20	2, 12	0.59	2, 11	-4.09	1	22	US
TYC 6215-184-1.....	ScoPMS 214	...	1.24	2	0.30	2, 12	0.82	2, 11	-4.17	1	22	US
TYC 6785-476-1.....	PZ99 J154106.7-265626	...	0.92	3	0.50	13	0.74	11, 13	-3.88	1	22	US
TYC 6208-1543-1.....	PZ99 J160158.2-200811	...	1.10	1	0.30	13	0.68	11, 13	-3.92	1	22	US
2UCAC 22492947.....	PZ99 J161329.3-231106	0.60	12, 13	0.86	11, 13	-4.28	1	22	US
TYC 6793-1406-1.....	PZ99 J161618.0-233947	...	0.64	1	0.40	12, 13	0.74	11, 13	-4.07	1	22	US
TYC 6779-305-1.....	V1149 Sco	HD 143006	0.75	1	0.07	1, 11	0.68	11	-4.05	1	22	US
TYC 6779-305-1.....	V1149 Sco	HD 143006	0.75	1	0.07	1, 11	0.68	11	-4.03	4	23	US
HIP 84586.....	V824 Ara	HD 155555	0.80	1	0.00	14	0.80	1, 14	-3.97	...	24	β Pic
HIP 92680.....	PZ Tel	HD 174429	0.78	1	0.00	14	0.78	1, 14	-3.78	1	25	β Pic
HIP 92680.....	PZ Tel	HD 174429	0.78	1	0.00	14	0.78	1, 14	-3.84	...	26	β Pic
HIP 25486.....	HR 1817	HD 35850	0.55	1	0.00	14	0.55	1, 14	-4.08	...	24	β Pic
HIP 25486.....	HR 1817	HD 35850	0.55	1	0.00	14	0.55	1, 14	-4.22	5	23	β Pic
HIP 25486.....	HR 1817	HD 35850	0.55	1	0.00	14	0.55	1, 14	-4.29	1	22	β Pic
TYC 7310-2431 1.....	MML 52	...	0.97	4	0.05	4	0.62	4, 11	-4.12	2	22	UCL
TYC 7319-749 1.....	MML 58	...	0.88	5	0.14	4	0.81	4, 11	-4.20	2	22	UCL
TYC 7822-158 1.....	MML 63	...	0.87	5	0.23	4	0.80	4, 11	-4.02	1	22	UCL
HIP 76673.....	MML 69	HD 139498	0.75	1	0.09	4	0.68	4, 11	-4.04	1	22	UCL
TYC 7331-782 1.....	MML 70	...	0.95	4	0.15	4	0.82	4, 11	-4.06	1	22	UCL
TYC 7333-1260 1.....	MML 74	HD 143358	0.73	4	0.05	4	0.59	4, 11	-4.04	2	22	UCL
HIP 59764.....	SAO 251810	HD 106506	0.60	1	0.06	15	0.55	1, 15	-3.95	1	25	LCC
HIP 59764.....	SAO 251810	HD 106506	0.60	1	0.06	15	0.55	1, 15	-3.97	...	26	LCC
HIP 66941.....	SAO 252423	HD 119022	0.74	1	0.12	4	0.62	1, 4	-4.03	...	25	LCC
HIP 66941.....	SAO 252423	HD 119022	0.74	1	0.12	4	0.62	1, 4	-4.06	...	26	LCC
HIP 490.....	SAO 214961	HD 105	0.59	1	0.00	14	0.59	1, 14	-4.36	1	25	Tuc
HIP 490.....	SAO 214961	HD 105	0.59	1	0.00	14	0.59	1, 14	-4.41	7	23	Tuc
HIP 1481.....	SAO 248159	HD 1466	0.54	1	0.00	14	0.67	1, 14	-4.36	1	25	Tuc
HIP 105388.....	SAO 246975	HD 202917	0.69	1	0.00	14	0.69	1, 14	-4.06	1	25	Tuc
HIP 105388.....	SAO 246975	HD 202917	0.69	1	0.00	14	0.69	1, 14	-4.09	...	26	Tuc
HIP 105388.....	SAO 246975	HD 202917	0.69	1	0.00	14	0.69	1, 14	-4.22	4	23	Tuc
HIP 116748A.....	DS Tuc A	HD 222259A	0.68	1	0.00	14	0.68	1, 14	-4.00	...	26	Tuc
HIP 116748A.....	DS Tuc A	HD 222259A	0.68	1	0.00	14	0.68	1, 14	-4.09	1	25	Tuc
TYC 3319-306-1.....	CI Melotte 20 350	...	0.69	6	0.10	16	0.60	6, 16	-4.04	1	22	α Per
TYC 3319-306-1.....	CI Melotte 20 350	...	0.69	6	0.10	16	0.60	6, 16	-4.21	1	22	α Per
TYC 3315-1080-1.....	CI Melotte 20 373	...	0.77	7	0.10	16	0.67	7, 16	-4.04	2	22	α Per
TYC 3319-589-1.....	CI Melotte 20 389	...	0.67	8	0.10	16	0.57	8, 16	-4.53	1	22	α Per
TYC 3320-1283-1.....	CI Melotte 20 622	...	0.82	6	0.10	16	0.72	6, 16	-3.78	1	22	α Per
2UCAC 47964793.....	CI Melotte 20 696	...	0.74	6	0.10	16	0.64	6, 16	-4.21	1	22	α Per
TYC 3320-545-1.....	CI Melotte 20 699	...	0.70	8	0.10	16	0.60	8, 16	-4.05	2	22	α Per
TYC 3320-423-1.....	CI Melotte 20 750	...	0.59	6	0.10	16	0.49	6, 16	-4.80	1	22	α Per
TYC 3320-2239-1.....	CI Melotte 20 767	...	0.61	6	0.10	16	0.52	6, 16	-4.62	2	22	α Per
TYC 3320-583-1.....	CI Melotte 20 935	...	0.63	6	0.10	16	0.53	6, 16	-4.16	1	22	α Per
TYC 3321-1655-1.....	CI Melotte 20 1101	...	0.69	7	0.10	16	0.59	6, 16	-4.00	1	22	α Per
TYC 3325-753-1.....	CI Melotte 20 1234	...	0.72	8	0.10	16	0.62	8, 16	-4.53	1	22	α Per
2UCAC 47800056.....	CI* Melotte 20 AP 93	...	0.94	9	0.10	16	0.84	9, 16	-4.05	1	22	α Per
TYC 1799-118-1.....	CI Melotte 22 102	...	0.72	6	0.04	6, 17	0.68	17	-4.45	1	22	Pleiades

TABLE 5—*Continued*

1270

Name	Alias	Alias	$B - V$ (mag)	References	$E(B - V)$ (mag)	References	$(B - V)_0$ (mag)	References	$\log R'_{\text{HK}}$ (dex)	N_{obs}	References	Group
TYC 1799-118-1.....	Cl Melotte 22 102	...	0.72	6	0.04	6, 17	0.68	17	-4.48	1	22	Pleiades
TYC 1799-102-1.....	Cl Melotte 22 120	...	0.71	6	0.04	6, 17	0.67	17	-4.35	1	22	Pleiades
TYC 1799-1268-1.....	Cl Melotte 22 129	...	0.88	6	0.05	6, 17	0.83	17	-4.27	1	27	Pleiades
TYC 1799-1037-1.....	Cl Melotte 22 164	HD 23158	0.49	6	0.03	6, 17	0.46	17	-4.33	2	27	Pleiades
TYC 1803-1351-1.....	Cl Melotte 22 173	...	0.85	6	0.04	6, 17	0.81	17	-4.20	1	22	Pleiades
TYC 1803-8-1.....	Cl Melotte 22 174	...	0.85	6	0.04	6, 17	0.81	17	-3.48	1	22	Pleiades
TYC 1799-1224-1.....	Cl Melotte 22 233	HD 23195	0.53	6	0.03	6, 17	0.49	17	-4.72	2	27	Pleiades
TYC 1803-818-1.....	Cl Melotte 22 250	...	0.69	6	0.05	6, 17	0.64	17	-4.49	1	22	Pleiades
TYC 1799-963-1.....	Cl Melotte 22 296	...	0.84	6	0.04	6, 17	0.80	17	-3.90	1	17	Pleiades
TYC 1803-574-1.....	Cl Melotte 22 314	...	0.66	6	0.04	6, 17	0.61	17	-4.21	1	22	Pleiades
TYC 1803-542-1.....	Cl Melotte 22 405	...	0.54	6	0.04	6, 17	0.49	17	-4.42	3	27	Pleiades
TYC 1803-808-1.....	Cl Melotte 22 489	...	0.63	6	0.10	6, 17	0.53	17	-3.94	2	27	Pleiades
TYC 1803-1061-1.....	Cl Melotte 22 514	...	0.70	6	0.04	6, 17	0.66	17	-4.34	1	22	Pleiades
TYC 1803-1156-1.....	Cl Melotte 22 571	...	0.78	6	0.03	6, 17	0.75	17	-4.40	1	22	Pleiades
GSC 1799-960.....	Cl Melotte 22 625	...	1.17	6	0.36	6, 17	0.82	17	-3.85	1	17	Pleiades
TYC 1799-974-1.....	Cl Melotte 22 708	...	0.61	6	0.03	6, 17	0.58	17	-3.88	2	27	Pleiades
TYC 1803-156-1.....	Cl Melotte 22 727	...	0.55	6	0.03	6, 17	0.52	17	-3.78	4	27	Pleiades
TYC 1803-944-1.....	Cl Melotte 22 739	...	0.62	6	0.04	6, 17	0.59	17	-3.97	1	17	Pleiades
TYC 1799-978-1.....	Cl Melotte 22 745	HD 282969	0.52	6	0.03	6, 17	0.50	17	-4.43	1	27	Pleiades
TYC 1800-1917-1.....	Cl Melotte 22 923	...	0.62	6	0.04	6, 17	0.58	17	-4.23	2	27	Pleiades
TYC 1804-2129-1.....	Cl Melotte 22 996	...	0.65	6	0.04	6, 17	0.60	17	-4.25	3	27	Pleiades
TYC 1804-2366-1.....	Cl Melotte 22 1015	...	0.65	6	0.04	6, 17	0.61	17	-4.55	1	22	Pleiades
TYC 1800-1620-1.....	Cl Melotte 22 1117	...	0.72	6	0.04	6, 17	0.68	17	-4.57	2	27	Pleiades
TYC 1800-1774-1.....	Cl Melotte 22 1182	...	0.64	6	0.04	6, 17	0.60	17	-4.44	1	22	Pleiades
TYC 1800-1627-1.....	Cl Melotte 22 1200	...	0.54	6	0.03	6, 17	0.51	17	-4.68	1	22	Pleiades
TYC 1804-2205-1.....	Cl Melotte 22 1207	...	0.63	6	0.04	6, 17	0.59	17	-4.29	1	27	Pleiades
TYC 1800-1616-1.....	Cl Melotte 22 1215	...	0.64	6	0.04	6, 17	0.60	17	-4.26	1	27	Pleiades
TYC 1800-1683-1.....	Cl Melotte 22 1613	...	0.54	6	0.05	6, 17	0.49	17	-4.42	1	27	Pleiades
TYC 1800-1632-1.....	Cl Melotte 22 1726	HD 23713	0.54	6	0.04	6, 17	0.51	17	-4.44	2	27	Pleiades
TYC 1804-2140-1.....	Cl Melotte 22 1776	HD 282958	0.72	6	0.04	6, 17	0.68	17	-4.07	1	17	Pleiades
TYC 1804-2140-1.....	Cl Melotte 22 1776	...	0.72	6	0.04	6, 17	0.68	17	-4.30	1	22	Pleiades
TYC 1800-1852-1.....	Cl Melotte 22 1797	...	0.56	6	0.04	6, 17	0.52	17	-4.36	1	27	Pleiades
TYC 1800-1716-1.....	Cl Melotte 22 1856	...	0.56	6	0.04	6, 17	0.51	17	-4.39	1	27	Pleiades
2UCAC 40300217.....	Cl Melotte 22 2027	...	0.86	6	0.04	6, 17	0.82	17	-4.71	1	27	Pleiades
2UCAC 39967447.....	Cl Melotte 22 2106	...	0.86	6	0.04	6, 17	0.82	17	-4.19	2	27	Pleiades
2UCAC 39967447.....	Cl Melotte 22 2106	...	0.86	6	0.04	6, 17	0.82	17	-3.94	1	22	Pleiades
2UCAC 39967452.....	Cl Melotte 22 2126	...	0.85	6	0.04	6, 17	0.81	17	-4.14	2	27	Pleiades
2UCAC 39967452.....	Cl Melotte 22 2126	...	0.85	6	0.04	6, 17	0.81	17	-4.16	1	17	Pleiades
TYC 1800-1091-1.....	Cl Melotte 22 2147	...	0.81	6	0.03	6, 17	0.78	17	-4.11	2	27	Pleiades
TYC 1800-1091-1.....	Cl Melotte 22 2147	...	0.81	6	0.03	6, 17	0.78	17	-3.94	1	22	Pleiades
TYC 1804-1179-1.....	Cl Melotte 22 2278	...	0.87	6	0.04	6, 17	0.83	17	-4.19	1	22	Pleiades
TYC 1800-471-1.....	Cl Melotte 22 2506	...	0.60	6	0.05	6, 17	0.55	17	-4.43	1	22	Pleiades
TYC 1804-305-1.....	Cl Melotte 22 2644	...	0.74	6	0.04	18	0.70	6, 18	-4.42	1	22	Pleiades
TYC 1800-1526-1.....	Cl Melotte 22 2786	...	0.61	6	0.04	6, 17	0.56	17	-4.38	1	22	Pleiades
TYC 1804-1400-1.....	Cl Melotte 22 3097	...	0.74	6	0.04	6, 17	0.70	17	-4.23	1	22	Pleiades
TYC 1804-1400-1.....	Cl Melotte 22 3097	...	0.74	6	0.04	6, 17	0.70	17	-4.29	1	22	Pleiades
TYC 1800-1415-1.....	Cl Melotte 22 3179	...	0.57	6	0.03	6, 17	0.53	17	-4.55	1	22	Pleiades
TYC 1813-126-1.....	Cl* Melotte 22 PELS 191	...	0.71	1	0.04	1, 17	0.67	17	-4.38	1	22	Pleiades

TABLE 5—*Continued*

Name	Alias	Alias	$B - V$ (mag)	References	$E(B - V)$ (mag)	References	$(B - V)_0$ (mag)	References	$\log R'_{\text{HK}}$ (dex)	N_{obs}	References	Group
HIP 13806.....	Cl Melotte 25 153	...	0.85	1	0.00	19	0.85	1, 19	-4.38	18	28	Hyades
HIP 14976.....	SAO 56256	HD 19902	0.73	1	0.00	19	0.73	1, 19	-4.57	10	28	Hyades
HIP 14976.....	SAO 56256	HD 19902	0.73	1	0.00	19	0.73	1, 19	-4.60	1	23	Hyades
HIP 15310.....	Cl Melotte 25 2	HD 20439	0.62	1	0.00	19	0.62	1, 19	-4.49	3	27	Hyades
HIP 15310.....	Cl Melotte 25 2	HD 20439	0.62	1	0.00	19	0.62	1, 19	-4.54	13	28	Hyades
HIP 16529.....	Cl Melotte 25 4	...	0.84	1	0.00	19	0.84	1, 19	-4.37	9	28	Hyades
HIP 18327.....	Cl Melotte 25 7	HD 258252	0.90	1	0.00	19	0.90	1, 19	-4.36	8	28	Hyades
HIP 19098.....	Cl Melotte 25 228	HD 285367	0.89	1	0.00	19	0.89	1, 19	-4.39	8	28	Hyades
HIP 19148.....	Cl Melotte 25 10	HD 25825	0.59	1	0.00	19	0.59	1, 19	-4.47	8	28	Hyades
HIP 19148.....	Cl Melotte 25 10	HD 25825	0.59	1	0.00	19	0.59	1, 19	-4.48	13	23	Hyades
HIP 19148.....	Cl Melotte 25 10	HD 25825	0.59	1	0.00	19	0.59	1, 19	-4.57	3	27	Hyades
HIP 19261 B.....	Cl Melotte 25 12	HD 26015B	0.65	1	0.00	19	0.65	1, 19	-4.28	8	28	Hyades
HIP 19781.....	Cl Melotte 25 17	HD 26756	0.69	1	0.00	19	0.69	1, 19	-4.42	21	28	Hyades
HIP 19781.....	Cl Melotte 25 17	HD 26756	0.69	1	0.00	19	0.69	1, 19	-4.47	27	27	Hyades
HIP 19786.....	Cl Melotte 25 18	HD 26767	0.64	1	0.00	19	0.64	1, 19	-4.39	2	27	Hyades
HIP 19786.....	Cl Melotte 25 18	HD 26767	0.64	1	0.00	19	0.64	1, 19	-4.44	15	28	Hyades
HIP 19786.....	Cl Melotte 25 18	HD 26767	0.64	1	0.00	19	0.64	1, 19	-4.48	9	23	Hyades
HIP 19793.....	Cl Melotte 25 15	HD 26736	0.66	1	0.00	19	0.66	1, 19	-4.42	24	27	Hyades
HIP 19793.....	Cl Melotte 25 15	HD 26736	0.66	1	0.00	19	0.66	1, 19	-4.42	17	28	Hyades
HIP 19796.....	Cl Melotte 25 19	HD 26784	0.51	1	0.00	19	0.51	1, 19	-4.49	1	27	Hyades
HIP 19796.....	Cl Melotte 25 19	HD 26784	0.51	1	0.00	19	0.51	1, 19	-4.54	11	28	Hyades
HIP 20130.....	Cl Melotte 25 26	HD 27250	0.74	1	0.00	19	0.74	1, 19	-4.45	8	28	Hyades
HIP 20130.....	Cl Melotte 25 26	HD 27250	0.74	1	0.00	19	0.74	1, 19	-4.47	12	27	Hyades
HIP 20146.....	Cl Melotte 25 27	HD 27282	0.72	1	0.00	19	0.72	1, 19	-4.45	45	27	Hyades
HIP 20146.....	Cl Melotte 25 27	HD 27282	0.72	1	0.00	19	0.72	1, 19	-4.46	9	28	Hyades
HIP 20237.....	Cl Melotte 25 31	HD 27406	0.56	1	0.00	19	0.56	1, 19	-4.45	8	28	Hyades
HIP 20237.....	Cl Melotte 25 31	HD 27406	0.56	1	0.00	19	0.56	1, 19	-4.48	161	27	Hyades
HIP 20480.....	Cl Melotte 25 42	HD 27732	0.76	1	0.00	19	0.76	1, 19	-4.46	8	28	Hyades
HIP 20480.....	Cl Melotte 25 42	HD 27732	0.76	1	0.00	19	0.76	1, 19	-4.48	10	27	Hyades
HIP 20492.....	Cl Melotte 25 46	HD 27771	0.85	1	0.00	19	0.85	1, 19	-4.39	8	28	Hyades
HIP 20492.....	Cl Melotte 25 46	HD 27771	0.85	1	0.00	19	0.85	1, 19	-4.81	1	27	Hyades
HIP 20557.....	Cl Melotte 25 48	HD 27808	0.52	1	0.00	19	0.52	1, 19	-4.50	8	28	Hyades
HIP 20557.....	Cl Melotte 25 48	HD 27808	0.52	1	0.00	19	0.52	1, 19	-4.52	183	27	Hyades
HIP 20577.....	Cl Melotte 25 52	HD 27859	0.60	1	0.00	19	0.60	1, 19	-4.45	102	27	Hyades
HIP 20577.....	Cl Melotte 25 52	HD 27859	0.60	1	0.00	19	0.60	1, 19	-4.47	1	22	Hyades
HIP 20577.....	Cl Melotte 25 52	HD 27859	0.60	1	0.00	19	0.60	1, 19	-4.47	9	28	Hyades
HIP 20741.....	Cl Melotte 25 64	HD 20899	0.66	1	0.00	19	0.66	1, 19	-4.47	9	28	Hyades
HIP 20741.....	Cl Melotte 25 64	HD 28099	0.66	1	0.00	19	0.66	1, 19	-4.50	81	27	Hyades
HIP 20741.....	Cl Melotte 25 64	HD 28099	0.66	1	0.00	19	0.66	1, 19	-4.62	1	22	Hyades
HIP 20815.....	Cl Melotte 25 65	HD 28205	0.54	1	0.00	19	0.54	1, 19	-4.58	8	28	Hyades
HIP 20815.....	Cl Melotte 25 65	HD 28205	0.54	1	0.00	19	0.54	1, 19	-4.60	144	27	Hyades
HIP 20826.....	Cl Melotte 25 66	HD 28237	0.56	1	0.00	19	0.56	1, 19	-4.46	8	28	Hyades
HIP 20826.....	Cl Melotte 25 66	HD 28237	0.56	1	0.00	19	0.56	1, 19	-4.46	2	27	Hyades
HIP 20826.....	Cl Melotte 25 66	HD 28237	0.56	1	0.00	19	0.56	1, 19	-4.48	5	23	Hyades
HIP 20826.....	Cl Melotte 25 66	HD 28237	0.56	1	0.00	19	0.56	1, 19	-4.55	1	22	Hyades
HIP 20850.....	Cl Melotte 25 178	HD 28258	0.84	1	0.00	19	0.84	1, 19	-4.43	9	28	Hyades
HIP 20899.....	Cl Melotte 25 73	HD 28344	0.61	1	0.00	19	0.61	1, 19	-4.44	33	27	Hyades
HIP 20899.....	Cl Melotte 25 73	HD 28344	0.61	1	0.00	19	0.61	1, 19	-4.46	7	23	Hyades

TABLE 5—*Continued*

Name	Alias	Alias	$B - V$ (mag)	References	$E(B - V)$ (mag)	References	$(B - V)_0$ (mag)	References	$\log R'_{\text{HK}}$ (dex)	N_{obs}	References	Group
HIP 20899.....	Cl Melotte 25 73	HD 28344	0.61	1	0.00	19	0.61	1, 19	−4.50	10	28	Hyades
HIP 20899.....	Cl Melotte 25 73	HD 28344	0.61	1	0.00	19	0.61	1, 19	−4.59	1	22	Hyades
HIP 20951.....	Cl Melotte 25 79	HD 285733	0.83	1	0.00	19	0.83	1, 19	−4.44	12	27	Hyades
HIP 20951.....	Cl Melotte 25 79	HD 285733	0.83	1	0.00	19	0.83	1, 19	−4.52	1	22	Hyades
HIP 20951.....	Cl Melotte 25 79	HD 285773	0.83	1	0.00	19	0.83	1, 19	−4.44	9	28	Hyades
HIP 20978.....	Cl Melotte 25 180	HD 28462	0.86	1	0.00	19	0.86	1, 19	−4.27	9	27	Hyades
HIP 20978.....	Cl Melotte 25 180	HD 28462	0.86	1	0.00	19	0.86	1, 19	−4.29	1	22	Hyades
HIP 20978.....	Cl Melotte 25 180	HD 28462	0.86	1	0.00	19	0.86	1, 19	−4.41	7	28	Hyades
HIP 21099.....	Cl Melotte 25 87	HD 28593	0.73	1	0.00	19	0.73	1, 19	−4.46	21	27	Hyades
HIP 21099.....	Cl Melotte 25 87	HD 28593	0.73	1	0.00	19	0.73	1, 19	−4.48	9	28	Hyades
HIP 21112.....	Cl Melotte 25 88	HD 28635	0.54	1	0.00	19	0.54	1, 19	−4.39	1	22	Hyades
HIP 21112.....	Cl Melotte 25 88	HD 28635	0.54	1	0.00	19	0.54	1, 19	−4.56	10	28	Hyades
HIP 21112.....	Cl Melotte 25 88	HD 28635	0.54	1	0.00	19	0.54	1, 19	−4.56	33	27	Hyades
HIP 21317.....	Cl Melotte 25 97	HD 28892	0.63	1	0.00	19	0.63	1, 19	−4.45	8	28	Hyades
HIP 21317.....	Cl Melotte 25 97	HD 28992	0.63	1	0.00	19	0.63	1, 19	−4.48	60	27	Hyades
HIP 21317.....	Cl Melotte 25 97	HD 28992	0.63	1	0.00	19	0.63	1, 19	−4.52	1	22	Hyades
HIP 21637.....	Cl Melotte 25 105	HD 29419	0.58	1	0.00	19	0.58	1, 19	−4.52	8	28	Hyades
HIP 21654.....	Cl Melotte 25 106	HD 29461	0.66	1	0.00	19	0.66	1, 19	−4.55	15	23	Hyades
HIP 21654.....	Cl Melotte 25 106	HD 29461	0.66	1	0.00	19	0.66	1, 19	−4.58	1	22	Hyades
HIP 22203.....	Cl Melotte 25 142	HD 30246	0.67	1	0.00	19	0.66	1, 19	−4.63	1	22	Hyades
HIP 22422.....	Cl Melotte 25 118	HD 30589	0.58	1	0.00	19	0.58	1, 19	−4.75	1	27	Hyades
HIP 22422.....	Cl Melotte 25 118	HD 30589	0.58	1	0.00	19	0.58	1, 19	−4.82	10	28	Hyades
HIP 23069.....	Cl Melotte 25 127	HD 31609	0.74	1	0.00	19	0.74	1, 19	−4.45	7	28	Hyades
HIP 23498.....	Cl Melotte 25 187	HD 32347	0.77	1	0.00	19	0.77	1, 19	−4.44	7	28	Hyades
HIP 23750.....	Cl* Melotte 25 S 140	HD 240648	0.73	1	0.00	19	0.73	1, 19	−4.43	7	28	Hyades
TYC 1265-569-1.....	Cl Melotte 25 49	HD 27835	0.59	6	0.00	19	0.59	6, 19	−4.62	1	22	Hyades
TYC 1265-569-1.....	Cl Melotte 25 49	HD 27835	0.60	1	0.00	19	0.60	1, 19	−4.52	8	28	Hyades
TYC 1265-569-1.....	Cl Melotte 25 49	HD 27835	0.60	1	0.00	19	0.60	1, 19	−4.53	12	27	Hyades
TYC 1266-1012-1.....	Cl Melotte 25 91	HD 28783	0.88	6	0.00	19	0.88	6, 19	−4.47	3	27	Hyades
TYC 1266-1012-1.....	Cl Melotte 25 91	HD 28783	0.88	6	0.00	19	0.88	6, 19	−4.80	1	22	Hyades
TYC 1266-1175-1.....	Cl Melotte 25 99	HD 29159	0.87	6	0.00	19	0.87	6, 19	−4.38	8	28	Hyades
TYC 1266-1175-1.....	Cl Melotte 25 99	HD 29159	0.87	6	0.00	19	0.87	6, 19	−4.40	9	27	Hyades
TYC 1266-1175-1.....	Cl Melotte 25 99	HD 29159	0.87	6	0.00	19	0.87	6, 19	−4.69	1	22	Hyades
TYC 1266-1286-1.....	Cl Melotte 25 92	HD 28805	0.73	1	0.00	19	0.73	1, 19	−4.44	7	28	Hyades
TYC 1266-1286-1.....	Cl Melotte 25 92	HD 28805	0.74	6	0.00	19	0.74	6, 19	−4.45	18	27	Hyades
TYC 1266-1286-1.....	Cl Melotte 25 92	HD 28805	0.74	6	0.00	19	0.74	6, 19	−4.61	1	22	Hyades
TYC 1266-149-1.....	Cl Melotte 25 93	HD 28878	0.89	6	0.00	19	0.89	6, 19	−4.40	8	28	Hyades
TYC 1266-149-1.....	Cl Melotte 25 93	HD 28878	0.89	6	0.00	19	0.89	6, 19	−4.63	1	22	Hyades
HIP 8486.....	GJ 9061B	HD 11131	0.65	1	0.00	14	0.65	1, 14	−4.47	4	25	UMa
HIP 8486.....	GJ 9061B	HD 11131	0.65	1	0.00	14	0.65	1, 14	−4.52	...	29	UMa
HIP 19859.....	HR 1322	HD 26923	0.57	1	0.00	14	0.57	1, 14	−4.55	...	29	UMa
HIP 19859.....	HR 1322	HD 26923	0.57	1	0.00	14	0.57	1, 14	−4.52	...	29	UMa
HIP 21276.....	GJ 3295	HD 28495	0.76	1	0.00	14	0.76	1, 14	−4.34	6	23	UMa
HIP 27072.....	HR 1983	HD 38393	0.48	1	0.00	14	0.48	1, 14	−4.77	3	25	UMa
HIP 27072.....	HR 1983	HD 38393	0.48	1	0.00	14	0.48	1, 14	−4.82	...	29	UMa
HIP 27913.....	HR 2047	HD 39587	0.59	1	0.00	14	0.59	1, 14	−4.46	...	29	UMa
HIP 27913.....	HR 2047	HD 39587	0.59	1	0.00	14	0.59	1, 14	−4.43	...	29	UMa
HIP 36704.....	HR 8883	HD 59747	0.86	1	0.00	14	0.86	1, 14	−4.37	1	23	UMa

TABLE 5—*Continued*

Name	Alias	Alias	$B - V$ (mag)	References	$E(B - V)$ (mag)	References	$(B - V)_0$ (mag)	References	$\log R'_{\text{HK}}$ (dex)	N_{obs}	References	Group
HIP 36704.....	HR 8883	HD 59747	0.86	1	0.00	14	0.86	1, 14	-4.46	...	29	UMa
HIP 42438.....	HR 3391	HD 72905	0.62	1	0.00	14	0.62	1, 14	-4.40	3	23	UMa
HIP 42438.....	HR 3391	HD 72905	0.62	1	0.00	14	0.62	1, 14	-4.48	1	22	UMa
HIP 80686.....	HR 6098	HD 147584	0.56	1	0.00	14	0.56	1, 14	-4.56	1	25	UMa
HIP 80686.....	HR 6098	HD 147584	0.56	1	0.00	14	0.56	1, 14	-4.58	...	29	UMa
HIP 88694.....	HR 6748	HD 165185	0.61	1	0.00	14	0.61	1, 14	-4.54	...	29	UMa
HIP 115312.....	HR 8883	HD 220096	0.82	1	0.00	14	0.82	1, 14	-4.39	1	23	UMa
2UCAC 35931542.....	CI* NGC 2682 SAND 0603	...	0.59	10	0.04	20	0.55	10, 20	-4.74	...	21	M67
2UCAC 35931521.....	CI* NGC 2682 SAND 0621	...	0.66	10	0.04	20	0.62	10, 20	-4.83	...	21	M67
2UCAC 35931673.....	CI* NGC 2682 SAND 0724	0.04	20	0.63	21	-4.86	...	21	M67
2UCAC 35931593.....	CI* NGC 2682 SAND 0746	...	0.71	10	0.04	20	0.67	10, 20	-4.85	...	21	M67
2UCAC 35931670.....	CI* NGC 2682 SAND 0747	...	0.70	10	0.04	20	0.67	10, 20	-4.47	...	21	M67
2UCAC 35931634.....	CI* NGC 2682 SAND 0748	...	0.83	10	0.04	20	0.79	10, 20	-4.75	...	21	M67
2UCAC 35931585.....	CI* NGC 2682 SAND 0753	...	0.63	10	0.04	20	0.59	10, 20	-4.77	...	21	M67
2UCAC 35931642.....	CI* NGC 2682 SAND 0770	...	0.68	10	0.04	20	0.64	10, 20	-4.88	...	21	M67
2UCAC 35931570.....	CI* NGC 2682 SAND 0777	...	0.67	10	0.04	20	0.64	10, 20	-4.82	...	21	M67
2UCAC 35931615.....	CI* NGC 2682 SAND 0779	...	0.69	10	0.04	20	0.65	10, 20	-4.94	...	21	M67
2UCAC 35931637.....	CI* NGC 2682 SAND 0785	...	0.70	10	0.04	20	0.66	10, 20	-4.79	...	21	M67
2UCAC 35931665.....	CI* NGC 2682 SAND 0789	...	0.66	10	0.04	20	0.62	10, 20	-4.82	...	21	M67
2UCAC 35931671.....	CI* NGC 2682 SAND 0801	...	0.72	10	0.04	20	0.68	10, 20	-4.98	...	21	M67
2UCAC 35931641.....	CI* NGC 2682 SAND 0802	...	0.72	10	0.04	20	0.68	10, 20	-4.92	...	21	M67
2UCAC 35931626.....	CI* NGC 2682 SAND 0829	...	0.63	10	0.04	20	0.59	10, 20	-4.88	...	21	M67
2UCAC 35931675.....	CI* NGC 2682 SAND 0937	...	0.59	10	0.04	20	0.55	10, 20	-4.84	...	21	M67
2UCAC 35931686.....	CI* NGC 2682 SAND 0942	...	0.63	10	0.04	20	0.59	10, 20	-4.78	...	21	M67
2UCAC 35931848.....	CI* NGC 2682 SAND 0943	...	0.76	10	0.04	20	0.72	10, 20	-5.08	...	21	M67
2UCAC 35931810.....	CI* NGC 2682 SAND 0945	...	0.67	10	0.04	20	0.63	10, 20	-4.83	...	21	M67
2UCAC 35931701.....	CI* NGC 2682 SAND 0951	...	0.72	10	0.04	20	0.68	10, 20	-4.94	...	21	M67
2UCAC 35931726.....	CI* NGC 2682 SAND 0958	0.04	20	0.62	21	-4.82	...	21	M67
2UCAC 35931749.....	CI* NGC 2682 SAND 0963	...	0.71	10	0.04	20	0.67	10, 20	-5.05	...	21	M67
2UCAC 35931815.....	CI* NGC 2682 SAND 0965	...	0.76	10	0.04	20	0.72	10, 20	-4.83	...	21	M67
2UCAC 35931793.....	CI* NGC 2682 SAND 0969	...	0.67	10	0.04	20	0.63	10, 20	-4.83	...	21	M67
GSC 814-1735.....	CI* NGC 2682 SAND 0981	...	0.71	10	0.04	20	0.67	10, 20	-5.00	...	21	M67
2UCAC 35931819.....	CI* NGC 2682 SAND 0982	...	0.61	10	0.04	20	0.57	10, 20	-4.66	...	21	M67
2UCAC 35931700.....	CI* NGC 2682 SAND 0991	...	0.68	10	0.04	20	0.65	10, 20	-4.96	...	21	M67
2UCAC 35931814.....	CI* NGC 2682 SAND 1004	...	0.76	10	0.04	20	0.72	10, 20	-4.86	...	21	M67
2UCAC 35931816.....	CI* NGC 2682 SAND 1012	...	0.74	10	0.04	20	0.70	10, 20	-4.80	...	21	M67
2UCAC 35931821.....	CI* NGC 2682 SAND 1014	...	0.71	10	0.04	20	0.67	10, 20	-4.72	...	21	M67
2UCAC 35931731.....	CI* NGC 2682 SAND 1033	...	0.61	10	0.04	20	0.57	10, 20	-4.74	...	21	M67
2UCAC 35931828.....	CI* NGC 2682 SAND 1041	...	0.73	10	0.04	20	0.69	10, 20	-4.93	...	21	M67
2UCAC 35931843.....	CI* NGC 2682 SAND 1048	...	0.69	10	0.04	20	0.65	10, 20	-4.92	...	21	M67
GSC 814-1295.....	CI* NGC 2682 SAND 1050	...	0.66	10	0.04	20	0.62	10, 20	-4.38	...	21	M67
2UCAC 35931775.....	CI* NGC 2682 SAND 1057	...	0.68	10	0.04	20	0.64	10, 20	-4.82	...	21	M67
GSC 814-1233.....	CI* NGC 2682 SAND 1064	...	0.66	10	0.04	20	0.62	10, 20	-4.94	...	21	M67
GSC 814-1221.....	CI* NGC 2682 SAND 1065	...	0.80	10	0.04	20	0.76	10, 20	-4.85	...	21	M67
2UCAC 35931734.....	CI* NGC 2682 SAND 1068	...	0.75	10	0.04	20	0.71	10, 20	-4.87	...	21	M67
2UCAC 35931840.....	CI* NGC 2682 SAND 1078	...	0.66	10	0.04	20	0.62	10, 20	-4.88	...	21	M67
2UCAC 35931804.....	CI* NGC 2682 SAND 1087	...	0.64	10	0.04	20	0.60	10, 20	-4.82	...	21	M67
2UCAC 35931713.....	CI* NGC 2682 SAND 1089	...	0.67	10	0.04	20	0.63	10, 20	-4.98	...	21	M67

TABLE 5—*Continued*

Name	Alias	Alias	$B - V$ (mag)	References	$E(B - V)$ (mag)	References	$(B - V)_0$ (mag)	References	$\log R'_{\text{HK}}$ (dex)	N_{obs}	References	Group
2UCAC 35931762.....	CI* NGC 2682 SAND 1093	...	0.64	10	0.04	20	0.60	10, 20	-4.78	...	21	M67
2UCAC 35931696.....	CI* NGC 2682 SAND 1095	...	0.65	10	0.04	20	0.61	10, 20	-4.92	...	21	M67
2UCAC 35931717.....	CI* NGC 2682 SAND 1096	...	0.66	10	0.04	20	0.62	10, 20	-4.88	...	21	M67
2UCAC 35931684.....	CI* NGC 2682 SAND 1106	...	0.69	10	0.04	20	0.65	10, 20	-5.06	...	21	M67
GSC 814-1789.....	CI* NGC 2682 SAND 1107	...	0.64	10	0.04	20	0.60	10, 20	-4.62	...	21	M67
2UCAC 35931906.....	CI* NGC 2682 SAND 1203	...	0.71	10	0.04	20	0.68	10, 20	-4.82	...	21	M67
2UCAC 35931884.....	CI* NGC 2682 SAND 1208	0.04	20	0.79	21	-4.84	...	21	M67
2UCAC 35931970.....	CI* NGC 2682 SAND 1212	...	0.78	10	0.04	20	0.74	10, 20	-4.86	...	21	M67
2UCAC 35931925.....	CI* NGC 2682 SAND 1213	...	0.60	10	0.04	20	0.56	10, 20	-4.81	...	21	M67
2UCAC 35931900.....	CI* NGC 2682 SAND 1218	...	0.68	10	0.04	20	0.65	10, 20	-4.88	...	21	M67
2UCAC 35931880.....	CI* NGC 2682 SAND 1246	...	0.69	10	0.04	20	0.65	10, 20	-4.93	...	21	M67
2UCAC 35931918.....	CI* NGC 2682 SAND 1247	...	0.62	10	0.04	20	0.58	10, 20	-4.70	...	21	M67
2UCAC 35931894.....	CI* NGC 2682 SAND 1248	...	0.62	10	0.04	20	0.58	10, 20	-4.78	...	21	M67
2UCAC 35931973.....	CI* NGC 2682 SAND 1249	...	0.78	10	0.04	20	0.74	10, 20	-4.91	...	21	M67
2UCAC 35931980.....	CI* NGC 2682 SAND 1251	...	0.75	10	0.04	20	0.71	10, 20	-4.80	...	21	M67
2UCAC 35931939.....	CI* NGC 2682 SAND 1252	...	0.64	10	0.04	20	0.60	10, 20	-4.81	...	21	M67
2UCAC 35931911.....	CI* NGC 2682 SAND 1255	...	0.67	10	0.04	20	0.63	10, 20	-4.80	...	21	M67
GSC 814-1973.....	CI* NGC 2682 SAND 1258	0.04	20	0.61	21	-4.92	...	21	M67
GSC 814-1679.....	CI* NGC 2682 SAND 1260	...	0.62	10	0.04	20	0.59	10, 20	-4.79	...	21	M67
2UCAC 35931940.....	CI* NGC 2682 SAND 1269	...	0.76	10	0.04	20	0.72	10, 20	-4.99	...	21	M67
2UCAC 35931858.....	CI* NGC 2682 SAND 1278	...	0.78	10	0.04	20	0.74	10, 20	-5.00	...	21	M67
2UCAC 35931865.....	CI* NGC 2682 SAND 1289	...	0.76	10	0.04	20	0.72	10, 20	-5.03	...	21	M67
2UCAC 35931886.....	CI* NGC 2682 SAND 1307	...	0.81	10	0.04	20	0.77	10, 20	-5.05	...	21	M67
2UCAC 35931913.....	CI* NGC 2682 SAND 1318	...	0.62	10	0.04	20	0.58	10, 20	-4.64	...	21	M67
2UCAC 35931949.....	CI* NGC 2682 SAND 1330	...	0.66	10	0.04	20	0.62	10, 20	-4.62	...	21	M67
2UCAC 36114630.....	CI* NGC 2682 SAND 1341	...	0.74	10	0.04	20	0.71	10, 20	-4.72	...	21	M67
2UCAC 35932025.....	CI* NGC 2682 SAND 1406	...	0.55	10	0.04	20	0.51	10, 20	-4.75	...	21	M67
GSC 814-2433.....	CI* NGC 2682 SAND 1420	...	0.63	10	0.04	20	0.59	10, 20	-4.75	...	21	M67
2UCAC 35932087.....	CI* NGC 2682 SAND 1426	...	0.62	10	0.04	20	0.58	10, 20	-4.80	...	21	M67
2UCAC 35932080.....	CI* NGC 2682 SAND 1446	...	0.61	10	0.04	20	0.58	10, 20	-4.76	...	21	M67
2UCAC 35932033.....	CI* NGC 2682 SAND 1449	...	0.66	10	0.04	20	0.62	10, 20	-4.85	...	21	M67
2UCAC 35932057.....	CI* NGC 2682 SAND 1452	...	0.67	10	0.04	20	0.63	10, 20	-4.35	...	21	M67
2UCAC 35932039.....	CI* NGC 2682 SAND 1462	...	0.67	10	0.04	20	0.64	10, 20	-4.89	...	21	M67
2UCAC 35932031.....	CI* NGC 2682 SAND 1473	...	0.78	10	0.04	20	0.74	10, 20	-5.13	...	21	M67
2UCAC 35932013.....	CI* NGC 2682 SAND 1477	...	0.72	10	0.04	20	0.68	10, 20	-4.98	...	21	M67

REFERENCES.—(1) Perryman et al. 1997; (2) Walter et al. 1994; (3) Høg et al. 2000 (converted to Johnson using Mamajek et al. 2006); (4) Mamajek et al. 2002; (5) Wichmann et al. 1997; (6) Mermilliod 1991; (7) Stauffer et al. 1989; (8) Prosser 1992; (9) Messina 2001; (10) Montgomery et al. 1993; (11) unreddened $B - V$ color appropriate for spectral type given by other reference; (12) I have assumed $A_V/E(B - V) = 3.1$ in converting an A_V value to $E(B - V)$; (13) Preibisch & Zinnecker 1999; (14) star is within 75 pc and presumed to have no reddening; (15) Nordström et al. 2004; (16) Crawford & Barnes 1974; (17) Soderblom et al. 1993; (18) Stauffer & Hartmann 1987; (19) Taylor 2006; (20) VandenBerg & Stetson 2004; (21) Giampapa et al. 2006; (22) White et al. 2007; (23) Wright et al. 2004; (24) Gray et al. 2006; (25) Henry et al. 1996; (26) Soderblom et al. 1998; (27) Duncan et al. 1991, converted to $\log R'_{\text{HK}}$ following Noyes et al. 1984; (28) Paulson et al. 2002; (29) Gray et al. 2003.

TABLE 6
CLUSTER $\log R'_{\text{HK}}$ VALUES

Group Name (1)	Age (Myr) (2)	References (3)	$\log R'_{\text{HK}}$ Median (4)	68% CL (5)	N (6)	Activity-Color Slope m (7)	$\overline{\log R'_{\text{HK}}} (B - V)_{\odot}$ (8)
USco.....	5	1, 2, 3	-4.05 ± 0.03	0.13	9	-0.73 ± 0.62	-4.01
β Pic.....	12	4, 5	-4.03 ± 0.13	0.23	6	1.40 ± 0.30	-4.06
UCL+LCC.....	16	6, 7	-4.04 ± 0.01	0.07	10	-0.37 ± 0.27	-4.04
Tuc-Hor.....	30	6, 7, 8	-4.16 ± 0.13	0.16	8	3.02 ± 0.45	-4.23
α Per.....	85	9, 10, 11	-4.16 ± 0.08	0.27	13	2.04 ± 1.52	-4.16
Pleiades.....	130	9, 11, 12	-4.33 ± 0.04	0.24	56	0.75 ± 0.24	-4.27
UMa.....	500	13	-4.48 ± 0.03	0.09	17	0.80 ± 0.27	-4.50
Hyades.....	625	11, 14	-4.47 ± 0.01	0.09	87	0.14 ± 0.13	-4.50
M67.....	4000	15, 16	-4.84 ± 0.01	0.11	76	-1.03 ± 0.23	-4.85

NOTES.—Col. (1): Name of group. Col. (2): Age. Col. (3): Age and membership references. Col. (4): $\log R'_{\text{HK}}$ median and uncertainty (Gott et al. 2001). Col. (5): 68% confidence intervals on $\log R'_{\text{HK}}$. Col. (6): Number of data points per bin. Col. (7): OLS bisector slope $m = \Delta \log R'_{\text{HK}} / \Delta B - V$ and uncertainty. Col. (8): Mean $\log R'_{\text{HK}}$ interpolated at solar $(B - V)_{\odot}$. OLS $(Y|X)$ slopes and uncertainties were calculated using 10^4 jackknife sampling simulations, except for β Pic and Tuc-Hor, where the slope was analytically calculated, due to their small sample size. Estimation of the solar $\log R'_{\text{HK}}$ value is discussed in § 1.

REFERENCES.—(1) Preibisch et al. 2002; (2) Preibisch & Zinnecker 1999; (3) Walter et al. 1994; (4) Ortega et al. 2002; (5) Zuckerman & Song 2004; (6) Mamajek et al. 2002; (7) de Zeeuw et al. 1999; (8) Mamajek et al. 2004; (9) Barrado y Navascués et al. 2004; (10) Makarov 2006; (11) this work (§ 2.2); (12) Duncan et al. 1991; (13) King et al. 2003; (14) Perryman et al. 1998; (15) VandenBerg & Stetson 2004; (16) Giampapa et al. 2006, selected from Girard et al. 1989.

coeval with the Hyades and Coma Ber clusters (all ~ 0.6 Gyr), but “with the Hyades perhaps being only 100 Myr older.” This assessment is apparent in visual inspection of Figure 2 of King & Schuler (2005) of the MS turnoffs with overlaid evolutionary tracks appropriate for the metallicities of UMa and the Hyades. Based on this, we adopt the age of UMa from King et al. (2003), 500 Myr.

2.4.3. Hyades

The Hyades is the best studied cluster in terms of its chromospheric activity. Our primary source of membership assignment and age (625 Myr) for the Hyades is Perryman et al. (1998), adopting their members constrained by both proper motions and RVs. Additional non-*Hipparcos* Hyades candidates were gleaned from the $\log R'_{\text{HK}}$ surveys of Duncan et al. (1991), Paulson et al. (2002), and White et al. (2007), including CI Melotte 25 49, 91, 92, 93, 99, and 183 and CI Melotte 25 VA 115, 146, 354, 383, 502, and 637. Tycho-2 and UCAC2 proper motions for these stars were tested for Hyades membership using the de Bruijne et al. (2001) convergent point, and all of these candidates are kinematically consistent with Hyades membership with moving cluster distances of ~ 44 –52 pc.

Among the $\log R'_{\text{HK}}$ data for Hyades members were a handful of remarkably active and inactive stars. Further investigation of these objects was warranted to see whether we should include them in our sample statistics (critical for establishing what the spread in plausible activity levels is for stars of a given age). To see if the extreme outliers might be dominated by “supercluster” members or interlopers that might be unrelated to the Hyades nucleus, we plotted moving cluster distance versus $\log R'_{\text{HK}}$ and membership probability versus $\log R'_{\text{HK}}$ in Figure 1. The moving cluster distances and probabilities were calculated following Mamajek (2005) using the de Bruijne et al. (2001) convergent point solution with *Hipparcos*, Tycho-2, or UCAC2 proper motions (in order of preference). An intrinsic velocity dispersion of 1 km s^{-1} was assumed in the membership probability estimation, with relative ranking seen as more important than absolute values.

A few things are apparent from Figure 1. The $\log R'_{\text{HK}}$ values for the high membership probability stars in the Hyades ($P > 75\%$)

are consistent with a median value of $\log R'_{\text{HK}} = -4.47$ and remarkably small rms of 0.08 dex.⁸ The lower membership probability objects ($P < 75\%$) have a lower median $\log R'_{\text{HK}}$ (-4.51) and higher rms (0.14 dex). We attribute this to the likely inclusion in the current list of Hyades candidates of older field interlopers. It

⁸ Our literature search for Hyades activity measurements yielded three extremely active outliers that are excluded in our analysis: CI Melotte 25 76, 105, and 127. Coincidentally, the $\log R'_{\text{HK}}$ values for all three stars were estimated from single observations by the Mount Wilson survey that all took place 1977 July 22. All three were also observed by Paulson et al. (2002), and their $\log R'_{\text{HK}}$ values for these stars are more in line with other Hyades ($\log R'_{\text{HK}} = -4.47$, -4.52 , and -4.45 , for stars 76, 105, and 127, respectively). The idea that three stars in the Hyades could be flaring simultaneously on the same night at unprecedentedly high levels is extremely unlikely, so we exclude these Mount Wilson observations from our statistics.

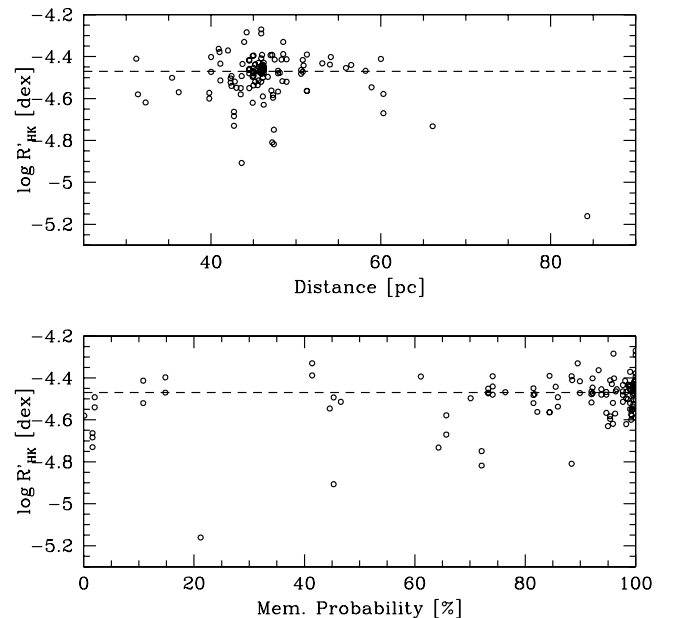


FIG. 1.—Top: Moving cluster distance vs. $\log R'_{\text{HK}}$ for candidate Hyades members. Bottom: Membership probability vs. $\log R'_{\text{HK}}$ for candidate Hyades members.

TABLE 7
log R'_{HK} DATA FOR ANCILLARY SAMPLES

Cluster Name (1)	Age (Myr) (2)	Age References (3)	Original log R'_{HK} (4)	Corrected log R'_{HK} (5)	log R'_{HK} References (6)
M34.....	200	1	−4.4:	...	7
Coma Ber.....	600	2	−4.51	−4.43	8
NGC 752.....	2000	3	−4.70	−4.70	8
M67.....	4000	4, 5	−4.82	−4.86	8
NGC 188.....	6900	4, 5	−4.98	−5.08	8
Old field.....	8000	6	−4.99	...	6

NOTES.—Col. (1): Name of group. Col. (2): Age. Col. (3): Age reference. Col. (4): Originally quoted mean log R'_{HK} value. Col. (5): Corrected mean log R'_{HK} value (only relevant for reference 8). Col. (6): Activity references.

REFERENCES.—(1) Jones et al. 1997; (2) King & Schuler 2005; (3) Dinescu et al. 1995; (4) Sarajedini et al. 1999; (5) VandenBerg & Stetson 2004; (6) this study (§ 2.4.6); (7) visual inspection of Fig. 1 of King et al. 2003; (8) data from Barry 1988, corrected following Soderblom et al. 1991.

is apparent that the stars at $d < 40$ pc and $d > 60$ pc tend to be less frequently active, probably due to inclusion of interlopers.

In summary, for our activity study, we conservatively include only those Hyades stars with membership probabilities $>50\%$ and cluster parallax distances within 1 tidal radius (± 10 pc) of the mean distance (46.3 pc; Perryman et al. 1998).⁹

2.4.4. M67

We adopt an age of 4.0 Gyr for the M67 cluster from Sarajedini et al. (1999) and VandenBerg & Stetson (2004) and include the M67 membership and HK observations of Giampapa et al. (2006) in our analysis. The log R'_{HK} values listed in Table 5 were converted from the HK emission equivalent widths by M. Giampapa (2008, private communication). The candidate RS CVn Sanders 1112 is listed in Table 5 but was excluded from the analysis (with log $R'_{\text{HK}} = -4.11$).

2.4.5. Ancillary Cluster Data

We believe that the cluster membership assignments in Table 5 are quite reliable. Any interlopers among the samples that we may not have caught are small in number and will have negligible impact on our findings. The ages reflect modern astrophysical understanding and are systematically older than those used in previous age–log R'_{HK} calibrations.

Notably the current sample is sparsely populated at ages of >1 Gyr. The historical lack of >1 Gyr old clusters in the age–activity calibration is due to the deficiency of nearby (<100 – 200 pc) older clusters with solar-type members bright enough for observations with the Mount Wilson photometer.

To overcome this shortcoming, Barry and collaborators determined Mount Wilson S -values with a lower resolution system

(Barry et al. 1987; Barry 1988). Soderblom et al. (1991) argued that the Barry et al. (1987) S -values were not on the Mount Wilson system, but that a linear correction could remedy this. While Soderblom’s correction is not well constrained at the high- or low-activity regimes, we nonetheless use it to correct cluster mean log R'_{HK} values from Barry et al. (1987) to log R'_{HK} values on the Mount Wilson system. These ancillary cluster age–activity data are compiled in Table 7. We omit a datum for the ~ 3 Myr old cluster NGC 2264 for two reasons: (1) the Soderblom et al. (1991) correction for the Barry et al. (1987) data does not extend to activity levels this high, and (2) the extrapolated mean log R'_{HK} value for NGC 2264 (-4.26) is ~ 0.2 dex lower than the mean values for the similarly aged Upper Sco, UCL, LCC, and β Pic groups.¹⁰ The Barry et al. (1987) data are nominally corrected to a standard color of $(B - V)_0 = 0.60$ mag; however, for our purposes the differences are negligible. As a check on the Soderblom et al. (1991) conversion, we find a nearly identical median log R'_{HK} value at solar color for the M67 sample (-4.86) as found in the high-resolution HK study of Giampapa et al. (2006) (-4.85).

There is a clear need for more modern derivation of log R'_{HK} activity diagnostics in fiducial older clusters such as M34, Coma Ber, NGC 752, and NGC 188. Recent studies of H and K emission in such members of older clusters (e.g., Pace & Pasquini 2004) did not provide log R'_{HK} values, only emission-line fluxes. Attempts by the authors and D. Soderblom (2008, private communication) to tie these observations to the Mount Wilson system have thus far failed.

2.4.6. Field Stars with Precise Isochronal Ages

To further augment the activity data for old stellar samples, we consider an additional sample of solar-type field dwarfs with well-constrained isochronal ages. Valenti & Fischer (2005, hereafter VF05) report spectroscopic properties and isochronal age estimates for 1040 solar-type field dwarfs in the Keck, Lick, and AAT planet search samples (the “SPOCs” sample). After estimating accurate temperatures, luminosities, metallicities, and α -element enhancements, VF05 interpolate isochronal ages for each star on the Yonsei-Yale evolutionary tracks (Yi et al. 2003). From their sample of 1040 solar-type stars (which includes some evolved stars), VF05 were able to constrain isochronal ages for 57 stars (5.5%) to better than 20% in both their positive and negative age uncertainties. As our activity relation is currently poorly constrained at the old ages (given the lack of suitable cluster samples),

⁹ Due to the distance constraint, we reject from our sample HIP 10672, HIP 13600, HIP 13976, HIP 15563, HIP 15720, HIP 17766, HIP 19386, HIP 19441, HIP 20949, HIP 21741, HIP 22566, HIP 24923, and HIP 25639. Due to low membership probability, we reject from our sample HIP 15304, HIP 17609, HIP 19082, HIP 19834, HIP 20082, HIP 20719, HIP 21280, and HIP 22380. Some stars failed both the distance and the membership criteria: HIP 19386 and HIP 20441. Some, and possibly even most, of the rejected stars in the first two lists may be bona fide Hyades members, although the stars in the last list are almost certainly nonmembers. Our goal is to create as clean a sample of Hyades members as possible for the study of their activity, hence our stringent membership criteria. We do not necessarily recommend rejecting these stars from future studies of the Hyades. Our selection criterion clips the two most inactive Hyades candidates studied by Paulson et al. (2002): HIP 25639 (log $R'_{\text{HK}} = -5.38$, $d = 86$ pc) and HIP 19386 (log $R'_{\text{HK}} = -5.16$, $d = 84$ pc). The least active Hyades star that satisfies our membership and color criteria is HIP 22422 (log $R'_{\text{HK}} = -4.82$; Paulson et al. 2002), while the most active is HIP 20978 (log $R'_{\text{HK}} = -4.27$; Duncan et al. 1991).

¹⁰ Notably, the form of the Donahue (1993) relation at high activity levels is driven largely by the NGC 2264 datum.

TABLE 8

OLD SOLAR-TYPE DWARFS FROM VF05 WITH AGE UNCERTAINTIES OF $<20\%$

HD (1)	$B - V$ (mag) (2)	τ (Gyr) (3)	$\log R'_{\text{HK}}$ (dex) (4)	References (5)	ΔM_V (mag) (6)
3823.....	0.564	6.7	-4.97	1	-0.37
20794.....	0.711	13.5	-4.98	2	+0.18
22879.....	0.554	13.9	-4.92	3	+0.58
32923.....	0.657	9.0	-5.15	4	-0.93
34297.....	0.652	13.4	-4.93	2	-0.30
36108.....	0.590	7.1	-5.01	1	-0.37
38283.....	0.584	5.7	-4.97	2	-0.56
45289.....	0.673	7.6	-5.01	2	-0.49
51929.....	0.585	12.4	-4.86	2	+0.14
95128.....	0.624	5.0	-5.02	4	-0.34
122862.....	0.581	5.9	-4.99	1	-0.61
142373.....	0.563	7.7	-5.11	3	-0.63
143761.....	0.612	8.7	-5.04	5	-0.37
153075.....	0.581	11.2	-4.88	2	+0.15
157214.....	0.619	11.6	-5.00	4	-0.01
186408.....	0.643	5.8	-5.05	4	-0.43
186427.....	0.661	8.0	-5.04	4	-0.26
190248.....	0.751	6.2	-5.00	2	-0.78
191408.....	0.868	15.0	-4.99	2	+0.39
193307.....	0.549	5.7	-4.90	2	-0.43
196378.....	0.544	5.3	-4.95	1	-0.91
201891.....	0.525	14.5	-4.86	3	+0.65
210918.....	0.648	8.5	-4.95	2	-0.27

NOTES.—Col. (1): HD name. Col. (2): $B - V$ color from Perryman et al. (1997). Col. (3): Isochronal age (VF05; uncertainties $<20\%$). Col. (4): Chromospheric activity $\log R'_{\text{HK}}$. Col. (5): Activity reference. Col. (6): Difference between stellar absolute magnitude and that for an MS star of the same $B - V$ color.

REFERENCES.—(1) Jenkins et al. 2006; (2) Henry et al. 1996; (3) Wright et al. 2004; (4) Hall et al. 2007; (5) Baliunas et al. 1996.

we include VF05 solar-type dwarfs within 1 mag of the MS and isochronal ages of 5–15 Gyr. The stars in this sample that have published $\log R'_{\text{HK}}$ data are listed in Table 8. As the sample is sparse ($N = 23$), to put it on equal footing with the cluster samples, we simply treat it as a single “cluster” with median age 8.0 ± 0.7 (± 3.9 ; 68% CL) Gyr or $\log \tau = 9.90 \pm 0.04$ (± 0.19 ; 68% CL) dex. The mean activity for the sample is $\log R'_{\text{HK}} = -4.99 \pm 0.02$ dex (± 0.07 ; 68% CL). The mean color for the sample is similar to that of the Sun: $\overline{B - V} \simeq 0.62$ mag.

3. Ca II H AND K ANALYSIS

With established membership lists and assembled R'_{HK} values deriving from a few large, homogeneous spectroscopic surveys, we proceed in this section to derive a modern activity-age relationship. We first consider various second parameter effects, e.g., color/temperature/mass, surface gravity, and composition. We investigate color dependencies by examining the R'_{HK} diagnostic for binary pairs having the same age/composition but substantial temperature differences (§ 3.1.1) and then for kinematic groups sampling a range of masses at different ages (§ 3.1.2). We proceed in § 3.2 to derive a preliminary empirical activity-age relation based on cluster and solar $\log R'_{\text{HK}}$ data.

3.1. Systematics in R'_{HK}

There is some evidence that R'_{HK} varies systematically not only as a function of age, but at a given age with stellar color (i.e., mass). Specifically, while Soderblom et al. (1991) found a flat $\log R'_{\text{HK}}$ versus $(B - V)_0$ relation for halo stars, they found a significant positive slope for members of the Hyades cluster

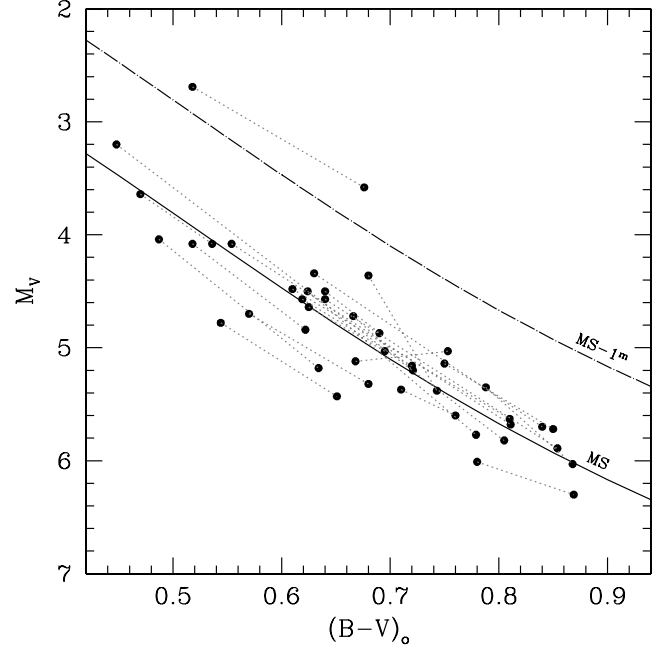


FIG. 2.—Color vs. absolute magnitude for 23 nonidentical [$(\Delta(B - V)) \geq 0.05$] stellar binaries (see § 3.1.1). Thin short-dashed lines connect the stellar binary components (filled circles). The solid line is the MS from Wright (2005), and the dot-dashed line is 1 mag brighter than the MS (approximately segregating post-MS stars from MS stars). The system above the “MS minus 1 mag” line (HD 5208) was retained as its color-magnitude slope was consistent with being a system of two MS stars. As the system has roughly solar metallicity (Marsakov & Shevlev 1995), it is possible that its *Hipparcos* parallax is significantly in error.

[$m = \Delta \log R'_{\text{HK}} / \Delta(B - V) = 0.391$]. Elsewhere in the literature, it appears that the color dependence of $\log R'_{\text{HK}}$ is largely ignored.

Spectral dependencies of R'_{HK} could systematically impact our calibration of R'_{HK} as an age estimator, if the distribution of colors differs among the different associations and clusters in our sample. To test whether the activity-age relation may be mass dependent, we study both binary pairs and kinematic groups, presuming in the respective samples that the components have the same age but different masses, and look for trends in R'_{HK} with color.

3.1.1. Trends among Binary Pairs

We plot in Figure 2 color versus absolute magnitude for the field binaries from Table 2 with significant color difference ($\Delta(B - V) > 0.05$ mag). The reddening toward these stars is small, according to their spectral types and $B - V$ colors, as well as their proximity to the Sun (most are within <75 pc and likely have negligible reddening). As can be seen, the pairs are generally aligned with the MS, although it is apparent that the systems have a modest range in metallicities that slide their individual MSs above and below the mean field MS.

In Figure 3 we show R'_{HK} as a function of color for the 24 pairs. Interstellar reddening, which should be negligible, should affect both components equally and therefore should not influence measurements of the activity-color mean slope. There is a range of slopes [$m = \Delta \log R'_{\text{HK}} / \Delta(B - V)$] characterizing the sample, with some negative and some positive. A statistical analysis of the individual slopes shows that one system is statistically deviant (HD 137763;¹¹ rejected by Chauvenet’s criterion; Bevington &

¹¹ HD 137763 appears to be a true pathology. While the B component HD 137778 is clearly an active K2 V dwarf, the A component is an inactive spectroscopic binary with the highest measured eccentricity ever reported ($e = 0.975$; Pourbaix et al. 2004). The spectroscopic companion Ab is likely applying torques to the primary (Duquenoey et al. 1992), altering its rotational evolution.

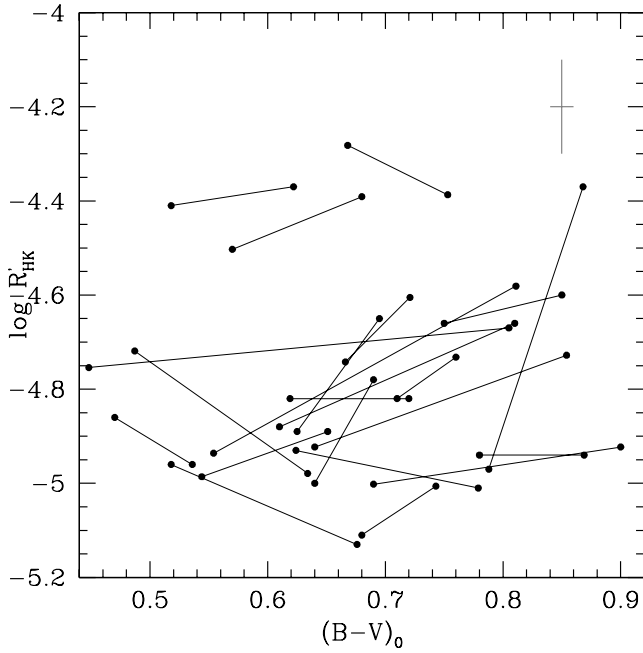


FIG. 3.—Color vs. activity for 23 nonidentical [$\Delta(B - V) \geq 0.05$] stellar binaries (see § 3.1.1). A typical error bar for $(B - V)$ colors (± 0.01 mag) and for a single $\log R'_{\text{HK}}$ observation (± 0.1 dex) is illustrated by the cross. The pair on the right side with the large slope is the pathological binary HD 137763.

Robinson 1992) and that the mean slope is $\bar{m} = 0.51 \pm 0.29$. The true median of the slope is $\tilde{m} = 0.60^{+0.34}_{-0.27}$ (Gott et al. 2001).

While the binary data alone are within $\sim 2\sigma$ of zero slope in $\Delta \log R'_{\text{HK}} / \Delta(B - V)$, there is some hint that the slope is indeed slightly positive. Donahue (1998) made a plot similar to Figure 3 (indeed, using many of the same systems) but did not explicitly state any conclusions regarding the existence of a color trend. As noted above, there is likely a range of ages represented by these binary pairs; we investigate now whether the observed variation in slope of R'_{HK} with color can be correlated with stellar age.

3.1.2. Trends among Stellar Kinematic Groups

In Figure 4 we plot $\log R'_{\text{HK}}$ versus $B - V$ color for the separate kinematically defined groups in our study. From 10^4 jackknife sampling simulations, the slopes [$m = \Delta \log R'_{\text{HK}} / \Delta(B - V)$] for each group were evaluated using ordinary least-squares linear regression with $\log R'_{\text{HK}}$ as the dependent variable and $(B - V)_0$ as the independent variable [OLS($Y|X$); Isobe et al. 1990]. These slopes, along with the median $\log R'_{\text{HK}}$ values, are provided in Table 5.

Examination of Table 5 shows that divining a unique slope applicable to all solar-type stars at all activity levels is not feasible. The <100 Myr old groups show a wide range of slopes ($-1 < m < 3$) with typically large uncertainties, but a mean slope for the ensemble of $m = 0.91 \pm 0.40$. The ~ 0.1 – 0.5 Gyr Pleiades and UMa clusters show similarly steep slopes of 0.75 ± 0.24 and 0.80 ± 0.27 , respectively. These values are $\sim 2\sigma$ steeper than the slope for the ~ 0.6 Gyr Hyades (0.14 ± 0.13). The oldest cluster (M67) also has the most negative slope (-1.0 ± 0.2). Together, the data suggest that the slope $\Delta \log R'_{\text{HK}} / \Delta(B - V)$ may flatten as a function of age. The mean slope for all of the clusters combined is $m = 0.37 \pm 0.14$, essentially identical to the Hyades slope ($m = 0.39$) found by Soderblom (1985). However, our Hyades slope appears to be flatter than that derived by Soderblom (1985) due to inclusion of additional lower activity stars at the

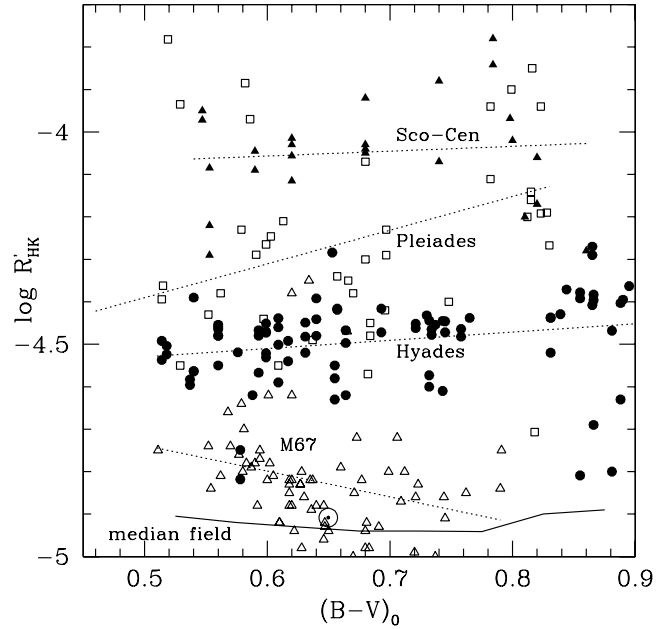


FIG. 4.— $(B - V)_0$ vs. $\log R'_{\text{HK}}$ for members of several stellar clusters in Table 5. Filled triangles are ~ 5 – 16 Myr Sco-Cen members (including Upper Sco, β Pic, UCL, LCC), open squares are ~ 130 Myr old Pleiades stars, filled circles are ~ 625 Myr old Hyades stars, and open triangles are ~ 4 Gyr old M67 members. Linear fits to the cluster data are shown by dashed lines. The circled dot is the Sun. The solid line represents the median $\log R'_{\text{HK}}$ for solar-type field stars (median $\log R'_{\text{HK}}$ values for 8 color bins from a sample of 1572 unique stars in the activity surveys of Henry et al. [1996] and Wright et al. [2004]).

blue and red edges of our color range. A sample of ~ 1500 unique solar-type field stars from the combined surveys of Wright et al. (2004) and Henry et al. (1996) is statistically consistent with having zero slope (see Fig. 4). Similarly, Soderblom et al. (1991) report a negligible slope for a sample of solar-type halo field stars.

For either the cluster (plus older field) sample alone or the binary sample alone, the significance of the activity-color slope is $< 3\sigma$. However, based on the fact that the measured slopes are consistent between these populations in the mean, and systematic with stellar age, we conclude that there is indeed an activity-color correlation that needs to be taken into account.

3.2. R'_{HK} -Age Calibration Using Cluster Stars

3.2.1. Assembled Cluster Data

With estimates of the mean $\log R'_{\text{HK}}$ values and color trends for stellar samples of known age, we can proceed toward an improved activity-age relation. In Figure 5 we plot histograms of the distribution of $\log R'_{\text{HK}}$ values for the stellar groups in our study (Table 6). For each cluster, we use the individual $\Delta \log R'_{\text{HK}} / \Delta(B - V)$ slopes calculated above to interpolate a mean $\log R'_{\text{HK}}$ value for a hypothetical cluster member of solar color [$(B - V)_0 = 0.65$ mag]. These are quoted in the last column of Table 5 and adopted in the analysis that follows.

3.2.2. A New R'_{HK} -Age Relation

In Figure 6 we plot the mean $\log R'_{\text{HK}}$ values versus cluster age. The data are the combined set of individually assessed $\log R'_{\text{HK}}$ measurements from Table 5, along with their 1σ confidence levels, and adopted mean $\log R'_{\text{HK}}$ values from Table 7. In both cases the ordinate values have been corrected to a nominally solar-color

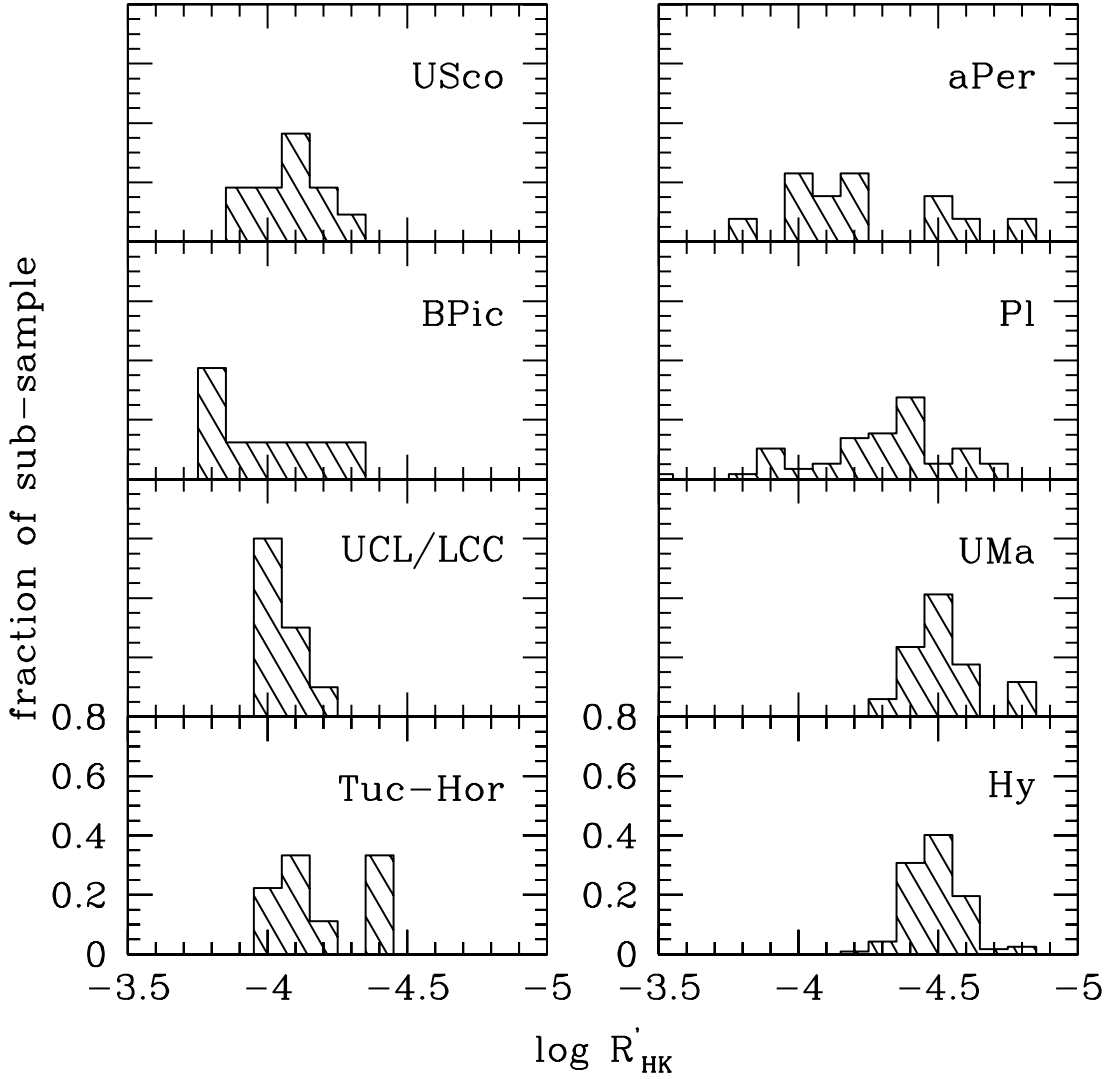


FIG. 5.—Normalized histograms showing the distribution of $\log R'_{\text{HK}}$ values within each stellar cluster or association, as compiled in Table 5. Individual kinematic groups show a dispersion in activity that is driven by both measurement error and astrophysical variation; the latter appears to be at a maximum at α Per and Pleiades ages.

population. The best unweighted quadratic fit to the cluster data¹² is

$$\log \tau = -38.053 - 17.912 \log R'_{\text{HK}} - 1.6675 \log(R'_{\text{HK}})^2 \quad (3)$$

and its inverse (better fitted as a trinomial)

$$\log R'_{\text{HK}} = 8.94 - 4.849 \log \tau + 0.624(\log \tau)^2 - 0.028(\log \tau)^3, \quad (4)$$

where τ is the age in years, and where the fit is only appropriate approximately between $\log R'_{\text{HK}}$ values of -4.0 and -5.1 and $\log \tau$ of 6.7 and 9.9 (the approximate range covered by our cluster samples). Our new function is plotted with the cluster mean activity values and the previously published activity-age relations in Figure 6. Along the active sequence ($-5.0 < \log R'_{\text{HK}} < -4.3$) corresponding to ages older than the Pleiades, the observed rms in

the fit is only $\log(\tau/\text{yr}) = 0.11$ dex ($\sim 29\%$). When the lower accuracy ancillary cluster data (§ 2.4.5) are removed, the rms for $\log R'_{\text{HK}} < -4.3$ is only ~ 0.07 dex in $\log(\tau/\text{yr})$. We believe that the latter value is more representative of the fidelity of our activity-age relation (eq. [3]). For the very active stars having $\log R'_{\text{HK}} > -4.3$, the rms in the fit is $\log(\tau/\text{yr}) = 0.23$ dex ($\sim 60\%$). While the age calibration has an unquantified systematic uncertainty due to the uncertainty in the cluster age scale, these rms values represent lower limits on the calibration uncertainty assigned to ages from $\log R'_{\text{HK}}$ measurements.

What is the typical uncertainty due to observational uncertainties or variability? To quantify this, we apply equation (3) to our binary and cluster samples. For the binary samples, the mean age inferred for the binary from the two $\log R'_{\text{HK}}$ values is assumed to be the correct system age. Among the 20 color-separated solar-type dwarf binaries in Table 2, the mean dispersion in the ages for the 40 components is ± 0.15 dex (1σ). Among the 14 near-identical solar-type dwarf binaries in Table 3, the mean dispersion in the ages for the 28 components is ± 0.07 dex (1σ). The age dispersions observed among the various stellar samples are summarized in the second column of Table 9. Applying the relation to the well-populated Hyades and M67 activity samples yields dispersions in the predicted ages of 0.25 and 0.20 dex, respectively.

¹² If the “classical” ages for the α Per and Pleiades clusters are adopted (51 and 77 Myr, respectively; Mermilliod 1981) instead of the Li depletion ages, there is negligible impact on this fit: $\log(\tau) = -36.331 - 17.213 \log R'_{\text{HK}} - 1.5977 \log(R'_{\text{HK}})^2$. The general effect is that the very active stars become $\sim 5\%$ younger.

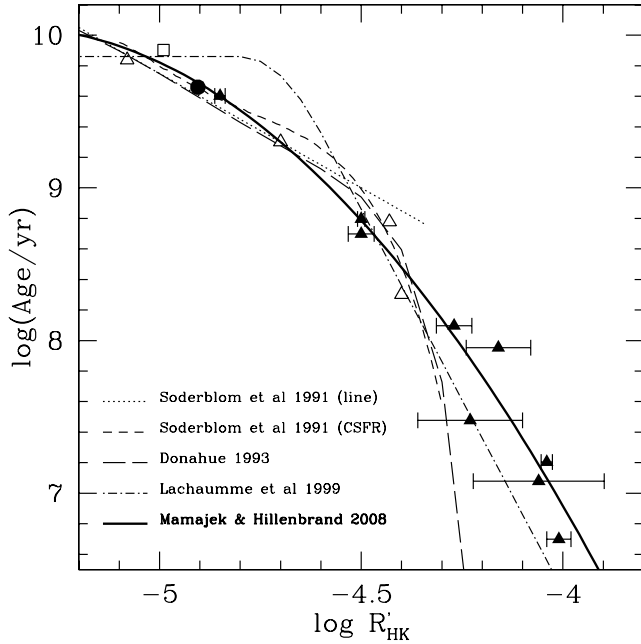


FIG. 6.— Mean $\log R'_{\text{HK}}$ cluster values (interpolated to solar $B - V$) vs. cluster age. Filled triangles are cluster mean $\log R'_{\text{HK}}$ values. Open triangles are ancillary cluster mean $\log R'_{\text{HK}}$ values listed in Table 7. The open square is the mean datum for the 5–15 Gyr old solar-type dwarfs from VF05 with isochronal age uncertainties of $< 20\%$. The filled circle is the Sun. Previously published activity-age relations are plotted as dotted and/or dashed lines. Soderblom et al. (1991) attempted two fits: a linear fit to his cluster data (dotted line) and a fit that assumes a constant star formation rate (CSFR) taking into account disk heating (long-dashed line). Our best-fit polynomial to the data in Tables 6 and 7 is the thick solid line (eq. [3]).

Hence, we see slightly larger dispersions in inferred age from among the cluster samples than among the binary samples, the reasons for which are not entirely clear. Taking into account observational uncertainties, calibration uncertainties, and astrophysical scatter, we conclude that for solar-type dwarfs older than a few hundred megayears the revised activity-age relation yields age estimates with total accuracy $\sim 60\%$ (0.25 dex). For younger stars, the uncertainty is approximately 1 dex. In § 4.3 we compare these results to those of an alternative technique, tying together age-rotation and rotation-activity relations to quantify the activity-age relation as a function of color, which somewhat reduces the scatter.

Equation (3) is clearly an improvement on the previously published activity-age relations given the copious amount of new activity data that we have incorporated into our fit, especially for young clusters. However, some caveats to general applicability remain. For example, our analysis was unable to constrain quantitatively how the color-activity slope evolves with age. It is apparent from our cluster data that were we to adopt equation (3) for all solar-type stars, we would introduce systematic age effects as a function of stellar color (mass). We are thus motivated to see if we can find an empirical means of taking into account the color-dependent (mass-dependent) evolution of activity as a function of age.

4. ACTIVITY AGES VIA THE ROSSBY NUMBER AND GYROCHRONOLOGY

Thus far we have focused on calibrating the $\log R'_{\text{HK}}$ versus age relation empirically using cluster and young association stars of “known” age. In this section we demonstrate that an age versus activity calibration can also be derived by combining the observed

TABLE 9
DISPERSIONS IN AGE ESTIMATES

Sample	$\sigma(A)$ (dex)	$\sigma(B)$ (dex)
Upper Sco	0.60	...
β Pic.....	1.06	...
UCL+LCC.....	0.31	...
Tuc-Hor.....	0.66	...
α Per.....	1.01	...
Pleiades	1.12	1.06
Ursa Major.....	0.25	0.23
Hyades.....	0.25	0.22
M67.....	0.20	0.24
Color-separated pairs	0.15	0.07
Near-identical pairs.....	0.07	0.05
Sun	0.06	0.05

NOTES.—A: 68% CL range in ages derived from the $\log R'_{\text{HK}}$ -age formula (eq. [3]). B: 68% CL range in ages derived from $\log R'_{\text{HK}} \rightarrow \text{Ro} \rightarrow \text{Period} \rightarrow \tau$ (§§ 4.1 and 4.2).

correlation between Rossby number and $\log R'_{\text{HK}}$ demonstrated by Noyes et al. (1984) with a rendition of the empirical “gyrochronology” rotational evolution formalism of Barnes (2007). In this section we update both the activity versus Rossby number relation of Noyes et al. (1984) and the rotation versus age relation of Barnes (2007) and then combine these into an activity-age relation to be compared to the activity-age relation in § 3 (eq. [3]).

4.1. Rossby Number versus Activity

4.1.1. Rossby Number Correlated with R'_{HK} Measuring Chromospheric Activity

In their classic chromospheric activity study, Noyes et al. (1984) attempt to understand the evolution of $\log R'_{\text{HK}}$ in terms of the stellar dynamo (e.g., Parker 1979). Chromospheric activity is a manifestation of heating by surface magnetic fields, which for the Sun are presumed to be generated near the base of the convective envelope. Chromospheric activity should, theoretically, scale with magnetic dynamo number; however, dynamo models are parameterized by variables whose functional forms remain poorly constrained both observationally and theoretically (e.g., Noyes et al. 1984; Donahue et al. 1996; Montesinos et al. 2001; Charbonneau & MacGregor 2001). Noyes et al. (1984) demonstrated that the mean levels of stellar chromospheric activity for solar-type dwarfs decay as Rossby number increases. The Rossby number Ro is parameterized as the stellar rotation period P divided by the convective turnover time τ_c or $\text{Ro} = P/\tau_c$. Some assumptions are necessary in arriving at values for Ro .

First, stars are not rigid rotators, so any estimate of the rotation rate of an unresolved stellar disk via either chromospheric activity or starspot modulation will be a latitudinal mean that may vary with time during the course of stellar activity cycles (Donahue et al. 1996). Second, the Rossby number is dependent on a convective turnover time that is an estimate, based directly on stellar interior models (e.g., Kim & Demarque 1996) or informed by the models but empirically calibrated (e.g., Noyes et al. 1984). Multiple studies have attempted to quantify the convective turnover time for solar-type MS stars (Noyes et al. 1984; Stepien 1994; Kim & Demarque 1996) and pre-MS stars (Jung & Kim 2007). Montesinos et al. (2001) show that the Noyes et al. (1984) color versus convective turnover time relation produces the tightest correlation between activity and Rossby number when compared to

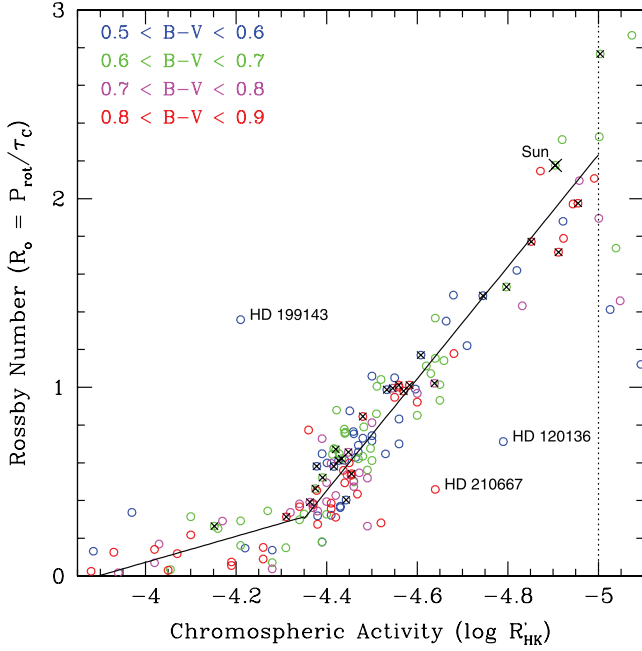


FIG. 7.—Rossby number (Ro) vs. $\log R'_{HK}$ for 169 solar-type MS or pre-MS stars with $0.5 \text{ mag} < (B - V)_0 < 0.9 \text{ mag}$ (the sample described in § 2.2). Stars are color-coded according to the legend. Mount Wilson HK survey stars with multiseasonal mean periods from Donahue et al. (1996) and multidecadal mean $\log R'_{HK}$ from Baliunas et al. (1996) are flagged with crosses. The best linear fits in the very active and active regimes are plotted (eqs. [5] and [7]). Stars with $\log R'_{HK} < -5.0$ appear to have a poor correlation between $\log R'_{HK}$ and Ro , possibly due to the increasing importance of gravity and metallicity toward low activity levels on the photospheric subtraction (J. Wright 2008, private communication). The Sun is marked with a large circle with a cross.

modern stellar models using mixing-length theory (MLT) and full turbulence spectrum (FTS) treatments of convection.

In light of the Montesinos et al. (2001) results, we adopt the Noyes et al. (1984) convective turnover time relation as a function of $B - V$ color. Indeed, from our own data set, the need for a color-dependent normalization of the rotation periods, i.e., the use of Rossby number Ro , is readily apparent from examination of period versus activity in which the color stratification is obvious. One caveat is that while the color-dependent convective turnover time should be adequate for MS stars, it will be systematically in error for pre-MS stars. As it is often unclear whether a given field star is pre-MS or MS (in most cases due to inadequate or lacking distance information), we adopt the MS convective turnover times for our calculations, independent of other age-constraining considerations.

In Figure 7 we plot chromospheric activity $\log R'_{HK}$ versus Rossby number Ro . The colored circles represent 169 solar-type MS and pre-MS (rejecting evolved stars more than 1 mag above the MS) stars having $0.5 \text{ mag} < (B - V)_0 < 0.9 \text{ mag}$ and both measured periods and $\log R'_{HK}$. A subsample of 28 of these stars have multiseasonal mean rotation periods and $\log R'_{HK}$ from Donahue et al. (1996) and Baliunas et al. (1996). These stars have the best determined rotation periods and mean $\log R'_{HK}$ values and are flagged with black crosses in the figure. With few exceptions, the Donahue-Baliunas stars all have published metallicity values within ± 0.5 dex of solar, and the majority are within ± 0.2 dex of solar (Cayrel de Strobel et al. 1997, 2001; Nordström et al. 2004; VF05).

Figure 7 suggests that the rotation versus activity relation should be clarified in three activity regimes. In the “very active”

regime¹³ ($\log R'_{HK} > -4.3$) there appears to be little correlation between $\log R'_{HK}$ and Ro (Pearson $r = -0.24$). In the “active” regime ($-5.0 < \log R'_{HK} < -4.3$) there is a very strong anticorrelation between activity and Rossby number (Pearson $r = -0.94$). Curiously, in the active and very active regimes the vertical scatter at a given activity level is roughly constant with $\log R'_{HK}$. In the “inactive” regime ($\log R'_{HK} < -5.0$), the correlation between activity and Rossby number is again very weak (Pearson $r = +0.33$). The inactive regime ($\log R'_{HK} < -5.0$) is exactly where Wright (2004) suggests that the age-activity correlation fails based on correlation of inferred $\log R'_{HK}$ with height above the MS. Wright (2005) suggests that the definition of $\log R'_{HK}$ may require inclusion of a gravity-sensitive correction. For the purposes of our study, we omit the inactive stars ($\log R'_{HK} < -5.0$) from further rotation-activity analysis.

In Figure 7 we fit an OLS bisector line to the active ($-5.0 < \log R'_{HK} < -4.3$) sequence of solar-type dwarfs, finding

$$Ro = (0.808 \pm 0.014) - (2.966 \pm 0.098)(\log R'_{HK} + 4.52) \quad (5)$$

and

$$\log R'_{HK} = (-4.522 \pm 0.005) - (0.337 \pm 0.011)(Ro - 0.814). \quad (6)$$

In this activity-rotation regime, the rms of the fits is ~ 0.16 in Ro and ~ 0.05 in $\log R'_{HK}$. Two obvious outliers were omitted in the analysis (HD 210667 and HD 120136).¹⁴

In the very active regime in Figure 7 ($\log R'_{HK} > -4.3$) the correlation between rotation and activity is very weak. However, we can still assess the empirical relation between rotation and activity in this regime, even if the predictability of the dependent variable on the independent variable is weak. Omitting the outlier HD 199143 (a pre-MS late F binary), for the stars with $Ro < 0.4$ in Figure 7, we fit

$$Ro = (0.233 \pm 0.015) - (0.689 \pm 0.063)(\log R'_{HK} + 4.23) \quad (7)$$

and

$$\log R'_{HK} = (-4.23 \pm 0.02) - (1.451 \pm 0.131)(Ro - 0.233). \quad (8)$$

¹³ Note that the monikers “very active,” “active,” and “inactive” have been defined somewhat differently in other papers (e.g., Henry et al. 1996; Saar & Brandenburg 1999; Wright et al. 2004). We delimit them based on the appearance of Fig. 7.

¹⁴ Multiple independent estimates of $\log R'_{HK}$ have been reported for HD 210667 (Duncan et al. 1991; Henry et al. 1996; Gray et al. 2003; Wright et al. 2004; White et al. 2007) and for HD 120136 (Duncan et al. 1991; Baliunas et al. 1996; Wright et al. 2004; Hall et al. 2007), so their activity levels are well constrained. HD 210667 would appear to be a normal inactive star in Fig. 7 if its period were 2 times that reported by Strassmeier et al. (2000; 9.1 days), so it is possible that this is a case of period aliasing (i.e., its true period is ~ 18 days?). The other outlier is the famous star HD 120136 (τ Boo), one of the first stars discovered to have a hot Jupiter (Butler et al. 1997). Mean rotation periods have been reported by Henry et al. (2000; 3.2 ± 0.5 days) and Walker et al. (2008; 3.5 ± 0.7 days), and the rotation rate is suspiciously close to the orbital period of 3.3 days for the planet (Butler et al. 1997). Walker et al. (2008) conclude that the planetary companion is magnetically inducing long-lived active regions on the star. Henry et al. (2000) similarly noted that the measured rotation period for τ Boo is significantly shorter than what one would infer from its activity level. Fig. 7 suggests that τ Boo’s unusual Rossby number vs. activity behavior is mimicked by less than a few percent of solar-type field dwarfs.

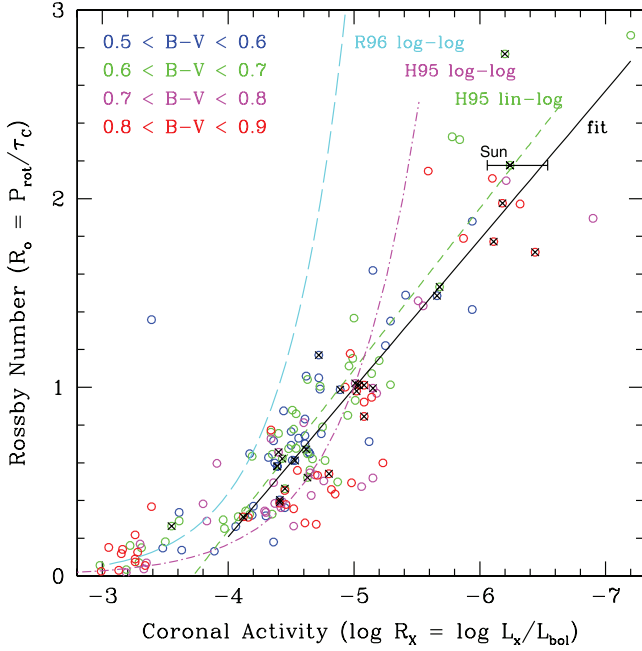


FIG. 8.— $\log R_X$ vs. Rossby number Ro for stars in our sample of solar-type stars with known rotation periods and chromospheric and X-ray activity levels. Donahue-Baliunas stars with well-determined periods also have thick crosses. Previously published R_X vs. Ro fits are drawn: the cyan long-dashed line is a log-log fit from Randich et al. (1996), the magenta dot-dashed line is a log-log fit from Hempelmann et al. (1995), and the green dashed line is a linear-log fit from Hempelmann et al. (1995). Our new loglinear fit for stars in the range $-7 < \log R_X < -4$ is the thick solid line, consistent with the Hempelmann linear-log relation. Saturated X-ray emission ($\log R_X > -4$) is consistent with $Ro < 0.5$.

The rms of the fits is ~ 0.10 in Ro and ~ 0.16 in $\log R'_{HK}$. While the rms in Ro is less for the very active than for the active sequence, the fractional uncertainty in Ro ($\sim 50\%$) is larger. As the low Pearson r for the data in the active regime of Figure 7 reflects, the power to predict activity given Ro , or vice versa, is limited with our current toolkit. The enhanced scatter for the very active stars is likely due to (1) increased variability, (2) only one or few $\log R'_{HK}$ measurements, and (3) inclusion of likely MS and pre-MS stars, implying a spread in convective turnover times that is not being taken into account. For our purposes, we match the very active and active sequence fits (eqs. [6], [5], [8], and [7]) at $\log R'_{HK} = -4.35$ and $Ro = 0.32$.

4.1.2. Rossby Number Correlated with R_X Measuring Coronal Activity

In addition to their chromospheric activity quantified via fractional Ca II H and K luminosity, $\log R'_{HK}$, young stars are often noted for copious coronal activity and X-ray emission. There appear to be at least two rotation-activity regimes inferred from X-ray surveys (e.g., Pizzolato et al. 2003): a “saturated” regime for very active, fast-rotating stars where there is little correlation between rotation and activity ($\log R_X \simeq -3.2$), and a “nonsaturated” regime of slower rotating, lower activity stars where rotation and X-ray emission are correlated ($-7 < \log R_X < -4$). As rotation slows with stellar age, one would surmise that X-ray emission (especially nonsaturated) can be a useful tool for estimating the ages of solar-type stars.

In Figure 8 we show that coronal activity can be related to Rossby number in a manner similar to that displayed in Figure 7 for the relation of chromospheric activity and Rossby number (see also, e.g., Hempelmann et al. 1995; Randich et al. 1996; Pizzolato et al. 2003 and references therein). As previous authors have noted,

finding a simple function form that adequately describes the relationship between $\log R_X$ and Ro over the full range of activity data available is difficult (e.g., Hempelmann et al. 1995). Figure 8 shows three previous fits to the $\log R_X$ versus Ro data, one from Randich et al. (1996) and two from Hempelmann et al. (1995) plotted over the full range of activity sampled by the respective authors. The Randich et al. (1996) fit in Figure 8 comes from a very small sample of stars in the young α Per cluster and appears to miss the majority of the data. The Hempelmann et al. (1995) log-log fit in Figure 8 passes through the majority of intermediate-activity stars but is a poor fit for the low-activity stars (overpredicting the Sun’s X-ray emission by an order of magnitude). The $\log R_X$ versus Ro (loglinear) fit of Hempelmann et al. (1995) is satisfactory for the intermediate- and low-activity stars, but extrapolation above $\log R_X > -4$ (i.e., the saturated X-ray regime) is not recommended.

Following Hempelmann et al. (1995), we fit a loglinear regression to the rotation-activity data. The range of fractional X-ray luminosities over which there is a good correlation between $\log R_X$ and Ro ($-7 < \log R_X < -4$) approximately overlaps the active regime in Figure 7 ($-5 < \log R'_{HK} < -4.3$; see the Appendix). Over the active sequence, the fit

$$Ro = (0.86 \pm 0.02) - (0.79 \pm 0.05)(\log R_X + 4.83) \quad (9)$$

produces an rms scatter of 0.25 in Rossby number Ro . The inverse relation is

$$\log R_X = (-4.83 \pm 0.03) - (1.27 \pm 0.08)(Ro - 0.86), \quad (10)$$

with an rms of 0.29 dex in $\log R_X$. The correlation between $\log R_X$ and Rossby number is very strong (Pearson $r = -0.89$). These fits are not applicable for stars with $\log R_X > -4$ that are nearing the saturated X-ray emission regime. Saturated X-ray emission appears to imply Rossby numbers $Ro < 0.5$ (rotation period < 6 days for a G2 dwarf) and hence can be used to estimate an upper limit to the rotation period. This transition region is similar to that seen for $\log R'_{HK}$ near $\log R'_{HK} \simeq -4.3$ (Fig. 7). In the Appendix we further quantify the relationship between these chromospheric and coronal activity indicators.

The rms scatter in Ro values inferred from $\log R_X$ is comparable to that inferred from $\log R'_{HK}$ values in single-measurement or multiyear surveys [$\S 4.1$; 0.25 vs. 0.16 in $\sigma(Ro)$], although the scatter for averaged data from multidecade Mount Wilson HK observations is smaller [0.10 in $\sigma(Ro)$]. This suggests that soft X-ray luminosities can be used to infer the rotation rate of old solar-type dwarfs almost as accurately as most $\log R'_{HK}$ values in the literature.

4.1.3. Considerations for a Rotation-Activity-Age Relation

In the next section ($\S 4.2$) we attempt to derive a rotation versus age relation for solar-type dwarfs of a given color. Our end goal is to combine an activity-rotation relation with a rotation-age relation ($\S 4.2$) to produce an activity-age relation to compare to equation (3). As we intend to infer rotation rates from activity levels, we would like to know how accurately the uncertainty in Ro reflects the uncertainty in rotation period from equations (7) and (5). From the definition of the Rossby number ($Ro = P/\tau_c$), the uncertainty in period is $\sigma_P \approx \tau_c \sigma_{Ro}$. While τ_c varies from star to star as a function of color, its mean value in our color range of interest is ~ 15 days, and hence a typical uncertainty in the predicted period σ_P is ~ 1.5 days (ranging from ~ 0.8 days for the late F stars to ~ 2.2 days for the late K stars). A good approximation

for the uncertainty in the period (in days) inferred from $\log R'_{\text{HK}}$ for late F through early K stars is

$$\sigma_P \simeq 4.4(B - V)(\sigma_{R_0}/0.1) - 1.7, \quad (11)$$

where $\sigma_{R_0} \simeq 0.1$ for stars with multidecadal $\log R'_{\text{HK}}$ means (Baliunas et al. 1996; i.e., Mount Wilson HK survey stars). For stars from Wright et al. (2004) with typically dozens of $\log R'_{\text{HK}}$ measurements over a span of a few years, the scatter in R_0 as a function of $\log R'_{\text{HK}}$ is $\sigma_{R_0} \simeq 0.17$. For stars with measured rotation periods, but with a few to tens of $\log R'_{\text{HK}}$ measurements (e.g., Duncan et al. 1991; Henry et al. 1996; White et al. 2007), the scatter in R_0 as a function of $\log R'_{\text{HK}}$ is $\sigma_{R_0} \simeq 0.2$. In the limit of a single $\log R'_{\text{HK}}$ measurement, it appears that one should be able to estimate R_0 to ~ 0.2 – 0.3 (1σ) accuracy for solar-type dwarfs. This is comparable to the accuracy in R_0 that single X-ray observations can produce ($\sigma_{R_0} \simeq 0.25$; § 4.1.2). Surveying the suite of coronal and X-ray activity indicators published for thousands of stars, it appears that we can predict rotation for the majority to better than ± 0.25 in R_0 .

For the Sun's observed mean rotation period as measured through the Mount Wilson S-index (26.09 days; Donahue et al. 1996), one would predict the Sun's mean chromospheric activity to be $\log R'_{\text{HK}} = -4.98$. This can be compared to the observed value, time averaged over several solar cycles, of -4.91 (§ 1.1). As the observed rms in $\log R'_{\text{HK}}$ versus R_0 along the inactive sequence is only ~ 0.05 dex, the Sun's past 40 years of activity appears to be only $\sim 1.3\sigma$ higher than predicted for its period. This corroborates previous findings that the Sun appears to have more or less normal activity for its rotation period (e.g., Noyes et al. 1984).

From the results of large chromospheric activity surveys (e.g., Henry et al. 1996; Wright et al. 2004) for solar-type stars within 1 mag of the MS, it appears that $\sim 76\%$ of solar-type field stars fall within the active sequence ($-5.0 < \log R'_{\text{HK}} < -4.35$), $\sim 3\%$ fall within the very active sequence ($\log R'_{\text{HK}} > -4.35$), and $\sim 21\%$ are inactive ($\log R'_{\text{HK}} < -5.0$). The coronal activity surveys show a similar distribution. Hence, for roughly three-quarters of the solar-type dwarfs, we have a well-determined empirical rotation-activity relation where we can reliably use activity to predict rotation period, or vice versa. This corroborates the results of Noyes et al. (1984). More importantly, we provide a modern, well-established activity-rotation relationship using the best available data. Our next step is to revisit the rotation-age relationship, with the eventual goal of producing an activity-rotation-age relationship with more predictive power than an activity-age relation.

4.2. Gyrochronology

In the course of their evolution, solar-type stars lose angular momentum via magnetic braking due to their mass loss (Weber & Davis 1967). This inexorably leads to a steady slowdown in rotation rates, first quantified by Skumanich (1972) as projected rotation speed $v \sin i \propto \text{age}^{-0.5}$. Detailed surveys of solar-type stars in open clusters (beginning with the summary in Kraft 1967) have shown that the evolution in rotation period has a mass dependence.

Recently, Barnes (2007) used existing literature data to derive a color-dependent version of the Skumanich law (“gyrochronology”). For a given age, Barnes finds that the majority of solar-type stars in clusters follow what he calls the *interface* or “I” rotational sequence. The choice of nomenclature is theoretically motivated, as it is believed that these stars are producing their magnetic flux near the convective-radiative interface. Barnes dubs

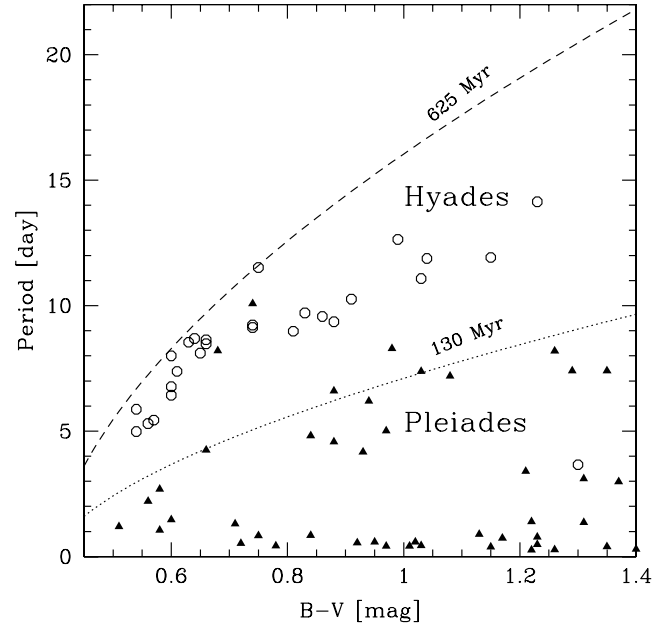


FIG. 9.—Rotation period vs. $B - V$ for solar-type stars in the Pleiades (filled triangles) and Hyades (open circles) compared to gyrochrones from Barnes (2007) for ages 130 and 625 Myr. The offsets between the gyrochrones and the observed period distributions for these benchmark clusters motivated us to rederive the parameters in the gyro relations.

the population of ultrafast rotators the “C” or *convective* rotational sequence and posits that these stars lack large-scale dynamos and hence break their rotation very inefficiently (see also Endal & Sofia 1981; Stauffer et al. 1984; Soderblom et al. 1993). According to Barnes (2007), the rotation periods for I-sequence stars evolve with age as

$$P(B - V, t) = f(B - V)g(t), \quad (12)$$

$$f(B - V) = a[(B - V)_0 - c]^b, \quad (13)$$

$$g(t) = t^n. \quad (14)$$

With the age of the star t given in Myr, Barnes finds $a = 0.7725 \pm 0.011$, $b = 0.601 \pm 0.024$, the “color singularity” $c = 0.40$ mag, and the time-dependent power law $n = 0.5189 \pm 0.0070$. In practice, Barnes segregates the I- and C-sequence rotators at the 100 Myr *gyrochrone* and does not attempt to estimate ages for faster rotating stars. These coefficients are claimed to satisfy the above gyrochronology relation for the Sun and several young open clusters and to match well a sample of color-separated binaries with known rotation periods (e.g., α Cen, 61 Cyg).

An independent assessment of data for the Sun, Hyades, and Pleiades reveals discrepancies when using the gyrochronology relations from Barnes (2007). As illustrated in Figure 9, the Barnes “gyrochrone” for an age of 625 Myr overpredicts the periods of Hyades members as a function of color by as much as 50%, suggesting the need for modification in a and/or b . For the Pleiades (130 Myr), the agreement is better overall, but disagreement is most prevalent for the bluer members, suggesting that the value of c needs revision. To produce suitable fits over a wide range of ages within the Barnes formalism, we were forced to rederive the parameters a , b , c , and n .

Considering the clusters of Tables 6 and 7, we find after a thorough literature search that only a few have sufficient data on stellar rotation periods for inclusion in this exercise. They are the usual

TABLE 10
REVISED GYROCHRONOLOGY PARAMETERS

Parameter	Value
a	0.407 ± 0.021
b	0.325 ± 0.024
c	0.495 ± 0.010
n	0.566 ± 0.008

suspects: α Per (Prosser et al. 1995), Pleiades (Prosser et al. 1995; Krishnamurthi et al. 1998), M34 (Meibom et al. 2008), and Hyades (Radick et al. 1987, 1995; Prosser et al. 1995; Paulson et al. 2004; Henry 2006, private communication). Rotation data for benchmark clusters older than the Hyades (such as Coma Ber, NGC 752, M67, and NGC 188) are hard to come by given the long mean periods of >10 days. However, increased interest in both planet searches and stellar oscillation studies may soon rectify this situation. We also include the Sun as an old anchor datum, adopting a period of 26.09 days, which is the latitudinal mean observed by Donahue et al. (1996) (the solar rotation ranges from ~ 25 days near the equator to ~ 32 days near the poles).

To rederive a gyro relation that more closely matches the cluster sequences and the Sun, we include in the fit only the obvious I-sequence rotators in the clusters and omit the ultrafast C-sequence rotators, as well as the two very slow rotators in the Pleiades (HII 2284 and HII 2341). For the four gyro parameters, we minimize the residuals in period for the cluster data and solar datum, but retaining only those fits that come within 0.1 days of the solar mean rotation rate at its age. Our method forces perhaps undue statistical significance on this one data point (the Sun); however, as we are lacking in cluster sequences or even single stars with accurate ages >625 Myr, the solar datum is unique and thus extremely important to reproduce. We also ignore the effects of metallicity on the cluster sequences, working in color rather than mass.

Our best estimates of the gyrochronology parameters are presented in Table 10. The errors reflect the uncertainties of the parameters for $\Delta\chi^2 = 1$, where $\text{rms} = 1.23$ days gives $\chi^2_\nu = 1$ for the best fit. In Figure 10 we demonstrate the match of these coefficients to the data from which they were established.

How well does our improved gyrochronology fit perform for the four sample solar-type dwarf binaries with known periods (§ 2.3)? In Figure 10 we also show that the color-period lines connecting the binary components appear to follow approximately the slopes of the curves predicted from our new gyrochrone curve (§ 4.2). In Table 11 we present revised estimates of the individual gyrochronological ages based on our revised parameters for equations (12)–(14).

Assuming that the systems are coeval, our revised fit to the gyro equations appears to yield stellar ages with precision of ± 0.05 dex (1σ ; $\pm 11\%$) in $\log(\tau/\text{yr})$. This is comparable to the precision claimed by Barnes (2007); however, the ages should be more accurate as the Pleiades and Hyades color sequence is more accurately modeled (cf. Figs. 10 and 9). For the best studied system (α Cen), the inferred gyro age (5.0 ± 0.3 Gyr) compares well to recent estimates from modeling asteroseismology data, which have been converging to a consensus age of 6 ± 1 Gyr in recent years: 4.85 ± 0.5 Gyr (Th  venin et al. 2002), ~ 6.4 Gyr (Thoul et al. 2003), 6.52 ± 0.3 Gyr (Eggenberger et al. 2004), $5.2\text{--}7.1$ Gyr (Miglio & Montalb  n 2005).

We conclude that our improved gyrochronology fit is probably precise to of order ~ 0.05 dex in $\log(\tau/\text{yr})$ for I-sequence rotators. This uncertainty does not include the absolute uncertainties in the

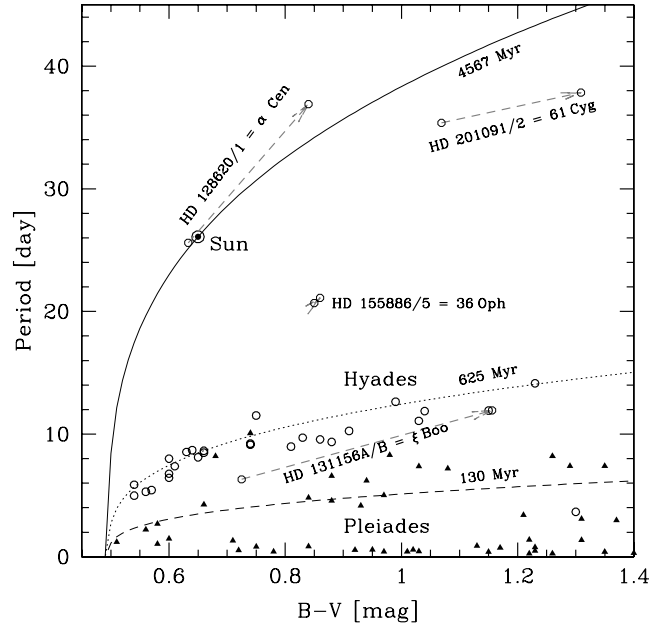


FIG. 10.—Rotation period vs. $B - V$ for solar-type stars of varying age compared to gyrochronology relations derived in this work. The Sun is a circled dot, members of the Pleiades are filled triangles, the Hyades are open circles, and (presumably coeval) field binary pairs are open circles joined by arrows.

cluster age scale (which are probably of similar magnitude; $\sim 15\%$). Clearly, new samples of stars with well-constrained rotation periods and ages at a range of colors are needed to constrain the rotational evolution of solar-type stars at ages of >1 Gyr. Our refined gyrochronology parameters represent our best attempt to empirically parameterize the rotational evolution of solar-type stars at present. However, we acknowledge that given the rapidly changing data landscape for cluster rotation studies, superior rotation versus age relations may soon be available.

4.3. Implications and Tests of New Gyro-Rossby Ages

Having calibrated the activity-rotation and rotation-age correlations with the best available data, we can now use the results from §§ 4.1 and 4.2 to predict the evolution of $\log R'_{\text{HK}}$ as a function of age and color for solar-type stars. In Figure 11 we illustrate the predicted activity tracks as a function of color and stellar age. In Figure 12 we plot the predicted activity-age relation for various colors of solar-type dwarfs. Considering these two plots leads us to a few conclusions. First, the subtle positive mean slopes in $\Delta \log R'_{\text{HK}}/\Delta B - V$ observed for the young clusters in Figure 4 and Table 6 can be understood in the context of mass-dependent

TABLE 11
REVISED GYRO AGES FOR FIELD BINARIES

System (1)	HD (2)	$\log \tau_A$ (yr) (3)	$\log \tau_B$ (yr) (4)	$\log \tau$ (yr) (5)
ξ Boo.....	131156AB	8.47	8.70	8.59
α Cen.....	128620/1	9.67	9.72	9.70
36 Oph.....	155886/6	9.28	9.28	9.28
61 Cyg.....	201091/2	9.57	9.53	9.55

NOTES.—Col. (1): Common name. Col. (2): HD name. Col. (3): Gyro age for component A. Col. (4): Gyro age for component B. Col. (5): Mean gyro age for the system. Gyro ages were estimated from the equation $P = a[(B - V)_0 - c]^b \times t^n$, where the coefficients are listed in Table 10.

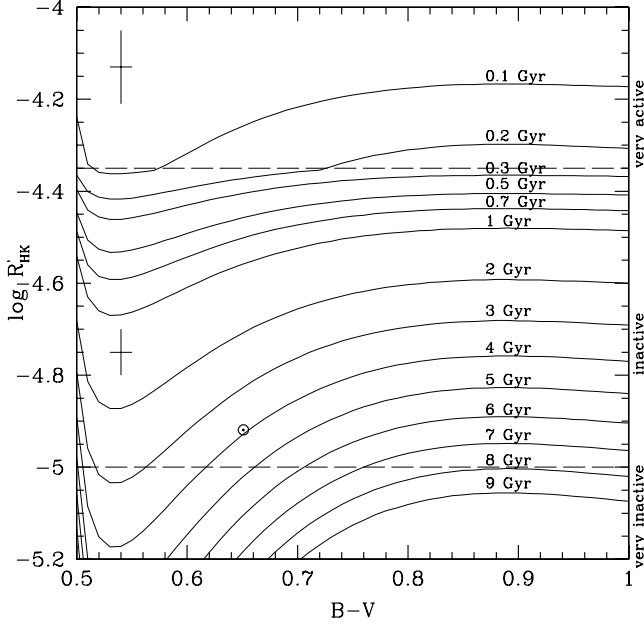


FIG. 11.—Predicted chromospheric activity levels as a function of age (“gyrochromochrones”), from combining the age-rotation relations in § 4.2 with the rotation-activity relations in § 4.1. Typical uncertainty bars are shown in the very active and active regimes, reflecting the rms in the Rossby number-activity fits and typical photometric errors. The behavior of the gyrochromochrones at the blue end (i.e., the obvious upturn) is not well constrained and is particularly sensitive to the c parameter in the gyrochronology fits.

rotation evolution combined with a rotation-activity relation (a notable exception is the old cluster M67). Second, the assumption of a single activity-age relation applicable to the wide range of solar-type dwarf colors [$\sim 0.5 \text{ mag} < (B - V)_0 < 0.9 \text{ mag}$; eqs. (3) and (4) and Fig. 6] we and others often considered is a

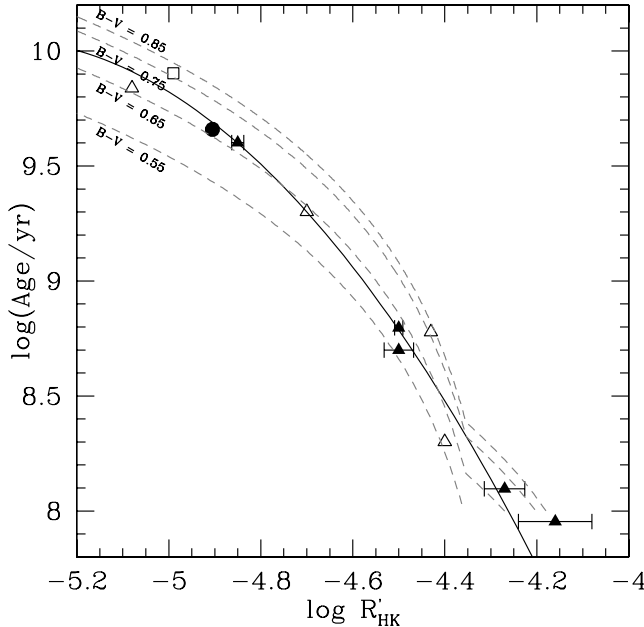


FIG. 12.—Predicted $\log R'_{\text{HK}}$ vs. age relation for solar-type dwarfs of different colors (dashed lines). The cluster samples and mean relation from Fig. 6 are plotted. The dashed lines represent the synthesis of the age-rotation gyrochronology relation (§ 4.2) with the rotation-activity relations (§ 4.1). These gyrochromochrones show that the assumption of an activity-age relation applicable to all solar-type dwarfs in the color range $0.5 \text{ mag} < (B - V)_0 < 0.9 \text{ mag}$ is probably an oversimplification. The kink in $\log R'_{\text{HK}}$ corresponds to the transition between the very active and active regimes.

TABLE 12
ACTIVITY-GYRO AGES FOR SOLAR-TYPE BINARIES

Primary (1)	Secondary (2)	$\log \tau_1$ (yr) (3)	$\log \tau_2$ (yr) (4)	$\overline{\log \tau}$ (yr) (5)
HD 531B.....	HD 531A	8.01	8.73	8.37 ± 0.36
HD 5190.....	HD 5208	9.59	9.86	9.73 ± 0.14
HD 13357A.....	HD 13357B	9.42	9.28	9.35 ± 0.07
HD 14082A.....	HD 14082B	8.59	8.43	8.51 ± 0.08
HD 23439A.....	HD 23439B	9.80	10.11	9.96 ± 0.15
HD 26923.....	HD 26913	8.76	8.64	8.70 ± 0.06
HD 53705.....	HD 53706	9.56	9.89	9.72 ± 0.16
HD 73668A.....	HD 73668B	9.47	9.46	9.47 ± 0.01
HD 103432.....	HD 103431	9.60	9.54	9.57 ± 0.03
HD 116442.....	HD 116443	9.82	9.85	9.84 ± 0.02
HD 134331.....	HD 134330	9.42	9.61	9.52 ± 0.10
HD 134439.....	HD 134440	9.62	9.75	9.68 ± 0.07
HD 135101A.....	HD 135101B	9.85	9.85	9.85 ± 0.00
HD 137763.....	HD 137778	9.86	8.72	9.29 ± 0.56^a
HD 142661.....	HD 142661B	9.43	9.32	9.37 ± 0.06
HD 144087.....	HD 144088	9.42	9.37	9.39 ± 0.02
HD 219175A.....	HD 219175B	9.48	9.58	9.53 ± 0.05

NOTES.—Col. (1): Name of primary. Col. (2): Name of secondary. Col. (3): Activity-gyro age for component A. Col. (4): Activity-gyro age for component B. Col. (5): Mean gyro age for the system.

^a HD 137763 is a pathological case discussed in footnote 10.

poor assumption. The predicted activity evolution curves in Figure 11 also warn that the search for Maunder minimum candidates (e.g., Donahue 1998; Wright 2004) should take into account that coeval stars may have different mean activity levels (~ 0.1 – 0.2 dex in $\log R'_{\text{HK}}$) as a function of $B - V$ color. The question remains, can we determine more accurate ages from an activity-rotation-age algorithm compared to the standard activity-age relations?

Similar to our analysis in § 3.2.2, we wish to test the consistency of our gyro-activity age predictions among two useful types of samples: field binary stars and open cluster members. In each of these groups, the constituents are expected to be coeval but to display a range in mass and to suffer from astrophysical scatter. How well do the predicted ages agree among these presumably coeval stars?

Our first test uses the 20 binary pairs of Table 2. We convert the individual R'_{HK} values to period via the R'_{HK} versus Rossby number correlation and use the gyrochronology relations to estimate ages. The ages for these binaries are listed in Table 12. The distribution of the periods (inferred from the R'_{HK} values) versus colors for the binaries is plotted in Figure 13, with the revised gyrochromochrones overlaid. Excluding the known pathological system HD 137763 (footnote 10), the remaining systems appear to give consistent ages with a statistical rms of ± 0.07 dex ($\sim 15\%$). Recall that using the simple activity-age relation (eq. [3]) produced consistent ages with rms of ~ 0.15 dex ($\sim 35\%$). So for the sample of nonidentical binaries, taking into account the color-dependent rotational evolution appears to significantly decrease the age uncertainties.

Our second test involves the cluster stars from Table 5. Rather than, as illustrated in Figure 5, adopting the mean activity level for a cluster and turning it into a mean age that can be compared to individually predicted ages, we convert the individual R'_{HK} values via the Rossby number correlation to period and use the gyrochronology relations. This method assumes that the stars are participating in the so-called I-sequence identified by Barnes and are not ultrafast rotators of the so-called C-sequence. If this is not

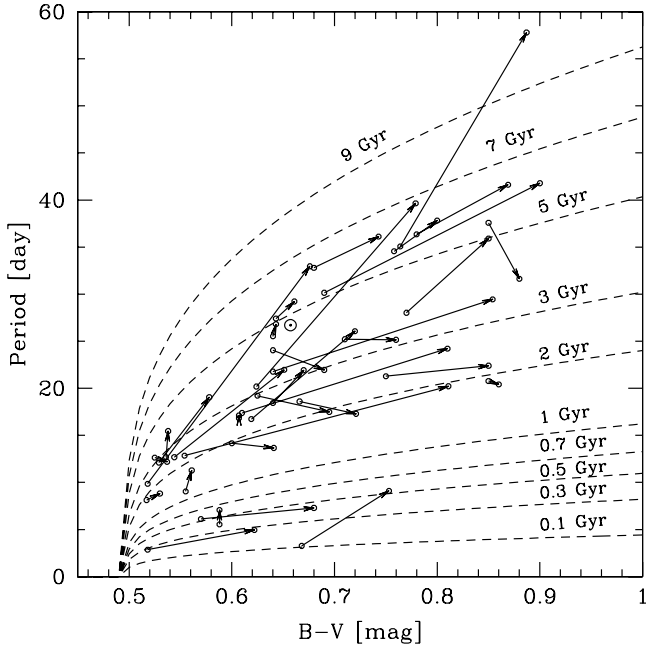


FIG. 13.—Predicted rotation periods for field binary stars with measured $\log R'_{\text{HK}}$. Periods were estimated from the activity-Rossby relations (eqs. [5] and [7]). Gyrochrone equations are from eqs. (12)–(14) using the constants in Table 10.

true in reality, some rapid rotators will have their ages underestimated via gyrochronology/activity. That the Rossby number versus R'_{HK} correlation of Figure 7 breaks down or saturates at high activity levels helps isolate us from this effect since those stars will not have reliable conversions to period. The resulting dispersions (68% CL) in the ages inferred for the cluster members are listed in Table 9, along with the dispersions observed for the two binary samples and the Sun. Also listed in Table 9 is the inferred age dispersion for the same samples when the simple activity-age relation (eq. [3]) is used to estimate ages.

From Table 9 we conclude the following regarding adopting a simple activity-age relation (§ 3.2.2) versus an activity-rotation-age prescription (§§ 4.1 and 4.2). First, among the six stellar samples (four open clusters and two binary samples), the activity-rotation-age technique resulted in smaller age dispersions for five of the six samples (the exception being M67). Quantifying the improvement is not so straightforward. The improvement among three of the clusters (Pleiades, UMa, Hyades) was typically a $\sim 10\%$ reduction in the age dispersion, equivalent to removing a ~ 0.1 dex source of systematic error. The two binary samples show marked improvements in their age dispersions; most notably, the dispersion in age estimates among the color-separated binaries was reduced significantly by using the activity-rotation-age technique rather than a simple activity-age relation. The results for M67 are somewhat perplexing and hint that our activity-rotation-age technique is not adequately modeling this ~ 4 Gyr old group. This is not surprising given that half of the M67 sample is hotter/bluer than the Sun, and as Figure 10 suggests, the gyro relations are not well constrained for late F/early G stars for ages older than the Hyades. We conclude by stating that the activity-rotation-age technique appears to give slightly more consistent ages among the older samples tested than by using a simple activity-age relation.

4.4. Inferred Ages for the Nearest Solar-Type Dwarfs

While a rigorous utilization of the revised age-deriving methods for studying the star formation history of the solar neighborhood is beyond the focus of this study, we briefly discuss some

implications of our results for a small volume-limited sample of solar-type dwarfs.

We use our new and improved age-deriving methods to estimate the ages for a volume-limited sample of the 108 solar-type dwarfs within 16 pc (Table 13). The sample consists of the nearest known dwarfs with $0.5 \text{ mag} < B - V < 0.9 \text{ mag}$ (the color region where both the R'_{HK} calculations and revised gyrochronology relations are constrained). A few of the entries are unresolved multiples, sometimes containing two or even three solar-type stars (e.g., ι Boo). Seven evolved stars lying more than 1 mag above the MS defined by Wright et al. (2004) have been omitted (i.e., $\Delta M_V < -1$: α Aur, η Boo A, μ Her, ζ Her, β Hyi, and 31 Aql). When multiple R'_{HK} measurements were found in the literature, we gave highest priority to those estimates that included the most observations. When multiple single observations were published by different authors, we preferentially adopted those from the largest surveys (e.g., Duncan et al. 1991; Henry et al. 1996; Wright et al. 2004). All parallaxes and V magnitudes are from the *Hipparcos* catalog (Perryman et al. 1997). MK spectral types are preferentially taken from compilations by Keenan and Gray and collaborators. Given the stated color, parallax, and absolute magnitude constraints, this catalog is likely to be complete for distances of < 16 pc.

Estimated ages using our methods are listed in the final two columns of Table 13. The first column of ages (τ_1) are from using the revised activity-age relation (§ 3.2.2, eq. [3]). The second column of ages (τ_2) are those inferred from converting the chromospheric activity levels to a rotation period via the Rossby number and then converting the rotation period to an age using the revised gyro relation (§ 4, eqs. [5]–[8] and [10]–[12]). The final column of ages τ_2 are the preferred age estimates. The inferred activity age for the extraordinarily active zero-age MS star AB Dor is ~ 1 Myr and clearly in error (apparently by 2 orders of magnitude; Luhman et al. 2005). As AB Dor painfully illustrates, the uncertainties in the inferred ages for the very active stars ($\log R'_{\text{HK}} > -4.3$) are large (~ 1 dex; e.g., Table 9). A conservative estimate of the typical age uncertainty is $\sim 50\%$ for the preferred ages τ_2 of the lower activity stars.

In Figure 14 we plot a histogram of the inferred ages τ_1 and τ_2 for the volume-limited sample of the solar-type dwarfs within 16 pc. The histogram cannot be strictly interpreted as a true star formation history as we have not accounted for disk heating (e.g., Soderblom et al. 1991; West et al. 2008). The effect preferentially removes older, higher velocity stars from the local sample but is subtle and small for the youngest age bins. The ages inferred from the simple activity-age relation (eq. [3]; *dashed histogram*) show a minimum at ~ 2 –3 Gyr seen in previous studies that corresponds to the “Vaughan-Preston gap” (Vaughan & Preston 1980; Barry 1988; see also Figs. 7 and 8 of Henry et al. 1996). However, when we examine the histogram of ages inferred from activity \rightarrow rotation (*solid histogram*), the minimum at ~ 2 –3 Gyr is not as obvious, revealing a more or less smooth distribution of ages between 0 and 6 Gyr (with a precipitous decrease at older ages, presumably due to disk heating and loss of evolved higher mass stars from the sample). Similarly, the stellar birth rate during the past gigayear appears unremarkable compared to the past ~ 6 Gyr. These results also call into doubt previous claims that the star formation rate during the past gigayear has been significantly enhanced (Barry 1988).

5. SUMMARY

The primary goal of this study was to derive a well-calibrated conversion between activity and age for stars younger than the Sun. To achieve this, we compiled from the literature R'_{HK} , R_X ,

TABLE 13
ACTIVITY AGES FOR THE SOLAR-TYPE DWARFS WITHIN 16 pc

HD	HIP	GJ	Alias	ϖ (mas)	$B - V$ (mag)	References	$\log R'_{\text{HK}}$ (dex)	References	V (mag)	M_V (mag)	ΔM_V (mag)	Spectral Type	References	τ_1 (Gyr)	τ_2 (Gyr)
166.....	544	5A	V439 And	72.98 ± 0.75	0.752	1	-4.328	5	6.07	5.39	-0.02	G8 V	8	0.2	0.2
1581.....	1599	17	ζ Tuc	116.38 ± 0.64	0.572	2	-4.839	6	4.23	4.56	0.25	F9.5 V	11	3.8	2.1
3443.....	2941	25AB	HR 159	64.38 ± 1.40	0.715	1	-4.903	7	4.61	5.19	-0.58	G8 V+G9 V	15	4.8	4.9
3651.....	3093	27A	54 Psc	90.03 ± 0.72	0.850	1	-4.991	7	5.88	5.65	-0.28	K0 V	8	6.4	7.7
4391.....	3583	1021	HR 209	66.92 ± 0.73	0.640	2	-4.55	6	5.80	4.93	0.23	G5 V Fe-0.8	11	0.8	0.9
4614.....	3821	34A	η Cas	167.99 ± 0.62	0.574	2	-4.958	5	3.46	4.59	0.20	F9 V	16	5.8	2.9
4628.....	3765	33	HR 222	134.04 ± 0.86	0.890	1	-4.852	7	5.74	6.38	0.25	K2.5 V	11	4.0	5.4
4813.....	3909	37	19 Cet	64.69 ± 1.03	0.514	1	-4.78	8	5.17	4.22	0.32	F7 V	8	2.9	1.7
6582.....	5336	53A	μ Cas A	132.40 ± 0.60	0.695	2	-4.964	5	5.17	5.78	0.65	K1 V Fe-2	8	5.9	5.3
7570.....	5862	55	ν Phe	66.43 ± 0.64	0.571	1	-4.95	9	4.97	4.28	-0.20	F9 V Fe+0.4	11	5.7	2.8
10307.....	7918	67	HR 483	79.09 ± 0.83	0.618	1	-5.02	10	4.96	4.45	-0.14	G1 V	8	7.0	4.2
10360.....	7751	66A	HR 487	122.75 ± 1.41	0.880	2	-4.899	11	5.96	6.26	0.36	K2 V	11	4.8	6.2
10361.....	7751	66B	HR 486	122.75 ± 1.41	0.850	2	-4.839	11	5.81	6.26	0.33	K2 V	11	3.8	5.2
10476.....	7981	68	107 Psc	133.91 ± 0.91	0.836	1	-4.912	7	5.24	5.87	0.02	K1 V	11	5.0	6.3
10700.....	8102	71	τ Cet	274.17 ± 0.80	0.727	1	-4.958	7	3.49	5.68	0.42	G8.5 V	11	5.8	5.8
10780.....	8362	75	V987 Cas	100.24 ± 0.68	0.804	1	-4.681	7	5.63	5.64	-0.06	G9 V	8	1.8	2.9
13445.....	10138	86A	HR 637	91.63 ± 0.61	0.820	2	-4.74	6	6.12	5.93	0.20	K1 V	11	2.4	3.7
13974.....	10644	92	δ Tri A	92.20 ± 0.84	0.607	1	-4.69	10	4.84	4.66	0.15	G0 V	16	1.9	1.5
14412.....	10798	95	HR 683	78.88 ± 0.72	0.724	1	-4.85	12	6.33	5.81	0.57	G8 V	11	3.9	4.3
17925.....	13402	117	EP Eri	96.33 ± 0.77	0.867	2	-4.311	7	6.05	5.97	-0.02	K1.5 V(k)	11	0.1	0.2
19373.....	14632	124	ι Per	94.93 ± 0.67	0.595	1	-5.02	10	4.05	3.94	-0.50	F9.5 V	8	7.0	3.7
20630.....	15457	137	96 Cet	109.18 ± 0.78	0.681	1	-4.420	7	4.84	5.03	0.05	G5 V	17	0.3	0.4
20766.....	15330	136	ζ^1 Ret	82.51 ± 0.54	0.641	1	-4.646	6	5.53	5.11	0.38	G2 V	11	1.5	1.5
20794.....	15510	139	82 Eri	165.02 ± 0.55	0.708	2	-4.998	6	4.26	5.35	0.18	G8 V	11	6.6	6.1
20807.....	15371	138	ζ^2 Ret	82.79 ± 0.53	0.600	1	-4.787	6	5.24	4.83	0.36	G0 V	11	3.0	2.0
22049.....	16537	144	ϵ Eri	310.75 ± 0.85	0.881	1	-4.455	7	3.72	6.18	0.10	K2 V(k)	11	0.4	0.8
22484.....	16852	147	10 Tau	72.89 ± 0.78	0.575	1	-5.12	12	4.29	3.60	-0.70	F9 IV-V	16	8.8	4.2
26965.....	19849	166A	40 Eri	198.24 ± 0.84	0.820	1	-4.872	7	4.43	5.92	0.14	K0.5 V	11	4.3	5.6
30495.....	22263	177	58 Eri	75.10 ± 0.80	0.632	1	-4.49	10	5.49	4.87	0.19	G1.5 V CH-0.5	11	0.6	0.6
32923.....	23835	188	104 Tau	63.02 ± 0.93	0.657	1	-5.15	10	4.91	3.91	-0.93	G1 V	8	9.3	6.8
34411.....	24813	197	λ Aur	79.08 ± 0.90	0.630	1	-5.067	5	4.69	4.18	-0.48	G1 V	8	7.9	5.0
36705.....	25647	...	AB Dor	66.92 ± 0.54	0.830	1	-3.88	11	6.88	6.01	0.18	K2 V(k)	11	<0.1	<0.1
37394.....	26779	211	V538 Aur	81.69 ± 0.83	0.840	1	-4.454	7	6.21	5.77	-0.11	K0 V	8	0.4	0.8
38858.....	27435	1085	HR 2007	64.25 ± 1.19	0.639	1	-4.87	10	5.97	5.01	0.29	G2 V	8	4.3	3.2
39587.....	27913	222	54 Ori	115.43 ± 1.08	0.594	1	-4.426	7	4.39	4.70	0.27	G0 V CH-0.3	11	0.4	0.3
41593.....	28954	227	V1386 Ori	64.71 ± 0.91	0.814	1	-4.42	5	6.76	5.82	0.07	G9 V	8	0.3	0.6
43834.....	29271	231	α Men	98.54 ± 0.45	0.720	2	-4.94	6	5.08	5.05	-0.14	G7 V	11	5.5	5.5
52698.....	33817	259	NLTT 17311	68.42 ± 0.72	0.894	2	-4.64	6	6.71	5.89	-0.20	K1 V(k)	11	1.4	2.5
63077.....	37853	288A	171 Pup	65.79 ± 0.56	0.589	1	-4.97	12	5.36	4.45	0.05	F9 V	11	6.0	3.2
69830.....	40693	302	HR 3259	79.48 ± 0.77	0.754	1	-4.95	12	5.95	5.45	0.03	G8+ V	11	5.7	6.1
72673.....	41926	309	HR 3384	82.15 ± 0.66	0.784	1	-4.95	12	6.38	5.95	0.39	G9 V	11	5.7	6.5
72905.....	42438	311	3 UMa	70.07 ± 0.71	0.618	1	-4.375	7	5.63	4.86	0.27	G0.5 V	16	0.2	0.2
75732.....	43587	324A	55 Cnc A	79.80 ± 0.84	0.860	2	-5.04	12	5.96	5.47	-0.55	K0 IV-V	8	7.4	8.7
82885.....	47080	356A	11 LMi	89.45 ± 0.78	0.770	1	-4.638	7	5.40	5.16	-0.35	G8+ V	8	1.4	2.3
86728.....	49081	376A	20 LMi	67.14 ± 0.83	0.676	1	-5.06	12	5.37	4.50	-0.45	G4 V	8	7.7	6.2
95128.....	53721	407	47 UMa	71.04 ± 0.66	0.624	1	-5.02	10	5.03	4.29	-0.34	G1 V	16	7.0	4.4
100623.....	56452	432A	HR 4458	104.84 ± 0.81	0.811	1	-4.89	12	5.96	6.06	0.33	K0 V	11	4.6	5.8

TABLE 13—*Continued*

HD	HIP	GJ	Alias	ϖ (mas)	$B - V$ (mag)	References	$\log R'_{\text{HK}}$ (dex)	References	V (mag)	M_V (mag)	ΔM_V (mag)	Spectral Type	References	τ_1 (Gyr)	τ_2 (Gyr)
101501.....	56997	434	61 UMa	104.81 ± 0.72	0.723	1	-4.546	7	5.31	5.41	0.17	G8 V	8	0.8	1.2
102365.....	57443	442A	HR 4523	108.23 ± 0.70	0.664	1	-4.95	6	4.89	5.06	0.18	G2 V	11	5.7	4.5
102870.....	57757	449	β Vir	91.74 ± 0.77	0.518	1	-4.99	10	3.59	3.40	-0.53	F8.5 IV-V	16	6.4	2.9
103095.....	57939	451A	CF UMa	109.21 ± 0.78	0.751	1	-4.896	7	6.42	6.61	1.19	K1 V Fe-1.5	8	4.7	5.3
104304.....	58576	454	HR 4587	77.48 ± 0.80	0.770	2	-4.92	12	5.54	4.99	-0.47	G8 IV	11	5.1	5.9
109358.....	61317	475	β CVn	119.46 ± 0.83	0.585	2	-4.99	10	4.26	4.64	0.23	G0 V	8	6.4	3.3
114710.....	64394	502	β Com	109.23 ± 0.72	0.572	1	-4.745	7	4.23	4.42	0.13	G0 V	16	2.5	1.5
115617.....	64924	506	61 Vir	117.30 ± 0.71	0.709	1	-5.001	7	4.74	5.09	-0.07	G7 V	11	6.6	6.1
118972.....	66765	1175	NLTT 34858	64.08 ± 0.81	0.855	1	-4.39	6	6.92	5.95	0.00	K0 V(k)	11	0.3	0.4
120136.....	67275	527A	τ Boo	64.12 ± 0.70	0.508	1	-4.731	7	4.50	3.54	-0.33	F7 IV-V	16	2.3	1.6
128620.....	71683	559A	α Cen A	742.12 ± 1.40	0.633	3	-5.002	6	-0.01	4.34	-0.82	G2 V	11	6.6	4.4
128621.....	71681	559B	α Cen B	742.12 ± 1.40	0.840	3	-4.923	6	1.35	5.70	-0.47	K2 IV	11	5.2	6.5
131156.....	72659	566A	ξ Boo A	149.26 ± 0.76	0.720	2	-4.344	5	4.72	5.59	0.37	G7 V	8	0.2	0.2
131511.....	72848	567	DE Boo	86.69 ± 0.81	0.833	1	-4.52	10	6.00	5.69	-0.19	K0 V	8	0.7	1.3
133640.....	73695	575	i Boo ABC	78.39 ± 1.03	0.647	1	-4.637	5	4.83	4.30	-0.47	G1 V+G8 V+K0 V	18	1.4	1.5
135599.....	74702	...	V739 Ser	64.19 ± 0.97	0.830	1	-4.52	12	6.92	5.96	0.13	K0 V	8	0.7	1.3
136352.....	75181	582	ν^2 Lup	68.70 ± 0.79	0.639	1	-4.91	6	5.65	4.83	0.11	G2 V	11	5.0	3.6
140538.....	77052	596.1A	ψ Ser	68.16 ± 0.87	0.684	1	-4.80	10	5.86	5.03	0.02	G5 V	16	3.2	3.2
140901.....	77358	599A	HR 5864	65.60 ± 0.77	0.715	1	-4.72	6	6.01	5.10	-0.10	G7 IV-V	11	2.2	2.7
141004.....	77257	598	λ Ser	85.08 ± 0.80	0.603	2	-5.004	7	4.42	4.07	-0.43	G0 IV-V	8	6.7	3.8
142373.....	77760	602	χ Her	63.08 ± 0.54	0.563	1	-5.18	7	4.60	3.60	-0.63	G0 V Fe-0.8	8	9.7	4.4
144579.....	78775	611A	LHS 3152	69.61 ± 0.57	0.734	1	-4.97	12	6.66	5.87	0.57	K0 V Fe-1.2	8	6.0	6.1
144628.....	79190	613	NLTT 42064	69.66 ± 0.90	0.856	1	-4.94	6	7.11	6.32	0.37	K1 V	11	5.5	6.8
145417.....	79537	615	LHS 413	72.75 ± 0.82	0.815	1	-5.06	6	7.53	6.84	1.09	K3 V Fe-1.7	11	7.7	8.8
146233.....	79672	616	18 Sco	71.30 ± 0.89	0.652	1	-4.93	10	5.49	4.76	-0.05	G2 V	8	5.3	4.1
147513.....	80337	620.1A	HR 6094	77.69 ± 0.86	0.625	1	-4.45	13	5.37	4.82	0.19	G1 V CH-0.4	11	0.4	0.4
147584.....	80686	624	ζ TrA	82.61 ± 0.57	0.550	2	-4.56	6	4.90	4.49	0.31	F9 V	11	0.9	0.6
149661.....	81300	631	12 Oph	102.27 ± 0.85	0.827	1	-4.583	7	5.77	5.82	0.01	K0 V(k)	11	1.0	1.9
154577.....	83990	656	NLTT 44221	73.07 ± 0.91	0.893	2	-4.815	9	7.38	6.70	0.58	K2.5 V(k)	11	3.4	4.8
155885.....	84405	663B	36 Oph B	167.08 ± 1.07	0.860	4	-4.559	7	5.11	6.23	0.25	K0 V	19	0.9	1.7
155886.....	84405	663A	36 Oph A	167.08 ± 1.07	0.850	4	-4.570	7	5.07	6.19	0.26	K0 V	19	1.0	1.8
156274.....	84720	666A	41 Ara	113.81 ± 1.36	0.777	1	-4.941	6	5.47	5.75	0.28	G9 V	19	5.5	6.3
157214.....	84862	672	72 Her	69.48 ± 0.56	0.619	1	-5.00	10	5.38	4.59	-0.01	G0 V	16	6.6	4.1
158633.....	85235	675	HR 6518	78.14 ± 0.51	0.759	1	-4.93	12	6.44	5.90	0.46	K0 V	20	5.3	5.9
160269.....	86036	684AB	26 Dra AB	70.98 ± 0.55	0.602	1	-4.62	14	5.23	4.49	0.00	F9 V+K3 V	21	1.3	1.1
160691.....	86796	691	μ Ara	65.46 ± 0.80	0.700	2	-5.04	13	5.12	4.20	-0.90	G3 IV-V	11	7.4	6.5
165341.....	88601	702A	70 Oph A	196.62 ± 1.38	0.860	1	-4.586	5	4.25	5.50	-0.48	K0 V	8	1.1	1.9
165908.....	88745	704A	99 Her A	63.88 ± 0.55	0.528	1	-5.02	12	5.08	4.11	0.11	F9 V mw	16	7.0	2.9
166620.....	88972	706	HR 6806	90.11 ± 0.54	0.876	1	-4.955	7	6.38	6.15	0.10	K2 V	8	5.8	7.1
170657.....	90790	716	NLTT 46596	75.71 ± 0.89	0.861	1	-4.65	12	6.81	6.21	0.22	K2 V	11	1.5	2.6

TABLE 13—*Continued*

HD	HIP	GJ	Alias	ϖ (mas)	$B - V$ (mag)	References	$\log R'_{\text{HK}}$ (dex)	References	V (mag)	M_V (mag)	ΔM_V (mag)	Spectral Type	References	τ_1 (Gyr)	τ_2 (Gyr)
172051.....	91438	722	HR 6998	77.02 ± 0.85	0.673	1	−4.90	12	5.85	5.28	0.35	G6 V	11	4.8	4.1
176051.....	93017	738AB	HR 7162	66.76 ± 0.54	0.594	1	−4.874	7	5.20	4.32	−0.11	F9 V+K1 V	21	4.3	2.6
182488.....	95319	758	HR 7368	64.54 ± 0.60	0.804	1	−5.06	5	6.37	5.42	−0.27	K0 V	17	7.7	8.7
185144.....	96100	764	σ Dra	173.41 ± 0.46	0.786	1	−4.832	7	4.67	5.87	0.27	G9 V	8	3.7	4.7
188512.....	98036	771A	β Aql	72.95 ± 0.83	0.855	1	−5.173	7	3.71	3.03	−2.93	G9.5 IV	11	9.6	11.4
190248.....	99240	780	δ Pav	163.73 ± 0.65	0.751	1	−4.999	6	3.55	4.62	−0.78	G8 IV	11	6.6	6.9
190360.....	98767	777A	HR 7670	62.92 ± 0.62	0.749	1	−5.102	7	5.73	4.72	−0.66	G7 IV−V	8	8.5	8.6
190404.....	98792	778	LHS 481	64.17 ± 0.85	0.815	1	−4.98	12	7.28	5.75	0.57	K1 V	8	6.2	7.3
191408.....	99461	783A	HR 7703	165.24 ± 0.90	0.868	1	−4.988	6	5.32	6.41	0.39	K2.5 V	11	6.4	7.7
192310.....	99825	785	HR 7722	113.33 ± 0.89	0.878	1	−5.048	11	5.73	6.00	−0.06	K2+ V	11	7.5	8.9
196761.....	101997	796	HR 7898	68.28 ± 0.82	0.722	1	−4.92	12	6.36	5.53	0.32	G8 V	11	5.1	5.2
205390.....	106696	833	NLTT 51629	67.85 ± 0.92	0.884	2	−4.53	9	7.14	6.30	0.23	K1.5 V	11	0.7	1.4
207129.....	107649	838	HR 8323	63.95 ± 0.78	0.601	1	−4.80	6	5.57	4.60	0.12	G0 V Fe+0.4	11	3.2	2.1
211415.....	110109	853A	HR 8501	73.47 ± 0.70	0.605	2	−4.86	6	5.36	4.69	0.13	G0 V	11	4.1	2.6
217014.....	113357	882	51 Peg	65.10 ± 0.76	0.666	1	−5.08	5	5.45	4.52	−0.37	G2 V+	11	8.1	6.1
224930.....	171	914A	85 Peg A	80.63 ± 3.03	0.673	2	−4.875	7	5.80	5.33	0.29	G5 V Fe−1	8	4.4	3.8

REFERENCES.—(1) Perryman et al. 1997; (2) Mermilliod 1991; (3) Bessell 1981; (4) Hoffleit & Jaschek 1991; (5) Duncan et al. 1991, calculated using equations in Noyes et al. 1984; (6) Henry et al. 1996; (7) Baliunas et al. 1996; (8) Gray et al. 2003; (9) Jenkins et al. 2006; (10) Hall et al. 2007; (11) Gray et al. 2006; (12) Wright et al. 2004; (13) Saffie et al. 2005; (14) estimated from *ROSAT* All-Sky Survey X-ray emission (Voges et al. 1999, 2000) via eq. (A1) (see also § 2.3); (15) Christy & Walker 1969; (16) Gray et al. 2001; (17) Keenan & McNeil 1989; (18) Hill et al. 1989; (19) Corbally 1984; (20) Cowley et al. 1967; (21) Edwards 1976.

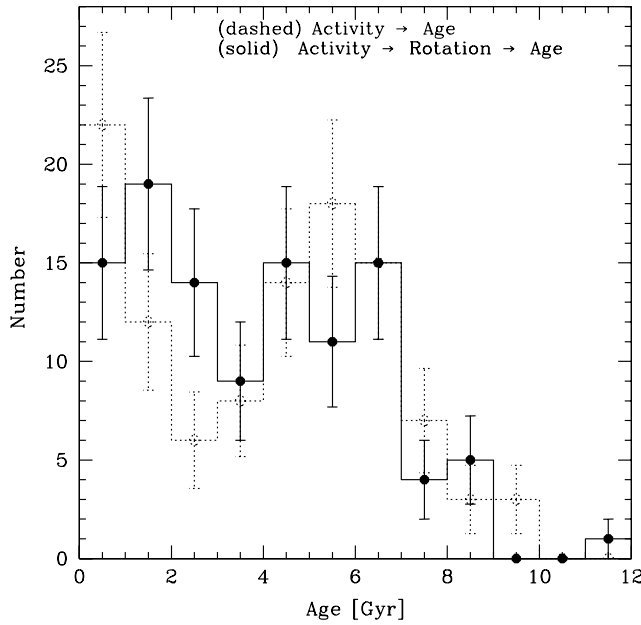


FIG. 14.—Histogram of the inferred ages for the solar-type dwarfs within 16 pc (F7–K2 V). The dashed histogram is for ages inferred directly from activity using eq. (3). The solid histogram is for ages derived from converting activity to rotation period (§ 4.1) and then converting rotation period and color to age using the revised gyro relation (§ 4.2). The ages inferred directly from activity show the familiar lull near ~ 3 Gyr noted in some studies (e.g., Barry 1988). Using the improved ages (from activity \rightarrow rotation \rightarrow age), the inferred star formation rate appears to be smoother between 0 and 6 Gyr.

and rotation period data for members of stellar associations and clusters; in particular, we have populated for the first time the young end of the chromospheric activity-age relation. We also used updated/modern ages for many young associations and clusters. We then fitted the following relations critical to assessing stellar ages of solar-type dwarfs: a chromospheric activity-age relation, a chromospheric activity-rotation relation, a coronal activity-rotation relation, and a rotation-age “gyrochronology” relation. Our main results drawn from study of the rotation and activity observed among binary stars and star cluster members with $0.5 \text{ mag} < B - V < 0.9 \text{ mag}$ can be summarized as follows:

1. We provide an improved $\log R'_{\text{HK}}$ versus age relation for solar-type stars that constrains especially the young, high-activity end relative to the relations of Soderblom et al. (1991), Donahue (1993), and Lachaume et al. (1999). The activity-age relation for solar-color stars appears to be absolutely calibrated to the modern cluster age scale to roughly ± 0.07 dex in $\log(\tau/\text{yr})$ for stars older than the Pleiades, and perhaps to only roughly ± 0.23 dex accuracy in $\log(\tau/\text{yr})$ for stars younger than the Pleiades. For young stars recently arriving on the MS (e.g., the Pleiades), $\log R'_{\text{HK}}$ is not very useful as a quantitative age estimator as the inferred rms spread in ages derived from chromospheric activity is an order of

magnitude. For older samples (> 0.5 Gyr) and typical $\log R'_{\text{HK}}$ measurements, it appears that our calibration can estimate the ages of solar-type dwarfs to roughly ± 0.25 dex ($\sim 60\%$; 1σ) accuracy, accounting for systematic errors in the calibration, random errors due to astrophysical scatter, variability of $\log R'_{\text{HK}}$, and measurement errors. This activity-age relation, however, does not account for color-dependent evolution effects that appear to be present.

2. We corroborate previous studies that find a tight relation between chromospheric activity and rotation for stars with $-5.0 < \log R'_{\text{HK}} < -4.35$, as well as coronal X-ray activity and rotation for stars with $-7 < \log R_X < -4$ (both via the Rossby number). In their respective saturated regimes ($\log R'_{\text{HK}} > -4.35$, $\log R_X > -4$), the correlation between chromospheric and coronal activity is poor. For stars with long-term $\log R'_{\text{HK}}$ averages and well-determined periods, we find that rotation period can predict mean $\log R'_{\text{HK}}$ to ± 0.05 dex (1σ) accuracy. For stars with multidecadal average $\log R'_{\text{HK}}$ measurements (e.g., Mount Wilson HK sample), $\log R'_{\text{HK}}$ can be used to predict Rossby number (period divided by convective turnover time) to ± 0.1 (1σ) accuracy. For shorter baseline $\log R'_{\text{HK}}$ measurements this uncertainty in Rossby number is larger, with the limit of a single $\log R'_{\text{HK}}$ measurement probably capable of predicting the Rossby number to $\sim 0.2\text{--}0.3$ (1σ) accuracy. Similarly, fractional X-ray luminosity R_X for nonsaturated X-ray emitters can be used to infer Rossby number to ~ 0.25 (1σ) accuracy.

3. We provide an improved gyrochronology relation (period as a function of color and age), which fits the young cluster data better than the coefficients provided by Barnes (2007). For so-called I-sequence rotators, the new fit is statistically accurate to ± 1.2 days in rotation between the age of the Pleiades and Sun. Our revised gyro relation predicts self-consistent ages with statistical accuracy of ± 0.06 dex (14% ; 1σ) for solar-type stars with well-determined periods.

4. Combining our activity-rotation relation (via the Rossby number; § 4.1) and our improved gyrochronology relations (rotation-color-age; § 4.2), we predict the evolution of activity as a function of color for solar-type dwarf stars. Our activity-rotation-age calibration appears to yield slightly better ages than using an activity-age relation alone. Statistical analysis of binary samples suggests that the activity-rotation-age technique can estimate ages of roughly ± 0.1 dex accuracy, whereas analysis of the cluster samples suggests an accuracy of more like roughly ± 0.2 dex.

We thank Mark Giampapa, David Soderblom, John Stauffer, Jason Wright, Debra Fischer, Sallie Baliunas, Søren Meibom, and Sydney Barnes for discussions and input. We acknowledge Greg Henry for allowing us access to his rotation period data for young MS stars in advance of publication. E. M. is supported through a Clay Postdoctoral Fellowship from the Smithsonian Astrophysical Observatory.

APPENDIX

X-RAY VERSUS CHROMOSPHERIC ACTIVITY

Sterzik & Schmitt (1997) demonstrated that fractional X-ray luminosity [$\log(L_X/L_{\text{bol}})$ or $\log R_X$ hereafter] and $\log R'_{\text{HK}}$ are well correlated over a wide range of masses and ages for solar-type dwarfs, and studies of the Sun and other solar-type dwarfs show that enhanced coronal activity traces enhanced chromospheric activity temporally as well (e.g., Hempelmann et al. 2003). Whereas R'_{HK} appears to drop by ~ 1 dex (see Fig. 6) between the T Tauri epoch ($\sim 1\text{--}10$ Myr) and the age of the Sun (~ 5 Gyr), $\log R_X$ declines by ~ 3 dex (Preibisch & Feigelson 2005). Further, the saturation of $\log R_X$ (Preibisch & Feigelson 2005) appears to occur at earlier ages than the saturation of $\log R'_{\text{HK}}$ (White et al. 2007). We conclude that at the high-activity end, $\log R_X$ may be a better diagnostic of age than $\log R'_{\text{HK}}$.

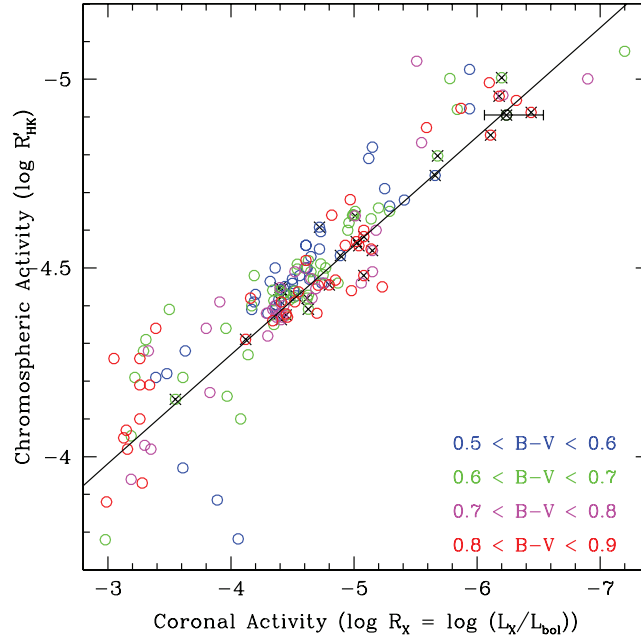


FIG. 15.— $\log R_X$ vs. $\log R'_{HK}$ for stars in our sample of solar-type stars with known rotation periods and chromospheric and X-ray activity levels. Donahue-Baliunas stars with well-determined periods also have thick crosses. Color bins are illustrated in the legend. The solar datum uses the mean $\log R'_{HK}$ calculated in § 1 and the mean $\log R_X$ calculated from Judge et al. (2003) (with systematic uncertainty of 50% in $\log R_X$ plotted).

The $\log R'_{HK}$ versus $\log R_X$ relation of Sterzik & Schmitt (1997) could be improved in two ways. First, their sample is X-ray biased, as it only includes stars with $\log R'_{HK}$ measurements that were detected in the RASS. Secondly, the relation is poorly constrained at the high-activity end due to the relative rarity of extremely young solar-type stars within 25 pc. To ameliorate this situation, we fit a $\log R'_{HK}$ versus $\log R_X$ relation to an unbiased sample of solar-type dwarfs and check that it fits the high-activity regime for solar-type stars. A convenient X-ray-unbiased sample of solar-type stars is the Baliunas-Donahue sample of 28 solar-type dwarfs from the Mount Wilson HK survey. This sample has well-determined rotation periods measured over more than five seasons by Donahue et al. (1996) and well-determined mean $\log R'_{HK}$ values from the Mount Wilson survey (Baliunas et al. 1996). Fortunately, *all* of these stars were detected in X-rays with *ROSAT*, and X-ray luminosities and R_X values were calculated by the authors (§ 2.2). An auxiliary sample of X-ray-biased solar-type stars was also constructed, so that the $\log R_X$ versus $\log R'_{HK}$ relation fitted to the X-ray-unbiased sample could be verified in the high-activity regime. This auxiliary sample is comprised of 199 solar-type dwarfs from the literature with $\log R'_{HK}$, $\log R_X$, and rotation period measurements. This sample was based on the compilation of Pizzolato et al. (2003) but added to, quality checked, and brought up to date.

We show in Figure 15 the correlation between the coronal and chromospheric activity indices for both the Baliunas-Donahue (X-ray unbiased) and auxiliary (X-ray biased) samples. For the X-ray-unbiased sample, the X-ray and chromospheric indices are remarkably well correlated (Pearson $r = 0.96$). We calculate the OLS bisector linear regression following Isobe et al. (1990). We find

$$\log R'_{HK} = (-4.54 \pm 0.01) + (0.289 \pm 0.015)(\log R_X + 4.92), \quad (A1)$$

with an rms scatter of 0.06 in $\log R'_{HK}$. The inverse relation is

$$\log R_X = (-4.90 \pm 0.04) + (3.46 \pm 0.18)(\log R'_{HK} + 4.53), \quad (A2)$$

with an rms of 0.19 dex ($\sim 55\%$) in $\log R_X$. Equation (A2) is statistically consistent with the relation found by Sterzik & Schmitt (1997), but our uncertainties are ~ 2 times smaller. Linear fits were also made for $\log R'_{HK}$ versus $\log R_X$, and its inverse, for the X-ray-based auxiliary sample. The resulting fits gave slopes statistically consistent with that estimated for the Baliunas-Donahue X-ray-unbiased sample, but with y -intercepts favored toward giving larger $\log R_X$ values (e.g., the X-ray-biased fit would predict $\log R_X$ for the solar $\log R'_{HK}$ value higher by ~ 0.2 dex compared to the X-ray-unbiased fit). We find that equations (A1) and (A2) are satisfactory for the high-activity stars also, so the fits are appropriate for the full range of $\log R_X$ and $\log R'_{HK}$ values seen for solar-type field dwarfs and pre-MS stars. The scatter in both relations increases substantially as the transition from the active regimes in both sequences to the very active regime above about -4.35 in $\log R'_{HK}$ and the saturated regime above about -4 in $\log R_X$ is approached.

If one combines equations (3) and (A1), one can derive an X-ray activity versus age relation for solar-type dwarfs:

$$\log \tau = 1.20 - 2.307 \log R_X - 0.1512 \log R_X^2. \quad (A3)$$

From the cluster X-ray data compiled in Pizzolato et al. (2003) it appears that the spread in $\log R_X$ among solar-type dwarfs in young clusters is roughly ± 0.2 – 0.6 dex (68% CL). If the chromospheric activity levels for the 4 Gyr old members of M67 (Giampapa et al. 2006) are converted to $\log R_X$ via equation (A2), one would predict a ± 0.4 dex (68% CL) spread in $\log R_X$ values among its solar-type

members. Based on this, a roughly ± 0.4 dex (68% CL) spread in $\log R_X$ values for a coeval population can be adopted and should be factored into any age uncertainty inferred from equation (A3).

The Baliunas et al. (1996) $\log R'_{\text{HK}}$ values are long-term averages from ~ 20 years of Mount Wilson HK observations, whereas the $\log R_X$ values typically represent only a few hundred second snapshot in the star's life. The correlation suggests that one can predict a multidecadal average of $\log R'_{\text{HK}}$ to within ± 0.1 (1σ) accuracy for a solar-type star from a few hundred seconds of X-ray data. Given the current state of X-ray and chromospheric activity data in the literature, we believe that these rms values are representative of how accurately these variables can be used to predict one another.

REFERENCES

- Asiain, R., Figueras, F., & Torra, J. 1999, *A&A*, 350, 434
- Baker, J., Bizzarro, M., Wittig, N., Connelly, J., & Haack, H. 2005, *Nature*, 436, 1127
- Baliunas, S., Sokoloff, D., & Soon, W. 1996, *ApJ*, 457, L99
- Baliunas, S. L., Donahue, R. A., Soon, W., & Henry, G. W. 1998, in *ASP Conf. Ser. 154, Cool Stars, Stellar Systems, and the Sun*, ed. R. A. Donahue & J. A. Bookbinder (San Francisco: ASP), 153
- Baliunas, S. L., & Soon, W. 1995, *ApJ*, 450, 896
- Baliunas, S. L., et al. 1995, *ApJ*, 438, 269
- Barnes, S. A. 2007, *ApJ*, 669, 1167
- Barrado y Navascués, D., Stauffer, J. R., & Jayawardhana, R. 2004, *ApJ*, 614, 386
- Barry, D. C. 1988, *ApJ*, 334, 436
- Barry, D. C., Cromwell, R. H., & Hege, E. K. 1987, *ApJ*, 315, 264
- Bazot, M., Bouchy, F., Kjeldsen, H., Charpinet, S., Laymand, M., & Vauclair, S. 2007, *A&A*, 470, 295
- Bessell, M. S. 1981, *Publ. Astron. Soc. Australia*, 4, 212
- Bevington, P. R., & Robinson, D. K. 1992, *Data Reduction and Error Analysis for the Physical Sciences* (2nd ed.; New York: McGraw-Hill)
- Bouwman, J., et al. 2008, *ApJ*, 683, 479
- Briceño, C., Preibisch, T., Sherry, W. H., Mamajek, E. A., Mathieu, R. D., Walter, F. M., & Zinnecker, H. 2007, in *Protostars and Planets V*, ed. B. Reipurth, D. Jewitt, & K. Keil (Tucson: Univ. Arizona Press), 345
- Butler, R. P., Marcy, G. W., Williams, E., Hauser, H., & Shirts, P. 1997, *ApJ*, 474, L115
- Cayrel de Strobel, G., Soubiran, C., Friel, E. D., Ralite, N., & Francois, P. 1997, *A&AS*, 124, 299
- Cayrel de Strobel, G., Soubiran, C., & Ralite, N. 2001, *A&A*, 373, 159
- Charbonneau, P., & MacGregor, K. B. 2001, *ApJ*, 559, 1094
- Christy, J. W., & Walker, R. L., Jr. 1969, *PASP*, 81, 643
- Close, L. M., et al. 2005, *Nature*, 433, 286
- Corbally, C. J. 1984, *ApJS*, 55, 657
- Cowley, A. P., Hiltner, W. A., & Witt, A. N. 1967, *AJ*, 72, 1334
- Cox, A. N. 2000, *Allen's Astrophysical Quantities* (4th ed.; New York: AIP)
- Crawford, D. L., & Barnes, J. V. 1974, *AJ*, 79, 687
- Deacon, N. R., & Hambly, N. C. 2004, *A&A*, 416, 125
- de Bruijne, J. H. J., Hoogerwerf, R., & de Zeeuw, P. T. 2001, *A&A*, 367, 111
- de Zeeuw, P. T., Hoogerwerf, R., de Bruijne, J. H. J., Brown, A. G. A., & Blaauw, A. 1999, *AJ*, 117, 354
- Dinescu, D. I., Demarque, P., Guenther, D. B., & Pinsonneault, M. H. 1995, *AJ*, 109, 2090
- Donahue, R. A. 1993, Ph.D. Thesis, New Mexico State Univ.
- . 1998, *ASP Conf. Ser. 154, The Tenth Cambridge Workshop on Cool Stars, Stellar Systems and the Sun*, ed. R. A. Donahue & J. A. Bookbinder (San Francisco: ASP), 1235
- Donahue, R. A., Saar, S. H., & Baliunas, S. L. 1996, *ApJ*, 466, 384
- Duncan, D. K., et al. 1991, *ApJS*, 76, 383
- Duquennoy, A., Mayor, M., Andersen, J., Carquillat, J. M., & North, P. 1992, *A&A*, 254, L13
- Edwards, T. W. 1976, *AJ*, 81, 245
- Eggenberger, P., Charbonnel, C., Talon, S., Meynet, G., Maeder, A., Carrier, F., & Bourban, G. 2004, *A&A*, 417, 235
- Endal, A. S., & Sofia, S. 1981, *ApJ*, 243, 625
- Famaey, B., Siebert, A., & Jorissen, A. 2008, *A&A*, 483, 453
- Fleming, T. A., Schmitt, J. H. M. M., & Giampapa, M. S. 1995, *ApJ*, 450, 401
- Fletcher, S. T., Chaplin, W. J., Elsworth, Y., Schou, J., & Buzasi, D. 2006, *MNRAS*, 371, 935
- García-López, R. J., Rebolo, R., Beckman, J. E., & McKeith, C. D. 1993, *A&A*, 273, 482
- Giampapa, M. S., Hall, J. C., Radick, R. R., & Baliunas, S. L. 2006, *ApJ*, 651, 444
- Girard, T. M., Grundy, W. M., López, C. E., & van Altena, W. F. 1989, *AJ*, 98, 227
- Gliese, W., & Jahreiss, H. 1991, *Preliminary Version of the Third Catalogue of Nearby Stars (Greenbelt: NASA GSFC) (CNS3)*
- Gott, J. R. I., Vogeley, M. S., Podariu, S., & Ratra, B. 2001, *ApJ*, 549, 1
- Gray, R. O., Corbally, C. J., Garrison, R. F., McFadden, M. T., Bubar, E. J., McGahee, C. E., O'Donoghue, A. A., & Knox, E. R. 2006, *AJ*, 132, 161
- Gray, R. O., Corbally, C. J., Garrison, R. F., McFadden, M. T., & Robinson, P. E. 2003, *AJ*, 126, 2048
- Gray, R. O., Napier, M. G., & Winkler, L. I. 2001, *AJ*, 121, 2148
- Hall, J. C., Lockwood, G. W., & Skiff, B. A. 2007, *AJ*, 133, 862
- Hallam, K. L., Altner, B., & Endal, A. S. 1991, *ApJ*, 372, 610
- Hartigan, P., & Kenyon, S. J. 2003, *ApJ*, 583, 334
- Hartigan, P., Strom, K. M., & Strom, S. E. 1994, *ApJ*, 427, 961
- Hartmann, L., Soderblom, D. R., Noyes, R. W., Burnham, N., & Vaughan, A. H. 1984, *ApJ*, 276, 254
- Hempelmann, A., Schmitt, J. H. M. M., Baliunas, S. L., & Donahue, R. A. 2003, *A&A*, 406, L39
- Hempelmann, A., Schmitt, J. H. M. M., Schultz, M., Ruediger, G., & Stepień, K. 1995, *A&A*, 294, 515
- Hempelmann, A., Schmitt, J. H. M. M., & Stepień, K. 1996, *A&A*, 305, 284
- Henry, G. W., Baliunas, S. L., Donahue, R. A., Fekel, F. C., & Soon, W. 2000, *ApJ*, 531, 415
- Henry, T. J., Soderblom, D. R., Donahue, R. A., & Baliunas, S. L. 1996, *AJ*, 111, 439
- Hill, G., Fisher, W. A., & Holmgren, D. 1989, *A&A*, 211, 81
- Hillenbrand, L. A., et al. 2008, *ApJ*, 677, 630
- Hines, D. C., et al. 2006, *ApJ*, 638, 1070
- . 2007, *ApJ*, 671, L165
- Hoffleit, D., & Jaschek, C. 1991, *Bright Star Catalog* (5th ed.; New Haven: Yale Univ. Obs.)
- Høg, E., et al. 2000, *A&A*, 355, L27
- Isobe, T., Feigelson, E. D., Akritas, M. G., & Babu, G. J. 1990, *ApJ*, 364, 104
- Jay, J. E., Guinan, E. F., Morgan, N. D., Messina, S., & Jassour, D. 1997, *BAAS*, 29, 730
- Jenkins, J. S., Jones, H. R. A., Pavlenko, Y., Pinfield, D. J., Barnes, J. R., & Lyubchik, Y. 2008, *A&A*, 485, 571
- Jenkins, J. S., et al. 2006, *MNRAS*, 372, 163
- Jones, B. F., Fischer, D., Shetrone, M., & Soderblom, D. R. 1997, *AJ*, 114, 352
- Judge, P. G., Solomon, S. C., & Ayres, T. R. 2003, *ApJ*, 593, 534
- Jung, Y. K., & Kim, Y.-C. 2007, *J. Astron. Space Sci.*, 24, 1
- Keenan, P. C., & McNeil, R. C. 1989, *ApJS*, 71, 245
- Kenyon, S. J., & Hartmann, L. 1995, *ApJS*, 101, 117
- Kim, J. S., et al. 2005, *ApJ*, 632, 659
- Kim, Y.-C., & Demarque, P. 1996, *ApJ*, 457, 340
- King, J. R., & Schuler, S. C. 2005, *PASP*, 117, 911
- King, J. R., Villarreal, A. R., Soderblom, D. R., Gulliver, A. F., & Adelman, S. J. 2003, *AJ*, 125, 1980
- Kraft, R. P. 1967, *ApJ*, 150, 551
- Krishnamurthi, A., et al. 1998, *ApJ*, 493, 914
- Lachaume, R., Dominik, C., Lanz, T., & Habing, H. J. 1999, *A&A*, 348, 897
- Livingston, W., Wallace, L., White, O. R., & Giampapa, M. S. 2007, *ApJ*, 657, 1137
- Lockwood, G. W., Skiff, B. A., Henry, G. W., Henry, S., Radick, R. R., Baliunas, S. L., Donahue, R. A., & Soon, W. 2007, *ApJS*, 171, 260
- Luhman, K. L., Stauffer, J. R., & Mamajek, E. E. 2005, *ApJ*, 628, L69
- Makarov, V. V. 2006, *AJ*, 131, 2967
- Mamajek, E. E. 2005, *ApJ*, 634, 1385
- Mamajek, E. E., Barrado y Navascués, D., Randich, S., Jensen, E. L., Young, P. A., Miglio, A., & Barnes, S. A. 2008, in *ASP Conf. Ser. 384, The 14th Cambridge Workshop on Cool Stars, Stellar Systems, and the Sun*, ed. G. van Belle (San Francisco: ASP), 374
- Mamajek, E. E., Meyer, M. R., Hinz, P. M., Hoffmann, W. F., Cohen, M., & Hora, J. L. 2004, *ApJ*, 612, 496
- Mamajek, E. E., Meyer, M. R., & Liebert, J. 2002, *AJ*, 124, 1670
- . 2006, *AJ*, 131, 2360
- Marsakov, V. A., & Shevelev, Y. G. 1995, *Bull. Cent. Donnees Stellaires*, 47, 13
- Meibom, S., Mathieu, R. D., & Stassun, K. G. 2008, *ApJ*, submitted (arXiv:0805.1040)
- Milliod, J. C. 1981, *A&A*, 97, 235
- . 1991, *Catalogue of Homogeneous Means in the UBV System* (Lausanne: Univ. de Lausanne)

- Messina, S. 2001, *A&A*, 371, 1024
- Mestel, L. 1968, *MNRAS*, 138, 359
- Meyer, M. R., et al. 2004, *ApJS*, 154, 422
- . 2006, *PASP*, 118, 1690
- . 2008, *ApJ*, 673, L181
- Miglio, A., & Montalbán, J. 2005, *A&A*, 441, 615
- Montesinos, B., Thomas, J. H., Ventura, P., & Mazzitelli, I. 2001, *MNRAS*, 326, 877
- Montgomery, K. A., Marschall, L. A., & Janes, K. A. 1993, *AJ*, 106, 181
- Moro-Martín, A., et al. 2007, *ApJ*, 658, 1312
- Nordström, B., et al. 2004, *A&A*, 418, 989
- Noyes, R. W., Hartmann, L. W., Baliunas, S. L., Duncan, D. K., & Vaughan, A. H. 1984, *ApJ*, 279, 763
- Ortega, V. G., de la Reza, R., Jilinski, E., & Bazzanella, B. 2002, *ApJ*, 575, L75
- Ortega, V. G., Jilinski, E., de La Reza, R., & Bazzanella, B. 2007, *MNRAS*, 377, 441
- Pace, G., & Pasquini, L. 2004, *A&A*, 426, 1021
- Padgett, D. L. 1996, *ApJ*, 471, 847
- Parker, E. N. 1979, *Cosmical Magnetic Fields: Their Origin and Their Activity* (Oxford: Clarendon Press)
- Paulson, D. B., Cochran, W. D., & Hatzes, A. P. 2004, *AJ*, 127, 3579
- Paulson, D. B., Saar, S. H., Cochran, W. D., & Hatzes, A. P. 2002, *AJ*, 124, 572
- Perryman, M. A. C., et al. 1997, *The Hipparcos and Tycho Catalogues* (ESA SP-1200; Noordwijk: ESA)
- . 1998, *A&A*, 331, 81
- Pizzolatto, N., Maggio, A., Micela, G., Sciortino, S., & Ventura, P. 2003, *A&A*, 397, 147
- Pourbaix, D., et al. 2004, *A&A*, 424, 727
- Preibisch, T., Brown, A. G. A., Bridges, T., Guenther, E., & Zinnecker, H. 2002, *AJ*, 124, 404
- Preibisch, T., & Feigelson, E. D. 2005, *ApJS*, 160, 390
- Preibisch, T., & Mamajek, E. 2008, in *Handbook of Star-forming Regions*, ed. B. Reipurth, in press
- Preibisch, T., & Zinnecker, H. 1999, *AJ*, 117, 2381
- Prosser, C. F. 1992, *AJ*, 103, 488
- Prosser, C. F., et al. 1995, *PASP*, 107, 211
- Radick, R. R., Lockwood, G. W., Skiff, B. A., & Baliunas, S. L. 1998, *ApJS*, 118, 239
- Radick, R. R., Lockwood, G. W., Skiff, B. A., & Thompson, D. T. 1995, *ApJ*, 452, 332
- Radick, R. R., Thompson, D. T., Lockwood, G. W., Duncan, D. K., & Baggett, W. E. 1987, *ApJ*, 321, 459
- Randich, S., Schmitt, J. H. M. M., Prosser, C. F., & Stauffer, J. R. 1996, *A&A*, 305, 785
- Robichon, N., Arenou, F., Mermilliod, J.-C., & Turon, C. 1999, *A&A*, 345, 471
- Saar, S. H., & Brandenburg, A. 1999, *ApJ*, 524, 295
- Saar, S. H., & Osten, R. A. 1997, *MNRAS*, 284, 803
- Saffe, C., Gómez, M., & Chavero, C. 2005, *A&A*, 443, 609
- Sarajedini, A., von Hippel, T., Kozhurina-Platais, V., & Demarque, P. 1999, *AJ*, 118, 2894
- Schatzman, E. 1962, *Ann. d'Astrophys.*, 25, 18
- Silverstone, M. D., et al. 2006, *ApJ*, 639, 1138
- Skumanich, A. 1972, *ApJ*, 171, 565
- Soderblom, D. R. 1983, *ApJS*, 53, 1
- . 1985, *AJ*, 90, 2103
- Soderblom, D. R., Duncan, D. K., & Johnson, D. R. H. 1991, *ApJ*, 375, 722
- Soderblom, D. R., King, J. R., & Henry, T. J. 1998, *AJ*, 116, 396
- Soderblom, D. R., Stauffer, J. R., Hudon, J. D., & Jones, B. F. 1993, *ApJS*, 85, 315
- Strassmeier, K., Washuettl, A., Granzer, T., Scheck, M., & Weber, M. 2000, *A&AS*, 142, 275
- Stauffer, J. R., Hartmann, L., Soderblom, D. R., & Burnham, N. 1984, *ApJ*, 280, 202
- Stauffer, J. R., & Hartmann, L. W. 1987, *ApJ*, 318, 337
- Stauffer, J. R., Hartmann, L. W., & Jones, B. F. 1989, *ApJ*, 346, 160
- Stauffer, J. R., Schultz, G., & Kirkpatrick, J. D. 1998, *ApJ*, 499, L199
- Stauffer, J. R., et al. 2005, *AJ*, 130, 1834
- Stepien, K. 1994, *A&A*, 292, 191
- Sterzik, M. F., & Schmitt, J. H. M. M. 1997, *AJ*, 114, 1673
- Taylor, B. J. 2006, *AJ*, 132, 2453
- Thévenin, F., & Idiart, T. P. 1999, *ApJ*, 521, 753
- Thévenin, F., Provost, J., Morel, P., Berthomieu, G., Bouchy, F., & Carrier, F. 2002, *A&A*, 392, L9
- Thoul, A., Scuflaire, R., Noels, A., Vatoquez, B., Briquet, M., Dupret, M.-A., & Montalbán, J. 2003, *A&A*, 402, 293
- Tinney, C. G., McCarthy, C., Jones, H. R. A., Butler, R. P., Carter, B. D., Marcy, G. W., & Penny, A. J. 2002, *MNRAS*, 332, 759
- Twarog, B. A., Ashman, K. M., & Anthony-Twarog, B. J. 1997, *AJ*, 114, 2556
- Valenti, J. A., & Fischer, D. A. 2005, *ApJS*, 159, 141 (VF05)
- VandenBerg, D. A., & Stetson, P. B. 2004, *PASP*, 116, 997
- Vaughan, A. H., & Preston, G. W. 1980, *PASP*, 92, 385
- Vaughan, A. H., Preston, G. W., & Wilson, O. C. 1978, *PASP*, 90, 267
- Voges, W., et al. 1999, *A&A*, 349, 389
- . 2000, *IAU Circ.*, 7432, 3
- Walker, G. A. H., et al. 2008, *A&A*, 482, 691
- Walter, F. M., Vrba, F. J., Mathieu, R. D., Brown, A., & Myers, P. C. 1994, *AJ*, 107, 692
- Weber, E. J., & Davis, L. J. 1967, *ApJ*, 148, 217
- West, A. A., Hawley, S. L., Bochanski, J. J., Covey, K. R., Reid, I. N., Dhital, S., Hilton, E. J., & Masuda, M. 2008, *AJ*, 135, 785
- White, O. R., & Livingston, W. C. 1981, *ApJ*, 249, 798
- White, R. J., Gabor, J. M., & Hillenbrand, L. A. 2007, *AJ*, 133, 2524
- Wichmann, R., Krautter, J., Covino, E., Alcalá, J. M., Neuhaeuser, R., & Schmitt, J. H. M. M. 1997, *A&A*, 320, 185
- Wilson, O. C. 1963, *ApJ*, 138, 832
- Wolff, S. C., Heasley, J. N., & Varsik, J. 1985, *PASP*, 97, 707
- Wright, J. T. 2004, *AJ*, 128, 1273
- . 2005, *AJ*, 129, 1776
- Wright, J. T., Marcy, G. W., Butler, R. P., & Vogt, S. S. 2004, *ApJS*, 152, 261
- Yi, S. K., Kim, Y.-C., & Demarque, P. 2003, *ApJS*, 144, 259
- Zuckerman, B., & Song, I. 2004, *ARA&A*, 42, 685